APPROPRIATE STOPE DESIGN WITH CONSIDERATION OF FRACTURED ROCK MASS WHEN TRANSITIONING FROM OPEN PIT MINING TO UNDERGROUND MINING FOR SEPON COPPER-GOLD MINE DEPOSIT, LAOS

ファイソファ, シーラエ

https://hdl.handle.net/2324/7182449

出版情報：Kyushu University, 2023, 博士（工学）, 課程博士
バージョン：
権利関係：

APPROPRIATE STOPE DESIGN WITH CONSIDERATION OF FRACTURED ROCK MASS WHEN TRANSITIONING FROM OPEN PIT MINING TO UNDERGROUND MINING FOR SEPON COPPER-GOLD MINE DEPOSIT, LAOS

SEELAE PHAISOPHA

MARCH, 2024

APPROPRIATE STOPE DESIGN WITH CONSIDERATION OF FRACTURED ROCK MASS WHEN TRANSITIONING FROM OPEN PIT MINING TO UNDERGROUND MINING FOR SEPON COPPER-GOLD MINE DEPOSIT, LAOS

A DOCTORAL DISSERTATION

SUBMITTED TO THE GRADUATE SCHOOL OF ENGINEERING
KYUSHU UNIVERSITY

AS A PARTIAL FULFILLMENT OF THE REQUIREMENTS FOR THE DEGREE OF

DOCTOR OF PHILOSOPHY OF ENGINEERING

BY

SEELAE PHAISOPHA

SUPERVISED BY

PROF. HIDEKI SHIMADA

CO-SUPERVISED BY

ASSCIATE PROF. TAKASHI SASAOKA

DEPARTMENT OF EARTH RESOURCES ENGINEERING

ROCK ENGINEERING AND MINING MACHINERY

LABORATORY

KYUSHU UNIVERSITY

FUKUOKA, JAPAN

MARCH, 2024

ABSTRACT

Laos, abundant in natural resources like forests, rivers, and minerals, has untapped potential for economic growth, notably in gold and copper mining. To attract foreign investors and leverage these resources, efforts have focused on promoting the mining sector. Notably, the Sepon gold copper mine, one of Laos's largest operations, faces challenges in shifting from surface to underground mining due to a high stripping ratio. Open stope mining is considered suitable for Sepon, but hazards must be addressed to ensure worker safety and mine integrity. Implementing measures like waste filling as support systems is crucial. Careful planning considering geological conditions and financial aspects is essential. Laos aims to develop its mining resources to boost economic growth and improve citizen livelihoods. To achieve this, understanding geotechnical aspects of gold deposits and designing an underground open stope mine is the research objective. It involves field investigations, lab tests, and numerical simulations with RS2 software across five dissertation chapters as follow:

Chapter 1: This chapter presents an overview of the research background, explores geotechnical considerations and technology pertinent to the open stope mining method, and outlines the goals and structure of this dissertation

Chapter 2: This chapter offers an overview of conditions at the Sepon Gold Copper mine site. Laboratory tests indicate that the underground rock is classified as quite weak and low-strength. It also discusses current underground stability, highlighting displacement issues in the hanging wall, especially when stopes extend into both the hanging wall and roof. The chapter emphasizes the need to enhance existing support systems for safety and stability. The Sepon underground mine is situated in the sout center part of Laos, an area marked by a complex tectonic structure exacerbated by the Leuy and Korat fault lines crossing the mine site. The geological context reveals sedimentary-hosted rocks, and the region belongs to the Southeast Asia Belt, known for significant granite and associated gold-copper deposits. The gold ores are found in jasperoid, decalcified shale, and dolomitize shale. In this mine, the overhand open stope mining method is employed, characterized by a small-scale and manual excavation approach. Field investigations and laboratory tests have shown that the rock mass condition at this site is poor, particularly at shallow depths due to the prevalence of a fracture system. This chapter also introduces the problem statement associated with the current mining method and outlines the research objectives, setting the stage for further exploration and analysis.

Chapter 3: This chapter explores the impact of employing the open stope mining method with a vein dip of 62° under varying mine conditions. Through numerical analysis, two distinct variations of the open stope technique were simulated to assess ground behavior and stress conditions within both the stope and crown pillar. The findings reveal that the overhand cut method consistently provides superior stability compared to the underhand approach. Additional investigations were conducted to assess the stability of the stope and crown pillar in the overhand variant across different mine conditions. The results indicate a higher likelihood of crown pillar failure in open stope mines with a vein dip less than 52°, a wider vein width of 20 m, weaker geological conditions like a GSI lower than 35 causing a higher scale of failure, and a higher stress ratio from 1.5 upwards also impacting the open stope. The stability of the stope can be maintained by considering stope size, GSI, sill pillar thickness, and rock mass condition around the open stope. However, increasing crown pillar and sill pillar thickness can result in decreased mining recovery due to retained ore

.**Chapter 4:** This chapter extensively investigates stability considerations for both the crown pillar and sill pillar when extracting a highly inclined vein with a 37° dip, specifically focusing on bedding and joint contact mining conditions. The strategically placed sill pillar acts as a crucial barrier between adjacent stopes, preventing potential collapses. Using practical applications of the open stope mining method, this exploration draws insights from comprehensive numerical simulations. These findings offer crucial insights into stability dynamics under diverse geological conditions. The study emphasizes the substantial impact of the Geological Strength Index (GSI) on stability, where a decreasing GSI significantly affects all elements' stability. Additionally, wider stopes, particularly at 10 m width and 25 m height, diminish overall stability for both the stope and sill pillar. To address this, employing the cut and fill mining method with waste rock fill and maintaining a minimum 10 m thickness for the sill pillar is recommended for stability in this complex mining setting. The chapter critically examines the importance of backfill material, demonstrating its significant impact on structural stability, particularly in areas with a GSI below 35. Strategic backfilling emerges as crucial for ensuring structural integrity. Moreover, backfill simulations suggest its potential efficacy in mitigating instability and contributing to overall mining structure stability.

Chapter 5: This chapter serves as the conclusion, summarizing the findings and contributions of this dissertation.

ACKNOWLEDGEMENTS

I would like to express my profound appreciation to Prof. Dr. Hideki Shimada, my esteemed research supervisor at the Laboratory of Rock Engineering and Mining Machinery, Kyushu University. His patient guidance, unwavering encouragement, and generous support throughout the course of this research have been invaluable. I am deeply grateful for his willingness to dedicate his time and expertise to my academic and research pursuits.

I extend my heartfelt gratitude to Prof. Dr. Takashi Sasaoka, my co-supervisor, and Akihiro Hamanaka, both of whom hail from the Laboratory of Rock Engineering and Mining Machinery, Kyushu University. Their invaluable and constructive suggestions during the planning and development stages of this research were instrumental. Additionally, I am thankful for their professional advice and the kind assistance that kept my progress on track.

I would like to convey my sincere thanks to the member of my examination committee, including Prof. Dr. Mamoru Kikumoto, from the Institute of Urban Innovation, Yokohama National University. His insightful comments and engaging discussions enriched the quality of my work, and I deeply appreciate the time they dedicated to providing valuable feedback.

I am grateful to the staff of the Sepon gold mine in Laos for graciously facilitating my visit to their mine site, enabling me to observe daily operations and collect the essential data required for this research.

I am particularly indebted to the JICA (KIZUNA program) for their generous financial support, which made my doctoral study at Kyushu University in Japan possible. This scholarship is a tremendous honor, and I am deeply appreciative of their assistance.

A very special thank you goes out to all my friends at the Laboratory of Rock Engineering and Mining Machinery, Kyushu University, for their unwavering assistance, encouragement, and the friendships we've formed. The time spent with them holds immeasurable value, beyond what words can express on this paper.

To my beloved dad, Khamsai Phaisopha, who resides forever in my thoughts, even though you have passed away. I carry immense pride in being your son, and I continue to miss you deeply. The fact that I bear your surname, which I still proudly use, serves as a constant reminder of you. I earnestly wish that you could witness my successes. Your presence is dearly missed.

My heartfelt and deepest gratitude is reserved for my mom, Bounhieng Phaisopha. Her unwavering love and boundless support have been a pillar of strength throughout my life's journey. She has always been there by my side, offering words of encouragement and a listening ear whenever I faced adversity.

Lastly, I want to express my appreciation to my wife, Buakhao Phongxayphon. Her love, care, patience, and unwavering encouragement have been instrumental in my academic pursuits in Japan, which I knew would be a challenging path. Despite the occasional disagreements, a normal part of any couple's life, her support has made all of this possible.

I must also extend my gratitude to the two little boys who have recently entered my life, my two sons, Thavixai Phaisopha and Thavixok Phaisopha. Their arrival has brought me boundless inspiration and serves as a reminder to never give up in the face of life's challenges. While I may not possess everything I desire, I am undeniably blessed to have both of you as an integral part of my life.

March 2024

SEELAE PHAISOPHA

TABLE OF CONTENTS

LIST OF FIGURES

LIST OF TABLES

CHAPTER 1
INTRODUCTION

Currently, transitioning from surface mining to underground mining is considered one of the best options for optimizing the environmental impact in the surface area of mineral exploration, promoting sustainable development. By shifting to underground mining, the disturbance on the surface can be significantly minimized, reducing the footprint and preserving the natural landscape. Additionally, underground mining methods offer the advantage of better control over dust, noise, and emissions, further mitigating the environmental impact. Laos is known to possess substantial undeveloped resources and undoubtedly holds undiscovered deposits of various commodities. With the potential for new discoveries, the transition to underground mining becomes even more relevant (Bakhtavar et al., 2009a, 2009b, 2012; Chung et al., 2022; Eberhardt et al., 2007; Olavarría et al., 2015; Potvin & Hudyma, 2016; Soltani Khaboushan et al., 2020), as it allows for the exploration and extraction of deeper, previously untapped deposits.

Recently, the preference has been for shallow surface mining over underground mining due to reasons ranging from economic considerations to safety concerns. However, in the research area, the adoption of underground open stopes has become necessary. The transition from surface mining to underground mining is driven by several factors, including the depletion of resources at shallow depths and an increasing stripping ratio that exceeds acceptable criteria. As a result, the need to ensure mine safety, promote economic development through natural resource exploitation, and preserve the environmental conditions of the mining area has led to the decision to transition to underground mining. The Sepon mine site, situated in Laos, is renowned as one of the largest open-pit mines and underground open stope mining systems for gold and copper operations. Its significance lies not only in its size but also in its potential to serve as a model for successful transitioning from surface mining to underground mining, ensuring sustainable resource extraction practices.

The study area is situated in a complex structure and mountainous region. As a result, mining activities in the area cause stress redistribution in the surrounding rocks, leading to surface movement and ground fissures. The presence of void spaces and the ongoing mining activities also contribute to these phenomena. However, the open stope method poses challenges in terms of mine safety, worker well-being, and transportation in the mined-out areas. Given the circumstances, it is crucial to evaluate the subsidence of shallow underground mines and compare it with the geometric characteristics of the problem statement at the Sepon deposit gold-copper mine. To accomplish this, the researcher emphasizes the significance of employing software simulations such as RS2. These simulations can provide valuable insights into the behavior of the mine structure and assist in predicting and mitigating potential subsidence issues.

The technique of filling the stope is considered the preferred method for mitigating instability in underground mines. By filling the excavated areas, it helps to provide support and prevent potential collapses or failures. However, despite the implementation of this technique, failures can still occur in the surrounding mined-out areas. These failures can be attributed to various factors, including the use of inadequate supporting methods or challenging geological conditions that have the potential to disrupt the surface of the mine, however, the failure can be control by adapting the stope dimension (Potvin & Hudyma, 2016) . It is essential to address these specific reasons for failures in order to ensure the stability and safety of the underground mine. This may involve improving the selection and implementation of supporting methods to match the geological conditions encountered. Additionally, conducting thorough geological assessments and monitoring the site continuously can aid in identifying potential instabilities and taking timely preventive measures.

To facilitate the development of gold metal mines and ensure control over mine instability, the mining industry must have a comprehensive understanding of the problem statement parameters and a well-defined mine design plan. By thoroughly assessing and analyzing these factors, potential risks and instabilities can be identified, and appropriate measures can be implemented to optimize the stability of underground mines. The findings and outcomes of this dissertation have the potential to significantly contribute to the optimization of underground mine stability. The knowledge gained from the research can be applied to enhance mining practices, mitigate instability-related challenges, and improve overall operational efficiency and safety.

Laos, with its abundance of gold resources, has a valuable opportunity to capitalize on its gold wealth. By strategically developing a large and sustainable gold industry, Laos can play a significant role in shaping the future market balance of the gold industry. This can have far-reaching economic impacts, creating employment opportunities, attracting investments, and positioning Laos as a key player in the global gold market.

1.1. Background

Sepon is situated in the Vilabouly District of Savannakhet Province, located in the South-Central part of Laos. Covering an area of 1,947 square kilometers, the Sepon project is approximately 40 kilometers north of the town of Sepon. The study area is specifically chosen within the Sepon Basin, which is located in the Vilabouly District of Savannakhet Province, Lao PDR. The Sepon Basin is renowned for its copper-gold mineralization district, as depicted in Figure 1.1. The Cu-Au mineralization in the SMD (Sepon Mineral District) is found along an east-trending corridor spanning approximately 40 kilometers in length and 10 kilometers in width.

Figure 1. 1 Location of Sepon Project

1.2. Sepon Mineral District

Porphyry deposits are significant resources of copper, gold, and molybdenum, and are defined as large volumes of magmatic-hydrothermal processes, in which sulfide and oxide ore minerals are precipitated from aqueous solution (Seedorff et al., 2005). Porphyry copper systems are composed of various mineralization types, including porphyry deposits centered on intrusion; skarn; carbonate-replacement; sediment-hosted, and high- and intermediate-sulfidation epithermal base and precious metals mineralization. Porphyry deposits are intimately associated with magmatic arcs developed along the convergent margin zone, together with calc-alkaline batholith and volcanic chains (Richards, 2003; Sillitoe, 1972).

Sepon Mineral District (SMD) is well known for its porphyry Cu-(Au-Mo) deposit, which occurs in the Sepon Basin, within the NW-trending Truongson fold belt in Vilabouly District, Savannakhet Province in the South-Central part of Laos (Fig. 1.2). The Cu-Au mineralization within the SMD occurred along the east-west trending corridor, approximately 40 km long by 10 km wide. The open-pit gold and copper mining activities and productions in the SMD were commenced in late 2002 and late 2004, respectively, within indicated and inferred resources of 83 Mt @ 1.8 g/t Au for 4.75 Moz plus 100 Mt @ 2% Cu for 2.0 Mt (Cannell & Smith, 2008; Smith et al., 2005).

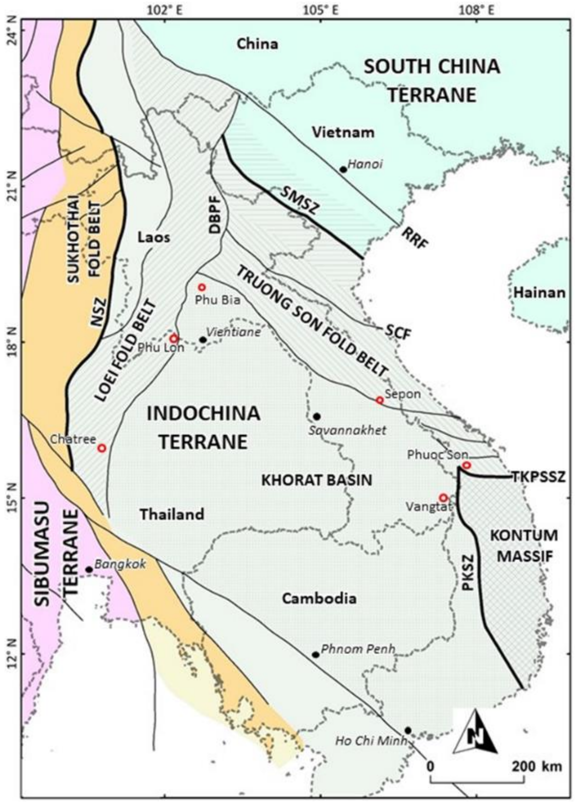

Figure 1. 2 Main lithotectonic terranes and domains of mainland Southeast Asia, and their associated metal deposits modified from (Sone & Metcalfe, 2008). Abbreviation: DBPF: Dien Bien Phu Fault; NSZ: Nan Suture Zone; PKSZ: Poko Suture Zone; RRF: Red River Fault; SCF: Song Ca Fault; SMSZ: Song Ma Suture Zone; TKPSSZ: Tam Ky-Phuoc Son Suture Zone

1.3. Geology and Mineralization

NW trending Truong Son fold belt (Fig. 1.2) is a volcanic arc that resulted from the collision between the Indochina and South China Terranes (Hutchison, 1989; Lepvrier et al., 1997; Metcalfe, 1998). Truong Son fold belt extends from northern Laos to central Vietnam and consists of metamorphic complexes with successor basins, including the Sepon Basin. The Sepon Basin is made up of poorly constrained Ordovician-Devonian clastic-carbonate sedimentary sequences with scattered intrusions of the volcanic rocks, consisting of sandstone, siltstone, mudstone, calcareous mudstone, shale, calcareous shale, limestone, bioclastic limestone, and chert (Fig. 1.3; (Morris, 2006). The E-W major structures together with NW trending steep dipping strike-slip faults are the main controls for the distribution of Cu-Au mineralization (Fig. 1.3; (Smith et al., 2005)).

Phadan and Thenkham are the major mineralized intrusion centers in the SMD, together with encompassed dike and sill intrusions. Three major types of mineralization have been recognized within the SMD, 1) Mo-(Cu) mineralization on the center of Phadan and Thengkham intrusions; 2) adjacent to the intrusion centers is skarn Cu-(Au) mineralization (e.g., Khanong, Thengkham N, and Thengkham S); and 3) further distal is the sediment-hosted gold deposit (e.g., Phavat, Nalou, Namkok W, Namkok E, Discovery, Vang Nang, and Huay Yeng) (Fig. 1.3, 1.4; Cannell & Smith, 2008; Smith et al., 2005).

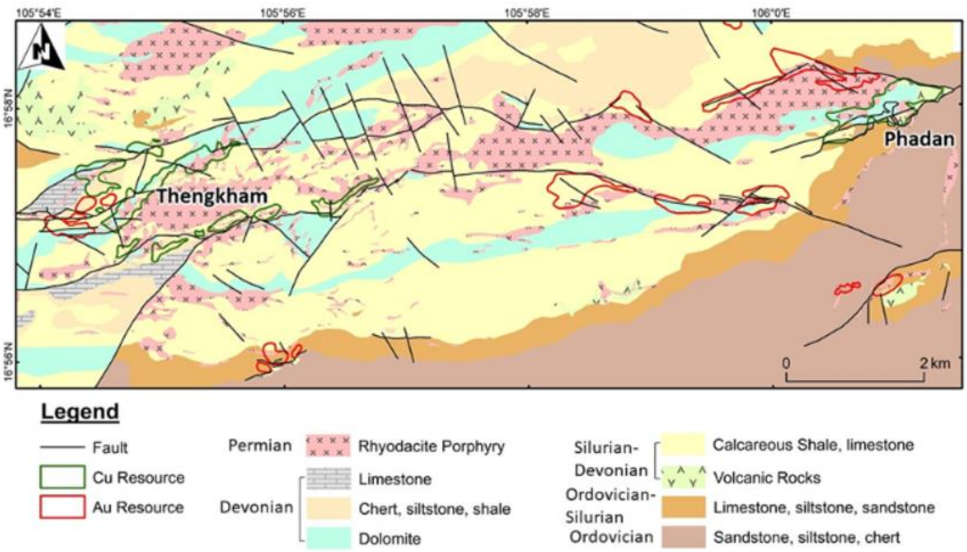

Figure 1. 3 Simplified geological map of Sepon Mineral District showing the main gold and copper deposits

1.3.1. Igneous Rocks

Rhyodacite porphyry (RDP), minor andesite, and lamprophyre are the igneous rocks that have been recognized in the SMD (Loader, 1999). The RDP intrusions are centered on Phadan and Thenkham (Fig. 1.3), together with dike sets and subsidiary intrusive centers widespread intruded the Sepon Basin sequence, oriented along the dominant E-W structural trend (Fig. 1.3). RDP is the mineralized intrusive rock in the SMD, which is characterized by the abundant of plagioclase phenocryst (up to 1 cm) and was later altered to K-feldspar (see below), quartz phenocryst constitute 10-25%, and <10% mafic minerals (Smith et al., 2005). RDP dike intrusions have been affected by regional fault structures that dominated the sedimentary sequence of the Sepon Basin and most of the RDP-sediment contacts are marked by shear structures. The magmatic-hydrothermal associated with RDP intrusions resulted in wall rocks alteration and Cu-(Au-Mo) mineralization.

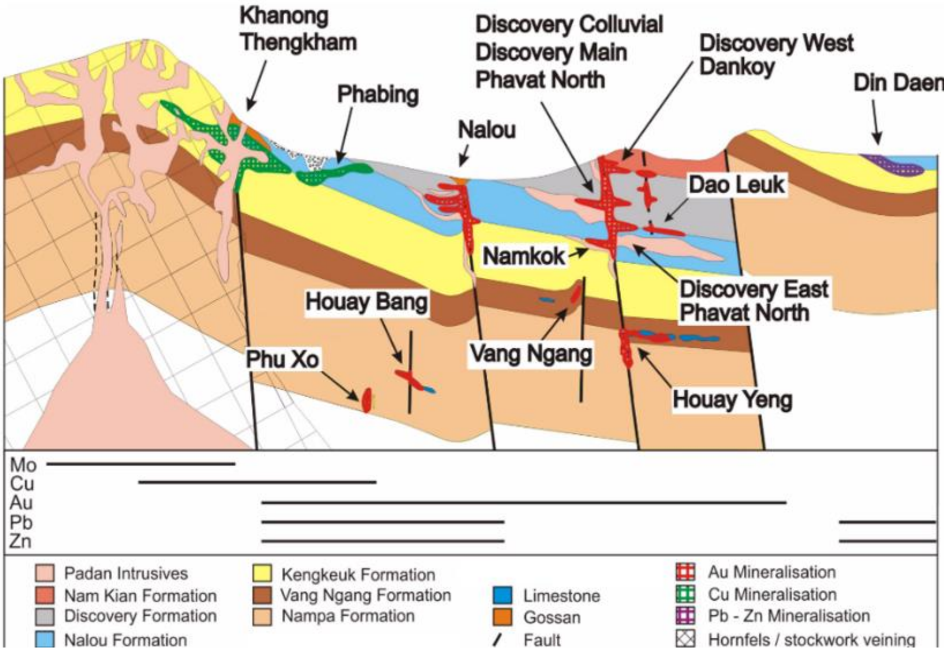

Figure 1. 4 Schematic model of Cu-Au mineralization at the SMD

1.3.2. Alteration and Mineralization

Three major types of mineralization have been recognized in the SMD, therefore the characteristics of wall rock alteration and mineralization are different in each environment and hydrothermal process.

1. Center on RDP intrusion: (Cromie, 2010) has classified four types of alteration in the RDP intrusion centers (i.e., Phadan and Thenkham); a) K-feldspar dominant replaced the primary (igneous) plagioclase in the phenocryst and groundmass; b) white mica with minor chlorite overprinted K-feldspar alteration; c) quartz vein with K-feldspar alteration halo and later by quartz-chlorite-pyrite-molybdenite-chalcopyrite-bornite-hematite vein; and d) massive barren quartz vein, vein stockwork. Cu and Mo sulfides are mainly present in the vein quartz and disseminated together with K-feldspar and white mica-chlorite alteration assemblages, however, the grades of Mo and Cu are slightly low, ranging from 40 to 1020 ppm Mo and <0.1 to 0.5% Cu, identifying sub-economic Mo and Cu mineralization in the SMD (LXML, 1999).

2. Contact between wall rock lithologies and RDP: the contact between wall rock lithologies, particularly carbonated rocks (e.g., calcareous shale, limestone, and dolomitic limestone) of Nalou and Kengkuek Formations (Fig. 1.3, 1.4) and RDP intrusions resulted in Cu-(Au) skarn

mineralization.(Cannell & Smith, 2008; Cromie, 2010; Seedorff et al., 2005) classified three types of skarn mineralization and alteration assemblage; a) garnet with minor pyroxene, biotite, and K-feldspar assemblages of prograde skarn, which were overprinted by b) chlorite, epidote, hematite, calcite, and sulfide (e.g., chalcopyrite-bornite-molybdenite±Au); and c) quartz, calcite, fluorite, pyrite±Au in the later stage. Primary copper mineralization presented in semi-massive sulfide zones is typically less than 1% Cu, though locally up to 5% Cu in chalcopyrite-rich zones (Cannell & Smith, 2008). Lower-grade gold, up to 1 ppm identified as a solid solution with chalcopyrite, and higher-grade gold, up to 290 ppm occurred as a solid solution in pyrite crystal structure during the later stage.

Economic ore zone within high-grade copper ore, >4% Cu occurred in the supergene enrichment zone near the surface, which is composed of secondary copper ore; chalcopyrite, malachite, azurite, cuprite, and native copper have been precipitate from groundwater distal from primary copper mineralization (Fig. 1.5; (Cannell & Smith, 2008)). The thickness and depth of the secondary ore zone are dependent on various factors, including the geometry of primary mineralization, the orientation of faults and RDP, and local hydrological factors.

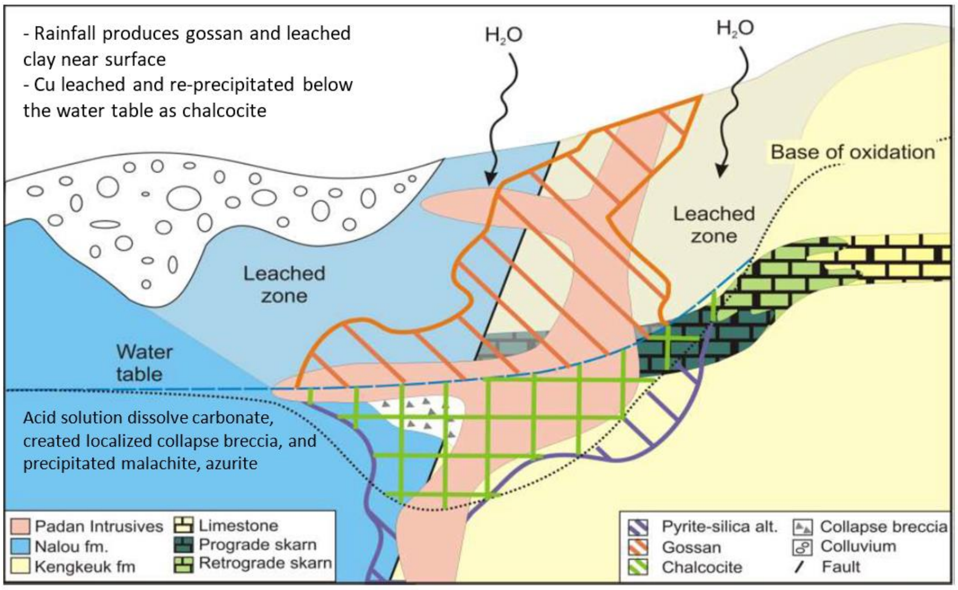

Figure 1. 5 Genetic model of secondary copper mineralization at the SMD

3. Sediment-hosted gold deposit: distal distance from the RDP intrusion centers, where the sets of dike and sill intruded calcareous mudstone and calcareous shale of Discovery Formation presented sediment-hosted gold deposits (Fig. 1.3, 1.4). Steep faults and secondary shallow to moderated dipping fault structures enhanced the RDP intrusions and elevated hydrothermal fluid ascending (Fig. 1.6), resulting in intensely silicified carbonated rocks or jasperoid and decalcified shale. Gold is predominantly found as invisible gold or gold in solid solution with

the crystallization of pyrite, most like disseminated and fracture controlled together with jasperoid and decalcified shale.

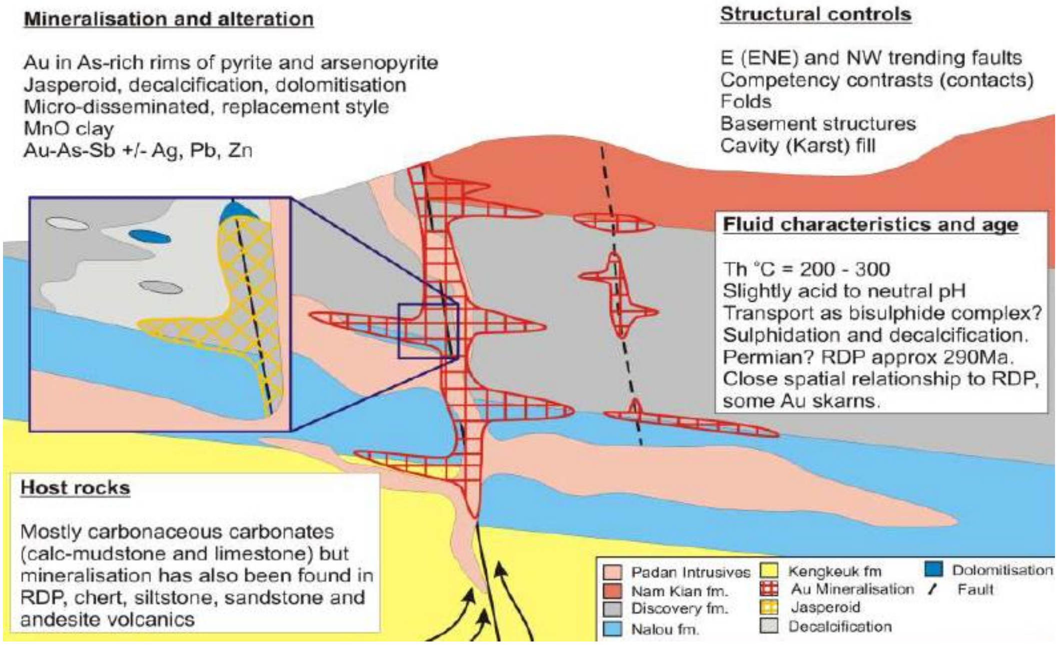

Figure 1. 6 Genetic model of gold mineralization at the SMD

1.4. Gold production; a global perspective

Indeed, Laos has been recognized as one of the resource-rich countries in Asia due to the identification of over 570 mineral deposits, which include valuable resources like gold, copper, zinc, and lead. These mineral deposits hold significant economic potential for the country (Kyophilvong, 2009). Therefore, Laos can be considered a resource-rich country, especially in terms of mineral resources. With estimated reserves of 500 tons of gold, Laos holds substantial potential in the gold mining industry. Gold is a valuable resource, and its extraction and export can make a significant contribution to the country's economy. Additionally, Laos is believed to have approximately 8 million tons of copper reserves. Copper is a vital industrial metal used in various applications, including electronics and construction. Exploiting this resource can lead to increased revenue and employment opportunities. Furthermore, Laos also produces zinc, with an estimated 2 million tons of zinc reserves. Zinc is crucial in industries such as galvanization, used to protect steel from corrosion, and it finds applications in the production of batteries, alloys, and more (Ngangnouvong, 2019). The Figure 1.7 shows the potential of mineral resource in Laos.

Figure 1. 7 The overview of gold copper and zinc production

The composition of Laos' export products is depicted in Figure 1.8, and it reveals an interesting distribution. Notably, mineral and mineral products stand out as the leading export category, representing approximately 52% of the country's total exports. This highlights Laos' significant mineral resources, including gold, copper, and zinc, which play a crucial role in its international trade.

Following closely behind, other industries and handicrafts contribute to the export sector, accounting for around 20% of total exports. These diverse industries showcase the nation's craftsmanship and manufacturing capabilities on the global stage. The export landscape also includes electricity, making up 13% of total exports. Laos has been increasingly harnessing its hydropower potential, and the export of electricity has become a notable source of revenue for the country. Agricultural products and live animals contribute about 10% to the export portfolio. This reflects the importance of agriculture in the Laotian economy, with products like rice, coffee, and rubber finding their way into international markets. Wood and wood products constitute another 4% of exports, emphasizing the presence of forestry resources in Laos. Finally, various other categories collectively make up less than 4% of the total export composition. The majority of Laos' mineral production, approximately 98%, is exported to

China, with the remaining 2% being shipped to Vietnam, Taipei, and Thailand as it is illustrated in Figure 1.9.

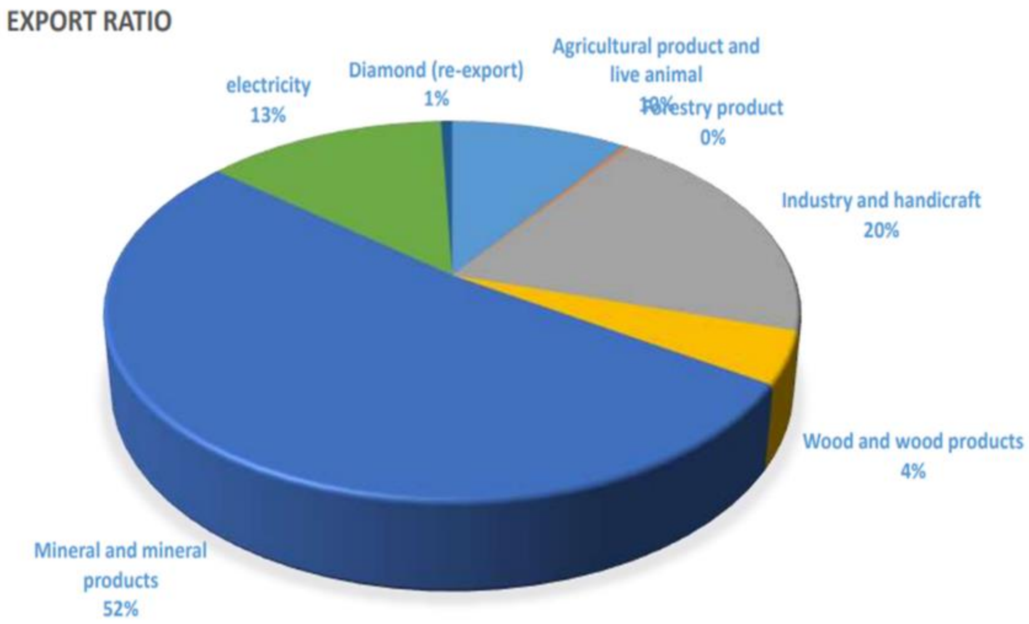

Figure 1. 8 The composition of export product in Laos

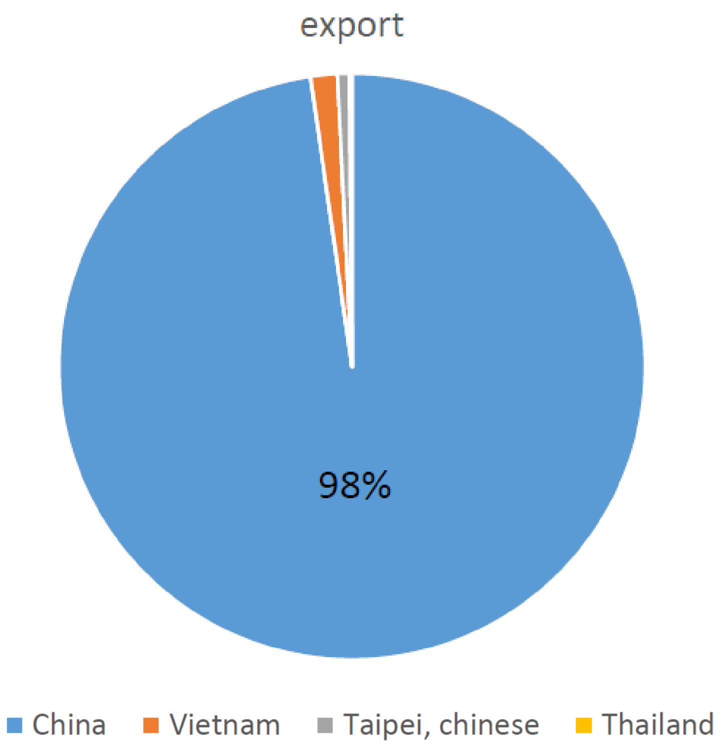

Figure 1. 9 The mineral export destination from Laos

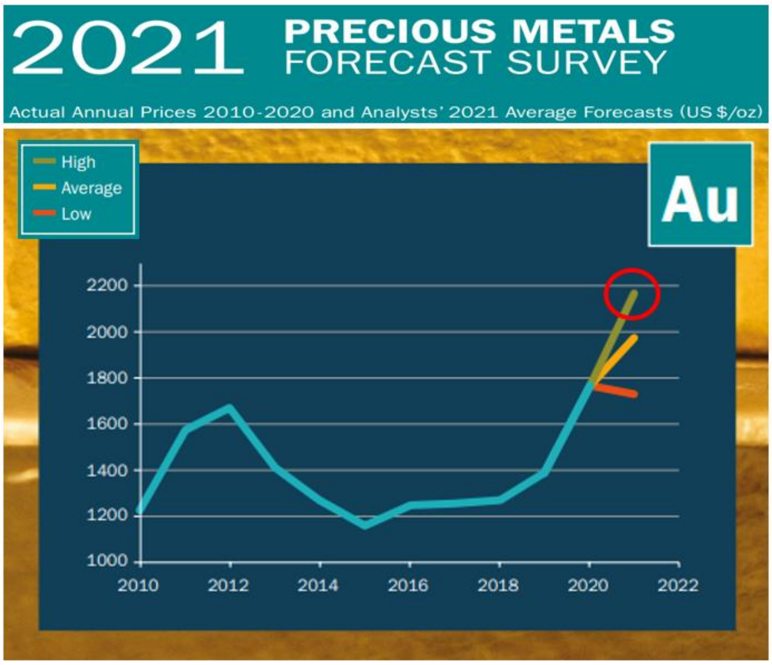

Figure 1. 10 The actual annual gold prices 2010 – 2020

Based on the information presented in Figure 1.10, it is evident that the price of gold exhibited various trends over the years. In 2012, the gold price saw a significant increase, reaching approximately 1,620 USD per ounce. Subsequently, the price experienced a downward trend, though with minor fluctuations, until 2018. However, starting in 2018 and continuing through 2022, there was a notable upward trajectory, culminating in a price of around 2,000 USD per ounce, with an average price hovering at approximately 1,900 USD per ounce. This pattern suggests a positive tendency for gold prices in the coming years. Given this scenario, it can be inferred that the prevailing gold price trends could potentially favor investors looking to engage in gold mining operations.

1.5. Deposit geology in Sepon Gold Mine

The geology section draws from the research of (Bouttathep, 2013; Cromie et al., 2006; Smith et al., 2005). In the Sepon vicinity, the regional geological setting is characterized by Devonian to Carboniferous-aged sediments, including continental fluvial and a range from shallow to deep marine deposits within a half-graben basin. Covering a 40-kilometer stretch at Sepon, there are six identified mineralized hydrothermal systems. These systems exhibit various mineralization styles, including porphyry Mo-Cu, Cu-Mo-Au skarn, Cu-Au carbonate replacement, and sediment-hosted Au.

The stratigraphic column in the Discovery Deeps area consists of the following formations:

- Nam Kian Formation (primarily calcareous shale (CSH)/chert)

- Discovery Formation (primarily calcareous shale CSH)
- Nalou Formation (primarily dolomite)
- Kengkeuk Formation (primarily shale/siltstone/dolomite)
- Vang Ngang Formation (primarily dolomitic shale)
- Nampa Formation
- Houay Formation
- Payee Formation

These formations make up the stratigraphic column in the Discovery Deeps area, providing a geological framework for understanding the subsurface geology and potential mineralization as it shown in Figure 1.11. In this specific study, the formations of primary relevance are located between the Nam Kian Formation and the Vang Ngang Formation. Among these formations, the Discovery, Nalou, and Kengkeuk Formations hold the highest significance, as they are central to the study's geological investigation and analysis.

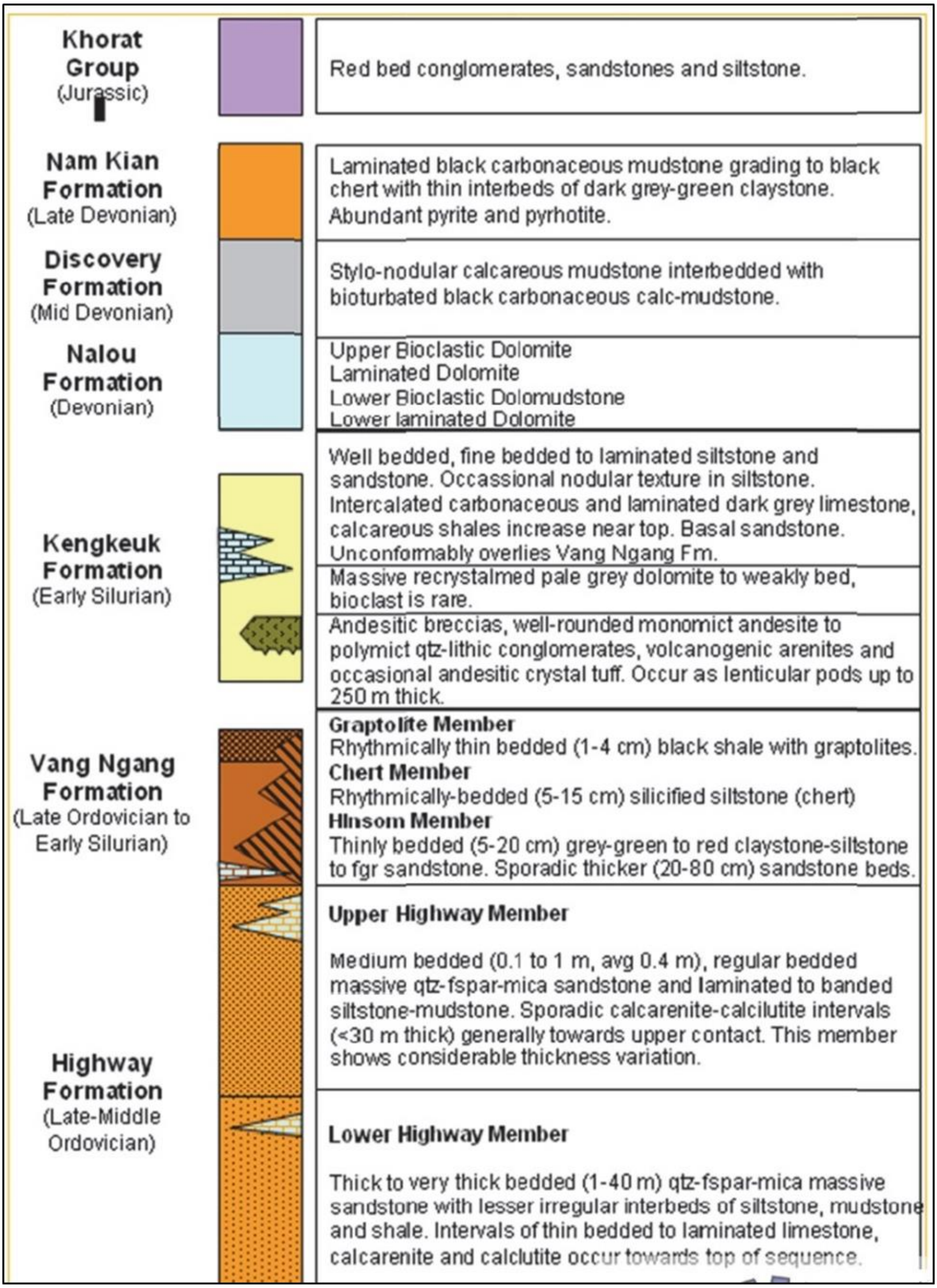

Figure 1. 11 Sepon Stratigraphic Column (Bouttathep, 2013)

1.6. The characteristic of orebody and geological features

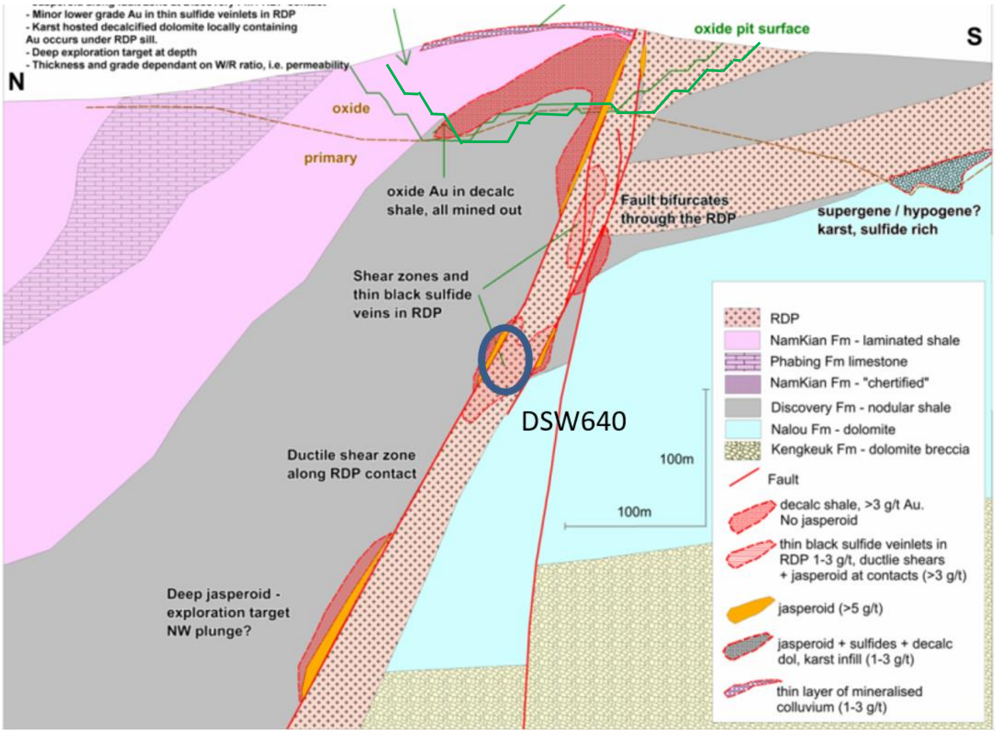

Figure 1. 12 The geological feature and orebody

Based on the information provided in Figure 1.12, we can gain valuable insights into both the geological composition and the nature of the orebody. This cross-sectional view offers a comprehensive overview of the mining operation. The geological formation in this region encompasses rhyodacite porphyry, shale, limestone, and dolomite breccia. Notably, the orebody itself consists of jasperoid, distinguished by a grade surpassing 5 grams per ton (g/t) of the desired material.

It's essential to highlight that mining activities have been discontinued at the surface, clearly indicated by the green line on the diagram. This cessation can be primarily attributed to the escalating stripping ratio, which has made further surface mining economically unviable. Consequently, there is a well-defined plan to transition from surface mining to the more economically sustainable approach of underground mining. Given the dip of the orebody, it becomes evident that underground open stope mining presents itself as a highly feasible option. This method allows for efficient extraction at various depths, with the orebody extending over 350 meters below the surface. Moreover, the orebody boasts an impressive width, ranging from 5 meters to 20 meters, providing a substantial area for extraction.

1.7. Classification of mining method

In the research area, a variety of mining methods are employed, including the open stope method, room and pillar method, shrinkage stoping method, cut and fill method, and sub-level stoping method. However, when all extraction activities occur beneath the surface, it is classified as an underground mine. Underground mining methods are typically chosen when the depth of the deposit and/or the waste-to-ore ratio (stripping ratio) make surface operations impractical, shape of vein and geological condition of ore and surrounding rock mass.

Once the economic feasibility of underground mining has been established, the most suitable mining methods must be carefully selected. This selection process takes into account a range of factors, including:

Spatial and geometric characteristics: These factors pertain to the natural attributes of the deposit, including its shape, size, thickness, plunge, and depth. These characteristics play a critical role in determining which mining method is most appropriate. For instance, a deposit with a unique shape may favor the use of cut and fill mining, while a vein with specific plunge characteristics might be better suited for sub-level stoping.

Strength of surrounding rock: It's crucial to assess the strength of the hanging wall, footwall, and ore body. This information helps in determining the level of support required for safe mining operations.

Economic value and ore grade distribution: Understanding the economic value of the ore and the distribution of ore grades within the deposit is essential. This information influences decisions regarding mining method selection and ore extraction strategy.

The choice of underground mining methods is primarily guided by the geological and spatial setting of the deposit. Candidate methods are then evaluated based on factors such as operational and capital costs, production rates, availability of labor and equipment, and environmental considerations. The method that offers the most reasonable and optimized combination of safety, economics, and ore recovery is selected.

For gold mine deposit, the following underground mining systems should be considered:

- The cut and fill method
- The room and pillar method
- The open stoping method
- The sub-level stoping method

- The shrinkage stoping method

It's worth noting that some mining methods are classified as unsupported methods, meaning they primarily rely on the natural competence of the rock walls and pillars for support, with minimal artificial support systems. Examples of unsupported methods include:

- The room and pillar mining method
- The shrinkage stoping method
- The sub-level stoping method

1.7.1. Basic room and pillar mining method

These methods are chosen when the geological conditions and structural stability of the deposit allow for such practices without compromising safety. Figures 1.13 illustrate different mining methods. Room and pillar mining is employed for the extraction of flat-dipping and tabular deposits (Hamrin, 1980). On the other hand, shrinkage and sub-level stoping techniques areapplied to vertical or steeply inclined ore bodies.

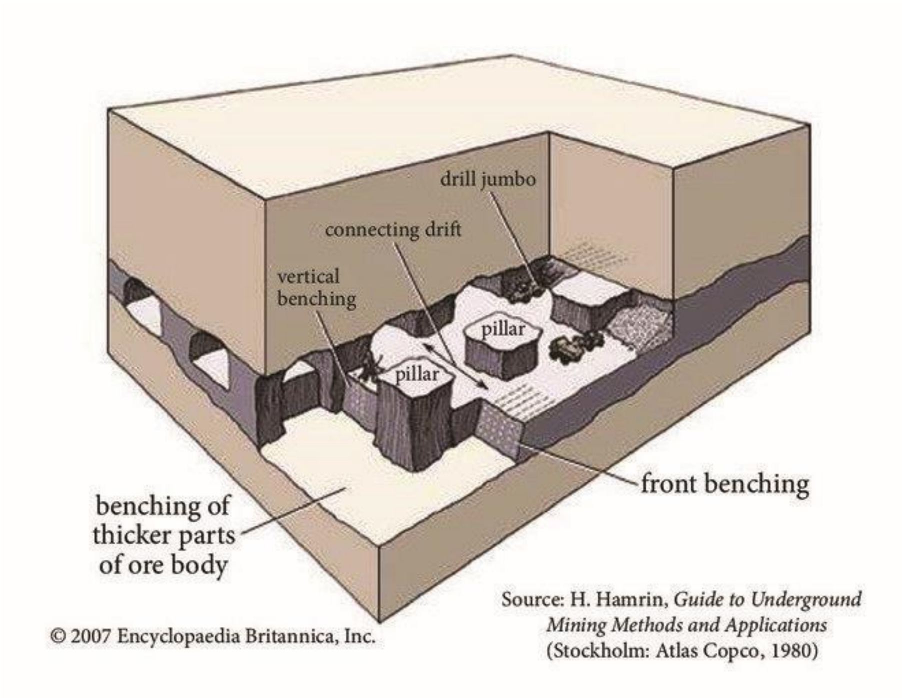

Figure 1. 13 Basic room and pillar mining method (Hamrin, 1980)

Room-and-pillar mining is a method designed for extracting resources from flat-bedded deposits of limited thickness, such as copper shale, coal, salt, potash, limestone, and dolomite. In this approach, open stopes are created while leaving supporting pillars to maintain the integrity of the roof. Miners aim to minimize pillar size to maximize ore recovery. Rock bolts are often used to reinforce the surrounding rock strata. The arrangement of rooms and pillars is typically organized in regular patterns, with pillars shaped as circular or square cross-sections or elongated walls separating the rooms. It's important to note that minerals contained within the pillars cannot be recovered and are not considered part of the mine's ore reserves. Geological conditions can lead to variations in room-and-pillar mining, and three common variations are outlined below. Classic room-and-pillar mining, as depicted in Figure 1.13, is suitable for flat deposits with moderate-to-thick beds and inclined deposits with thicker beds. It involves creating large open stopes where trackless machines can operate on a level floor. For ore bodies with significant vertical heights, mining occurs in horizontal slices, starting from the top and progressing downward in steps

1.7.2. Post room and pillar mining method

Post room-and-pillar mining, as depicted in Figure 1.14, is specifically employed for ore bodies with incline angles ranging from 20° to 55°. In these mining operations, vertical heights are substantial, and the mined-out areas are typically filled with material. This filling not only stabilizes the surrounding rock mass but also provides a stable work platform for mining the next ore slice.

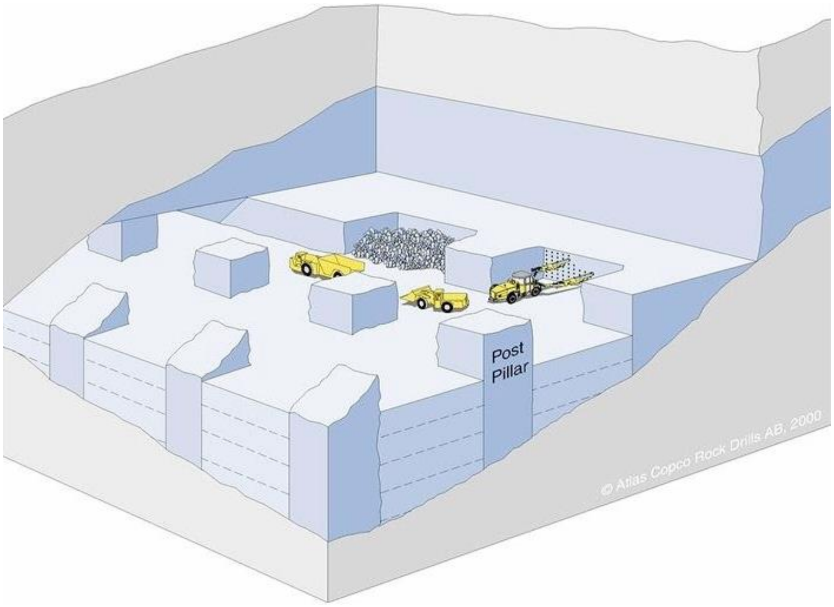

Figure 1. 14 Post room and pillar mining method (Atlas Copco Rock Drills AB,2000)

Post Room-and-Pillar Mining, also known as 'post-pillar' mining, is a hybrid mining method that combines aspects of both room-and-pillar and cut-and-fill stoping techniques. In this approach, ore extraction occurs in horizontal slices, starting from the bottom and progressing upwards. Pillars are intentionally left within the stope to provide roof support. Once a stope has been mined out, it is filled with tailings through hydraulic means, and the subsequent ore slice is excavated using machinery operating from the filled surface. These pillars extend through multiple layers of fill. The use of sandfill offers flexibility in adapting the stope layout to accommodate variations in rock conditions and ore boundaries. Both backfill and sandfill significantly enhance the pillar’s support capacity, allowing for a higher rate of ore recovery compared to traditional room-and-pillar mining. Post-pillar mining combines the advantages of cut-and-fill mining, such as the ability to work on level surfaces, with the spacious stopes characteristic of room-and-pillar mining. This method’s easy access to multiple production points is conducive to the efficient use of mechanized equipment.

1.7.3. Step-room mining of incline orebody

Step Room-and-Pillar Mining is a specialized variation tailored for the efficient utilization of trackless equipment within inclined ore bodies. While its applicability may vary, this method is particularly suited for tabular deposits with thicknesses ranging from 2 to 5 meters and dips spanning between 15° to 30°. The hallmark of this method is its unique layout, where stopes and haulage ways are organized along the dip of the ore body, resembling a polar coordinate system. By strategically orienting stopes at specific angles across the dip, stope floors are configured to facilitate smooth travel for trackless vehicles. Transport routes intersect in the opposite direction, allowing for roadway access to stopes and the transportation of blasted ore to the shaft.

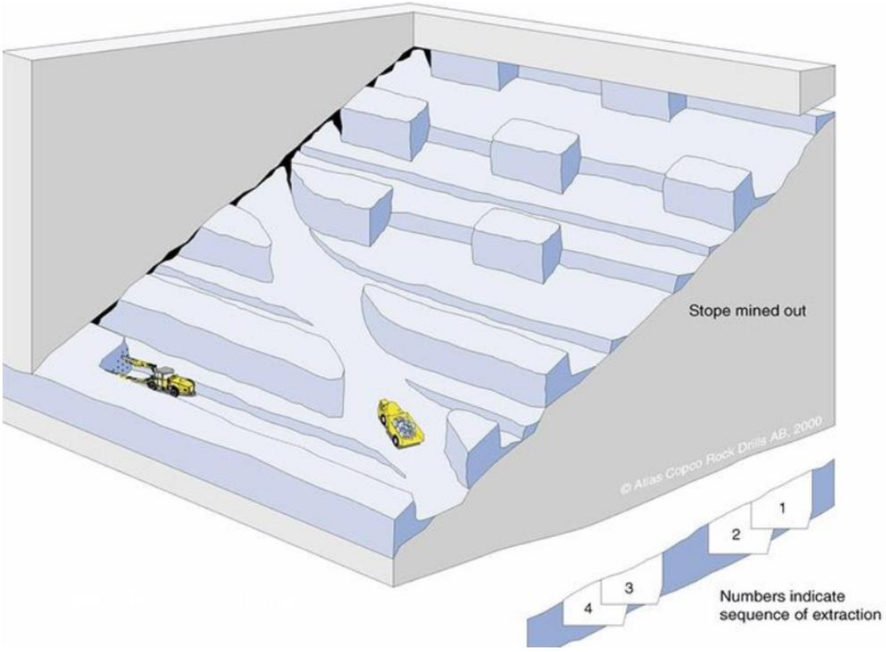

Figure 1. 15 Step-room mining of incline orebody (Atlas Copco Rock Drills AB,2000)

Key components of step room-and-pillar mining include a network of paralleh l transport drifts that traverse the ore body in predetermined directions. These drifts maintain graded floors suitable for selected trucks. Stopes are then excavated from these transport drifts, branching out at predefined step-room angles. The stope is advanced forward in a manner akin to drifting until it connects with the next parallel transport drive. The subsequent step involves excavating a similar drift or side slash one step down-dip and adjacent to the first drive. This process repeats until the span of the roof becomes almost too wide to remain stable. At this point, an elongated strip parallel to the stopes is left in place as a pillar. This method continues with the excavation of the next stope using the same procedure, progressing downward step by step. Figure 1.15 provides a visual representation of the extraction sequence, with numbers indicating the order of extraction.

1.7.4. Mining method in a narrow vein with steep dip

In vein mines, Figures 1.16, mineral deposit dimensions can vary widely, ranging from large, extensive formations spanning several square kilometers to narrow 0.5 m-wide quartz veins containing valuable minerals like gold at a concentration of 20 g/t. Miners aim to extract valuable minerals while preserving the surrounding waste rock in the hanging wall and footwall. In thicker deposits, machines operate efficiently within the ore body. However, in narrower mineralized zones, machines may be too wide, resulting in unnecessary waste production that dilutes the ore. An alternative is manual labor, but this approach is costly, inefficient, and finding labor willing to work with hand-held rock drills and physical effort can be challenging.

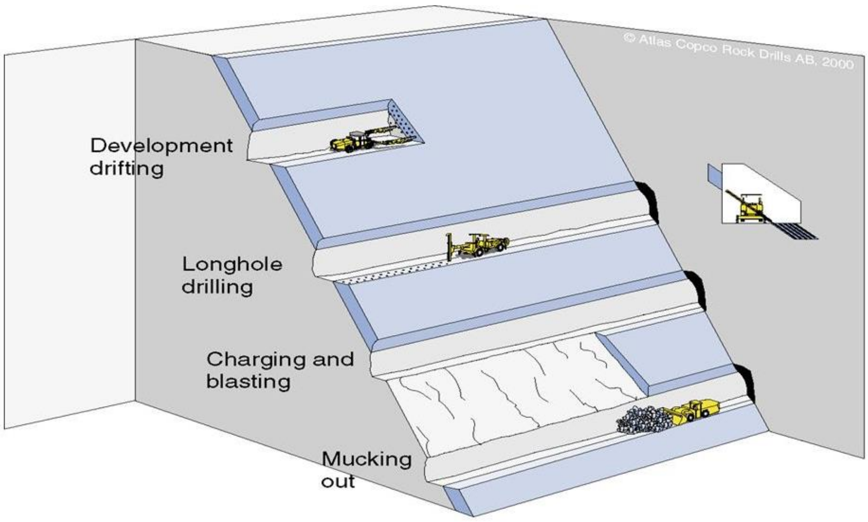

Figure 1. 16 Mining method in a narrow vein with steep dip (Atlas Copco Rock Drills AB,2000)

1.7.5. Shrinkage stoping, avertical stoping method

In shrinkage stoping, as depicted in Figure 1.17, ore is extracted in horizontal layers, commencing from the lowest point of the stope and progressing upward. A portion of the fragmented ore remains within the excavated stope, serving as a stable platform for mining the ore situated above and for supporting the stope walls. Due to blasting operations, the volume of rock expands by approximately 50%. Consequently, to maintain adequate clearance between the top of the blasted ore and the stope's roof, 40% of the blasted ore needs to be continuously removed during mining. Once the stope has reached the upper boundary of the planned mining area, mining activities cease, and the remaining 60% of the ore can then be recovered.

In sublevel open stoping, as illustrated in Figures 1.17 and, ore extraction takes place in open stopes that are typically backfilled once the mining is completed. These stopes are often quite substantial, especially in their vertical extent. The ore body is subdivided into distinct stopes, and areas between these stopes are set aside for the creation of pillars, which serve to support the overlying hanging wall. These pillars are typically designed as vertical columns that span the width of the ore body.

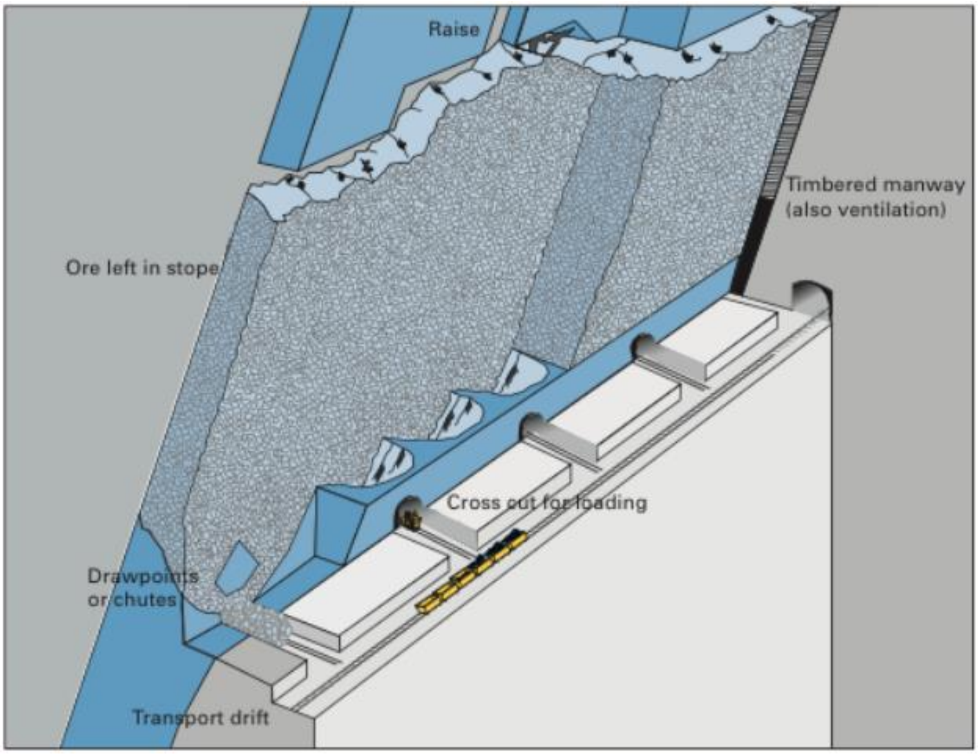

Figure 1. 17 Shrinkage stoping, avertical stoping method (Atlas Copco Underground Methods)

1.7.6. Sublevel open stoping

Horizontal sections of ore, known as crown pillars, are also deliberately left intact to provide support for mining activities conducted above the active stopes. The objective is to maximize mining efficiency by creating the largest possible stopes. However, it's crucial to consider the stability of the rock mass as a limiting factor when determining the sizes of both stopes and pillars. Sublevel stoping is the preferred method for extracting mineral deposits with specific characteristics:

- Steep dip: The footwall should have an inclination greater than the angle of repose.
- Stable rock mass: Both the hanging wall and the footwall need to be structurally stable.
- Competent ore and host rock: The ore and surrounding rock should be strong and capable of withstanding mining operations.
- Regular ore boundaries: Well-defined ore boundaries are essential for efficient extraction.

Sublevel drifts are excavated within the ore body between main levels to facilitate longhole drilling, which is conducted strategically to create blast patterns. The drill pattern specifies the precise locations, depths, and angles of each blast hole, demanding precision for a successful blast.

Drawpoints, located below the stope floor, are prepared for safe material removal using Load-Haul-Dump (LHD) vehicles, which may be combined with trucks or rail cars for longer-distance transport. Various layouts for undercut drawpoints are employed, and the trough-shaped stope floor is typically accessed via loading drifts at regular intervals. Developing this network of drifts and drawpoints beneath the stope is a labor-intensive and expensive process. An alternative layout, gaining popularity, integrates the loading level with the undercut. In this setup, mucking out is directly performed on the stope floor inside the open stope, with LHDs operating within the stope. For safety reasons, LHDs are operated via radio control by an operator stationed inside the access drift.

Sublevel stoping necessitates the presence of well-defined stope shapes and ore boundaries. Within the drill pattern, everything within the designated area qualifies as ore. In larger ore bodies, the region between the hanging wall and the footwall is divided into modules along the strike and extracted as primary and secondary stopes, as shown in Figure 1.18.

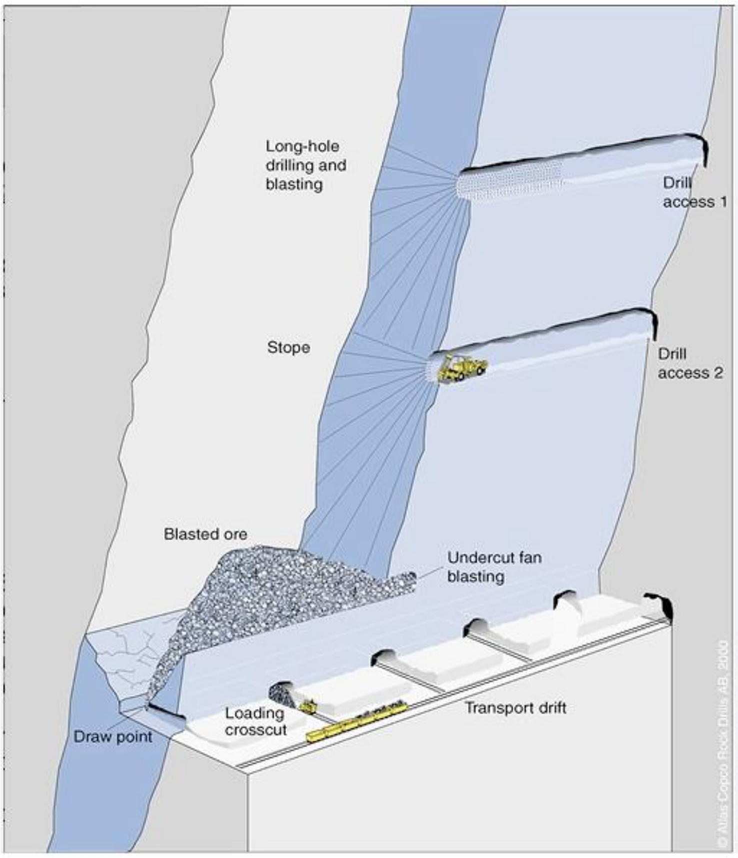

Figure 1. 18 Sublevel open stoping (Atlas Copco Rock Drills AB, 2000)

1.7.7. Bighole stoping method

Bighole stoping, as depicted in Figures 1.19, represents a significant scaling up of the sublevel open stoping mining method. This approach involves the use of longer blastholes with larger diameters, typically ranging from 140 to 165 mm. To create these holes, the in-the-hole (ITH) drilling technique is commonly employed. These blastholes can reach depths of up to 100 meters, which is double the depth achievable with conventional tophammer drilling rigs. The blast patterns utilized in bighole stoping are akin to those employed in sublevel open stoping.

In this method, a single 140-mm-diameter blasthole is capable of breaking a rock slice that is 4 meters thick, maintaining a 6-meter spacing from the toe. The distinct advantage of bighole stoping in comparison to sublevel stoping lies in its scalability. The ITH-drilled holes tend to be straight, enabling precision in drilling. Consequently, this accuracy can be harnessed to extend vertical spacings between sublevels. For instance, whereas sublevel open stoping typically has vertical spacings of 40 meters, bighole stoping allows for more generous 60-meter vertical spacings.

However, it's important to acknowledge that bighole stoping, due to its scale, does introduce certain risks related to potential damage to the surrounding rock structures. These risks necessitate careful consideration and management to ensure safe and effective mining operations when employing this method.

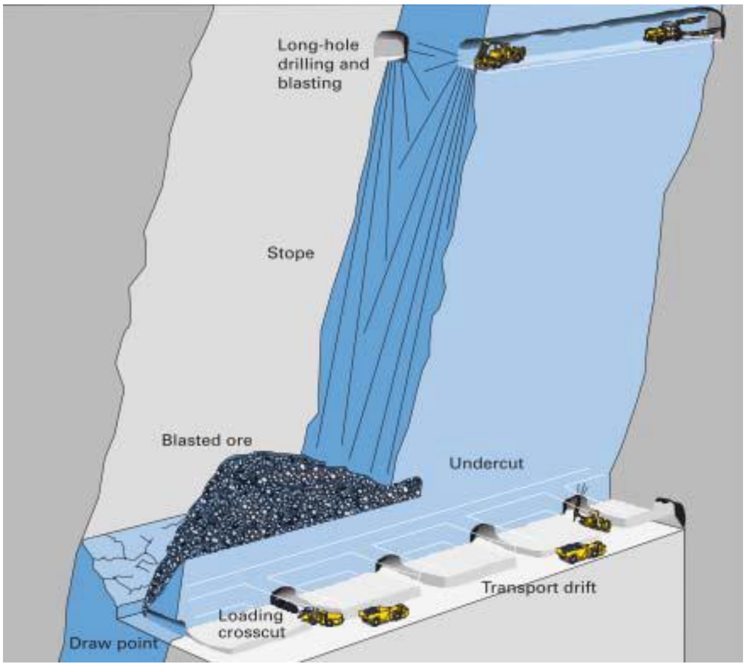

Figure 1. 19 Bighole stoping method (Atlas Copco Rock Drills AB, 2000)

However, the mining methods mentioned above are significant when considering the appropriate approach for real-underground mining conditions. In order to ensure the stability of the open stope and make it stable, the cut and fill mining method needs to be carefully evaluated. There are two types of cut and fill methods: the underhand cut and the overhand cut. It's crucial to select the most suitable method based on the characteristics of the orebody and the rock mass.

1.7.8. Underhand cut and fill mining method

The underhand cut and fill mining method is commonly employed in weak rock mass conditions, as noted by (Brechtel et al., 2001; Hustrulid et al., 2001; Kump et al., 2001). In this approach, mining begins with the uppermost slice and progresses downward shown in Figure 1.20. Once a slice is fully mined out, backfill material is introduced, and the subsequent slice is mined beneath it. The backfill material must possess sufficient strength to stabilize the surrounding country rock and protect mining operations at lower levels.

Among the various types of backfilling materials detailed by (Hartman et al., 1992) cemented hydraulic fill (CHF) is frequently utilized in this method. Cemented hydraulic fill offers several advantages, including the provision of the strongest possible fill compared to other alternatives, the reduction of rock bursting issues in deep mines, decreased dilution, and improved grade control. However, it does entail higher initial costs for the preparation plant and additional expenses due to the inclusion of cement. For instance, an application of cemented hydraulic fill at the Lucky Friday Mine in the USA cost approximately $4.52 US per ton of ore mined (Peppin et al., 2001).

While such high costs may pose a burden for companies mining low-grade deposits, they are more manageable for those operating high-grade deposits. In the case of the Sepon mine in Laos, one of the gold mining companies is considering the use of this method to extract ore with an average grade of 5g/t.

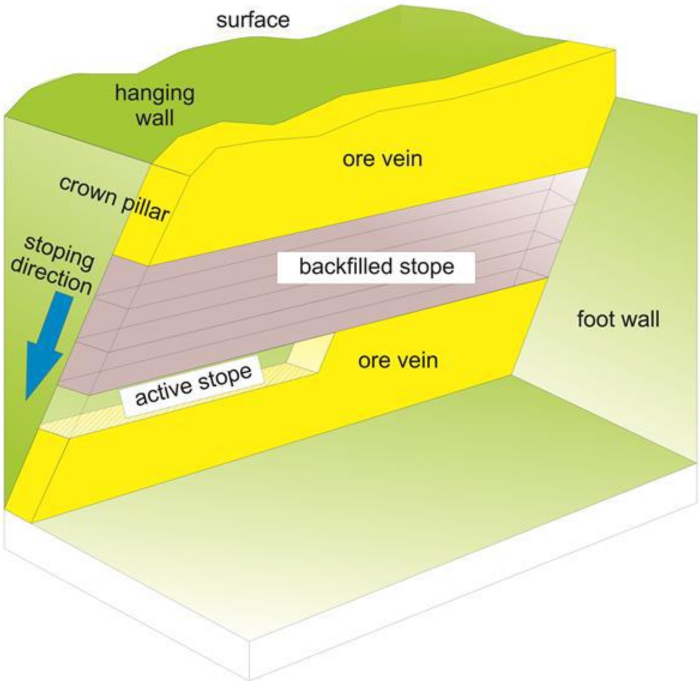

Figure 1. 20 Schematic of underhand cut and fill underground mining method

1.7.9. Overhand cut and fill mining method

When assessing the quality of the rock mass surrounding a deposit, the choice between the overhand cut and fill mining method and the underhand mining method depends on the rock conditions. Generally, if the rock mass is of good quality, the overhand cut and fill method is preferred. However, it's worth noting that applying the overhand cut and fill method in weak rock conditions can lead to a higher requirement for rock support, as observed in the study by Kump and Arnold (Kump et al., 2001). In such cases, the cost of rock support in weak rock may exceed the cost of installing cemented hydraulic fill.

In contrast to underhand stoping, where mining begins from the bottom level of the prospect, overhand stoping involves starting from the top and working downward. After each slice is fully mined, backfill material is introduced not only to provide additional support for the surrounding country rock but also to serve as a base for workers to operate on the upper levels, as depicted in Figure 1.21. Therefore, the strength of the filling material is not the primary consideration in selecting the filling type. Various fill types, including waste rock, pneumatic fill, or hydraulic fill, can be chosen based on factors such as availability, transportation cost, curing time, and others, as outlined in (Hartman et al., 1992). As a result, the overhand variant often offers cost advantages compared to the underhand method.

In the case of the two underground gold mines at Sepon Underground Gold Mine, both overhand and underhand variants can be employed in their operations. They use hydraulic backfill with an average cost of $1.5-1.6 per ton. The average gold grade at the Sepon gold mine is 5 g/t, which is considered economically viable for underground mining operations. In this study, considering the orebody's characteristics such as vein shape and rock mass properties, which exhibit a commendable GSI of 62, the overhand cut appears suitable. This method is particularly fitting when the strength of the ore vein is notably higher compared to the overhand cut.

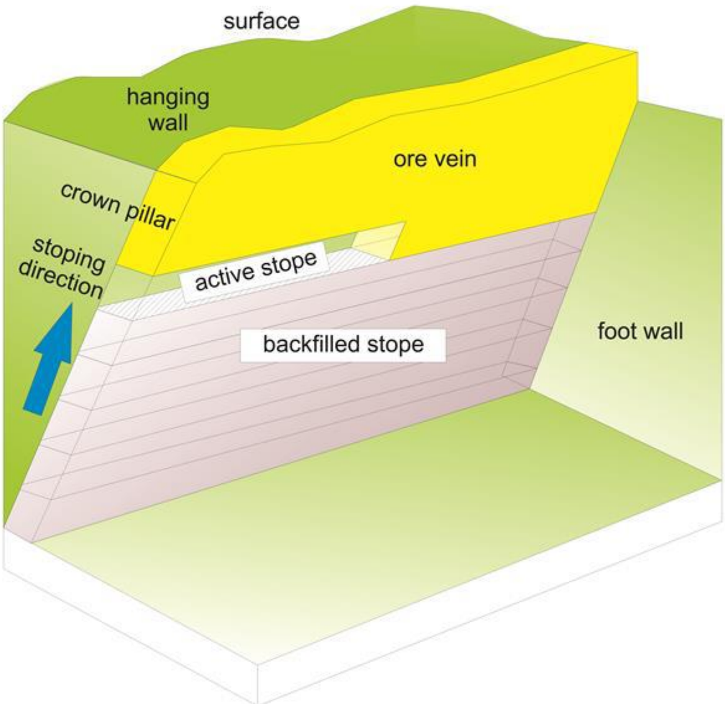

Figure 1. 21 Schematic of overhand cut and fill underground mining method

1.8. Surface subsidence related to underground mining

Numerous case studies worldwide have documented events in underground mining, both during active mining operations and after prolonged operation. A noteworthy example is the San Manuel Copper Mine in Southeastern Arizona, situated approximately 3 miles WSW of Mammoth within the San Pedro Valley. This mine serves as an illustrative case of ground subsidence associated with block cave mining. In the instance of the San Manuel Copper Mine, block caving activities led to ground subsidence, causing approximately 0.20 square miles of surface rock to collapse into the mine as shown in the Figure 1.22.

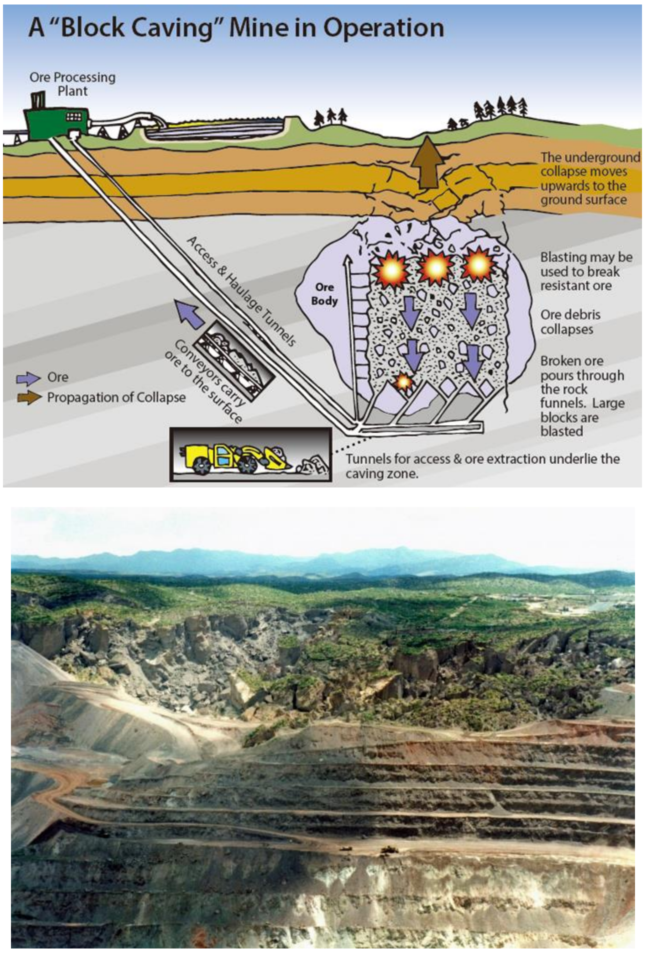

Figure 1. 22 Ground subsidence caused by block caving

The Telfer underground sub-level cave (SLC) operations are situated beneath the western wall of the main dome open pit at the Telfer Gold Mine in Australia, at depths ranging from approximately 600 to 1,000 m. The Telfer SLC commenced caving operations in 2006 and successfully broke through to the surface in 2009, resulting in the creation of a significant subsidence zone (Nicoll et al., 2017). Over time, this subsidence zone has continued to expand and evolve, with surface deformations occurring at a monthly rate ranging from 500 to 2,000 mm. The rate of surface deformation is directly linked to the pace of underground mining activities within the SLC operation as it illustrated in Figure 1.23.

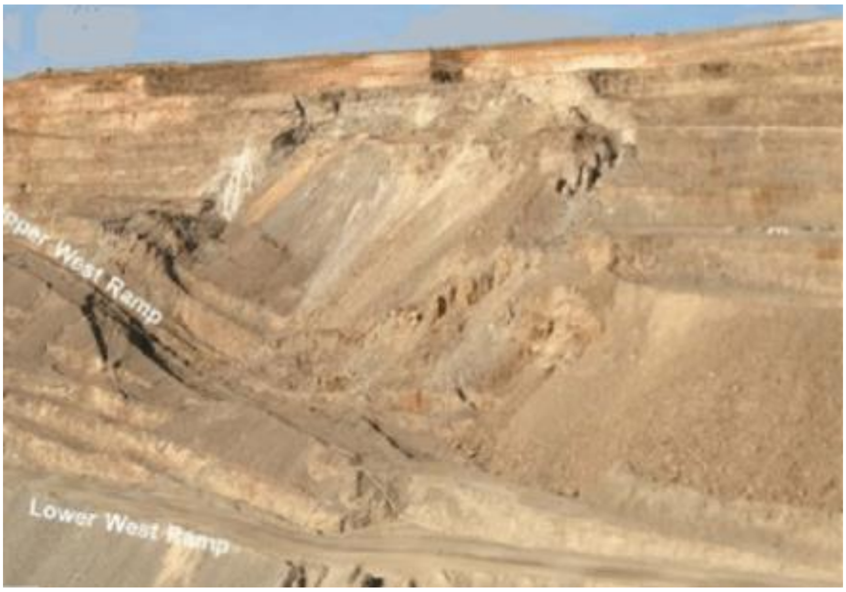

Figure 1. 23 Surface subsidence caused by sub-level cave (SLC)

In the context of this situation, the Sepon underground mining project has recently initiated its underground operations. Some sections of the open stope are situated in close proximity to the surface, approximately 35 meters above the crown pillar. Maintaining stability in these areas presents a significant challenge. The success of this endeavor depends on several critical factors, including the geological characteristics of the site, the condition of the rock mass, as well as the presence of faults and joints.

1.9. Dissertation Objectives

Based on the previous section's perspective, here are the revised objectives of the dissertation:

1. To analyze stress conditions in the vicinity of stope and crown pillar areas in shallow-depth mines under various conditions, including stoping direction, geological factors, vein geometry, and stress ratios.
2. To assess the effectiveness of conventional rock support systems or backfill techniques as mitigation measures for stope instability in diverse mine settings.
3. To propose alternative mitigation methods for addressing stope instability that are environmentally suitable for application in protected ground surface conditions.

1.10. Outline of the dissertation

To obtain objectives of dissertation, the five chapters are presented in this study. Following the first chapter, the rest of the chapters will be described as follow:

Chapter 2: This chapter presents the context and plan of the mining project, elucidating the methodology employed. The primary focus lies in analyzing the stability of mined-out areas, which is based on the mine production history. Furthermore, it outlines the main research objective. In this study, the overhand cut method is chosen due to the favorable strength characteristics of the orebody. Moreover, the shape of the vein is conducive to employing the open stope method.

Chapter 3: This chapter delves into the stress conditions within the stope and crown pillar areas in the context of open stope mining. The investigation places specific emphasis on stress variations attributed to different stoping directions, stope width, vein angle, geological factors like GSI, vein geometries, and stress ratios. To achieve this, a comparison between the overhand cut and underhand cut methods is conducted. The results indicate that the underhand cut method yielded slightly better outcomes. However, considering the orebody's strength properties, the overhand cut appears more suitable. The insights derived from this analysis will establish a foundational understanding crucial for evaluating the effectiveness of countermeasure methods, a topic explored in subsequent chapters.

Chapter 4: This chapter introduces the utilization of sill pillars as a strategic countermeasure to improve stope stability and optimize crown pillar recovery in an inclined orebody. The application of sill pillars will be simulated under various conditions identified in the previous chapter where suboptimal crown pillar support was observed. The rationale behind enhancing stope and crown pillar stability will be thoroughly explained in this chapter. Additionally, we explore alternative countermeasures aimed at improving the stability of open stopes situated at shallow depths. These countermeasures involve the use of backfill material. We initiate the discussion by outlining the process of determining material properties critical for our numerical analysis. Throughout this chapter, we assess the effectiveness of these support applications and deliberate on strategies to mitigate their impact on surface ground subsidence. Our objective is not only to enhance stope stability but also to minimize potential surface disturbances resulting from these measures.

Chapter 5: It is a summary of the conclusions from each chapter to form a general conclusion for the dissertation.

1.11. Reference

Bakhtavar, E., Shahriar, K., & Mirhassani, A. (2012). Optimization of the transition from open-pit to underground operation in combined mining using (0-1) integer programming. *Journal of the Southern African Institute of Mining and Metallurgy*, *112*(12), 1059–1064.

Bakhtavar, E., Shahriar, K., & Oraee, K. (2009a). Mining method selection and optimization of transition from open pit to underground in combined mining. *Archives of Mining*

Sciences, *54*(3), 481–493.

Bakhtavar, E., Shahriar, K., & Oraee, K. (2009b). Transition from open-pit to underground as a new optimization challenge in mining engineering. *Journal of Mining Science*, *45*(5), 485–494. https://doi.org/10.1007/s10913-009-0060-3

Bouttathep, B. (2013). Geology of the Sepon copper and gold deposits, Laos. *Proceedings of 2nd Lao–Thai Technical Conference on Geology and Mineral Resources. Department of Geology and Minerals, Lao PDR*, 164–187.

Brechtel, C. E., Struble, G. R., & Guenther, B. (2001). Underhand cut-and-fill mining at the Murray Mine, Jerritt Canyon Joint Venture. *Underground Mining Methods: Engineering Fundamentals and International Case Studies. Society of Mining, Metallurgy and Exploration, 8307 Shaffer Parkway, Littleton, CO 80127, USA, 2001.*, 333–337.

Cannell, J., & Smith, S. (2008). High-grade supergene enriched and exotic copper deposits in the Sepon Mineral District, Lao PDR. *Proceedings of PACRIM Congress*, 355–361.

Chung, J., Asad, M. W. A., & Topal, E. (2022). Timing of transition from open-pit to underground mining: A simultaneous optimisation model for open-pit and underground mine production schedules. *Resources Policy*, *77*(March), 102632. https://doi.org/10.1016/j.resourpol.2022.102632

Cromie, P. . (2010). Geological setting, geochemistry and genesis of the Sepon gold and copper deposits, Laos. *Unpublished PhD Thesis, ARC Centre of Excellence in Ore Deposits (CODES), University of Tasmania, Hobart, Austalia, 395p.*

Cromie, P. W., Smith, S. ., & Codes, U. (2006). New insights through LA-ICP-MS and sulphur isotope investigations into the occurrence of gold in the Sepon gold deposits, Laos. *ASEG Extended Abstracts*, *2006*(1), 1–3. https://doi.org/10.1071/aseg2006ab028

Eberhardt, E., Woo, K., Stead, D., & Elmo, D. (2007). Transition from surface to underground mining : Integrated mapping , monitoring and modeling data to better understand complex rock mass interaction. *ISRM Congress 2015 Proceedings - Int'l Symposium on Rock Mechanics*, *I*(June 2016).

Hamrin, H. (1980). *Guide to underground mining: methods and applications*. Atlas Copco.

Hartman, H. L., Britton, S. G., Mutmansky, J. M., Gentry, D. W., Schlitt, W. J., Karmis, M., & Singh, M. M. (1992). *SME mining engineering handbook* (Vol. 2). Society for Mining, Metallurgy, and Exploration Denver.

Hustrulid, W. A., Hustrulid, W. A., & Bullock, R. L. (2001). *Underground mining methods: Engineering fundamentals and international case studies*. SME.

Hutchison, C. S. (1989). *Geological evolution of South-east Asia* (Vol. 13). Clarendon Press Oxford.

Kump, D., Arnold, T., & Hustrulid, W. (2001). Underhand cut-and-fill at the Barrick bullfrog mine. *Underground Mining Methods: Engineering Fundamentals and International Case Studies*, 345–350.

Kyophilvong, P. (2009). Mining sector in Laos. *Ide-Jetro*, *17 June 2006*, 69–100.

Lepvrier, C., Maluski, H., Van Vuong, N., Roques, D., Axente, V., & Rangin, C. (1997). Indosinian NW-trending shear zones within the Truong Son belt (Vietnam): 40Ar-39Ar Triassic ages and Cretaceous to Cenozoic overprints. *Tectonophysics*, *283*(1–4), 105–127. https://doi.org/10.1016/S0040-1951(97)00151-0

Loader, S. E. (1999). Supergene enrichment of the Khanong copper resource, Sepon project, Lao PDR. *PACRIM*, *99*, 263–270.

LXML. (1999). *Drill hole report, 1999, LXML, Unpublished company report.*

Metcalfe, I. (1998). Palaeozoic and Mesozoic geological evolution of the SE Asian region: multidisciplinary constraints and implications for biogeography. *Biogeography and Geological Evolution of Southeast Asia*, *January 1998*, 25–41.

Morris, D. G. (2006). Revision of the Stratigraphy of the Sepon Basin. In *ACT Exploration Consultants Pty Ltd, Unpublished company report for Oxiana Limited, p. 1-17.*

Ngangnouvong, I. (2019). Mining in Laos, economic growth, and price fluctuation. *United Nations Conference on Trade and Development*, *April 2019*. https://unctad.org/meetings/en/Presentation/MYEM2019_Itthilith_Ngangnouvong_15042019.pdf

Nicoll, S., Bar, N., & Du Plessis, P. (2017). Managing Risks on an Active Haul Road Adjacent to a Propagating Subsidence Zone at Telfer Gold Mine. *Procedia Engineering*, *191*, 172–178. https://doi.org/10.1016/j.proeng.2017.05.169

Olavarría, S., Adriasola, P., & Karzulovic, A. (2015). Transition from open pit to underground mining at chuquicamata, Antofagasta, Chile. *International Symposium of Stability of Rock Slopes in Open Pit Mining and Civil Engineering*, 421–434.

Peppin, C., Fudge, T., Hartman, K., Bayer, D., & DeVoe, T. (2001). Underhand cut-and-fill mining at the Lucky Friday Mine. *Underground Mining Methods, Engineering Fundamentals and International Case Studies*, 313–318.

Potvin, Y., & Hudyma, M. (2016). *Open Stope Mining in Canada OPEN STOPE MINING IN CANADA Yves Potvin and Marty Hudyma Australian Centre for Geomechanics*. *January 2000*.

Richards, J. P. (2003). Tectono-magmatic precursors for porphyry Cu-(Mo-Au) deposit formation. *Economic Geology*, *98*(8), 1515–1533. https://doi.org/10.2113/gsecongeo.98.8.1515

Seedorff, E., Dilles, J. H., Proffett, J. M., Einaudi, M. T., Zurcher, L., Stavast, W. J. A., Johnson, D. A., & Barton, M. D. (2005). Porphyry Deposits: Characteristics and Origin of Hypogene Features: Economic Geology 100th Anniversary Volume. *Economic Geology*, 251–298.

Sillitoe, R. H. (1972). A plate tectonic model for the origin of porphyry copper deposits. *Economic Geology*, *67*(2), 184–197.

Smith, S., Olberg, D., & Manini, T. (2005). The Sepon gold deposits, Laos: exploration, geology and comparison to Carlin-type gold deposits in the Great Basin. *Geological Society of Nevada Symposium, Reno, Nevada*, 899–915.

Soltani Khaboushan, A., Osanloo, M., & Esfahanipour, A. (2020). Optimization of open pit to underground transition depth: An idea for reducing waste rock contamination while maximizing economic benefits. *Journal of Cleaner Production*, *277*, 123530. https://doi.org/10.1016/j.jclepro.2020.123530

Sone, M., & Metcalfe, I. (2008). Parallel Tethyan sutures in mainland Southeast Asia: new insights for Palaeo-Tethys closure and implications for the Indosinian orogeny. *Comptes Rendus Geoscience*, *340*(2–3), 166–179.

CHAPTER 2
OVERVIEW OF THE RESEARCH AREA

2.1. Introduction

In the first chapter, it is discussed how copper and gold metals play an essential role in our daily lives. This chapter provides a concise overview of the historical background of the Sepon mines under investigation. Since its inception in 2003, (L.X.M.L) Sepon has successfully produced more than 1.1 million T of copper cathode and over 53 T of gold. In 2022, Sepon recorded a production of 6,600 T of copper and 6.7 T of gold. Looking ahead to 2023, our projected production stands at over 6 T of gold and 7,000 T of copper. L.X.M.L has significantly contributed to the Lao Government, providing more than US$1.7 billion in direct revenue through taxes, royalties, and dividends. The indirect benefits, including employment, training, community support, and local business development programs, have also made substantial contributions to social and economic development in the Lao PDR.

The Sepon mine deposit is a classic sedimentary-hosted rock deposit. As of 2023, Sepon has initiated underground gold mining operations, with an annual production exceeding 600,000 T of ore (Au) at a cutoff grade of 5g/T, which is deemed profitable. However, the current scenario presents challenges, as both the price of gold and operational costs have increased.

The mine's initial discovery dates back to 1998 when it was identified by C.R.A (now Rio Tinto). It has since maintained uninterrupted operations for over two decades, from 2003 to the present day. The mine holds great promise for metal production due to the abundance of high-grade ore. Initially, the mining method involved open-pit operations for both gold and copper. However, as the easily accessible shallow ore near the surface is exhausted, the shift to underground mining becomes imperative to ensure continued productivity. The primary objective of this chapter is to investigate the geological features and identify the challenges present in the underground environment. This investigation includes a detailed examination of the methodology and essential material properties such as Geological Strength Index (GSI), Rock Quality Designation (RQD), and disturbance factors. These parameters are crucial as input variables for application within the RS2 software to analyze the finite element behavior.

2.2. Study area and mineralogy

The study area is located at approximately latitude 16° 57' 37" North and longitude 105° 59' 56" East. The Sepon Gold and Copper Operation is situated in south-central Laos, specifically in the Vilabouly District of Savannakhet Province. It is approximately 235 Km east of the town of Savannakhet and about 40 Km to the north of the town of Sepon. The journey from Savannakhet to the Vilabouly site typically takes around 4 hours. Figures 2.1 (a) and (b) depict the mine's geographical location and its layout.

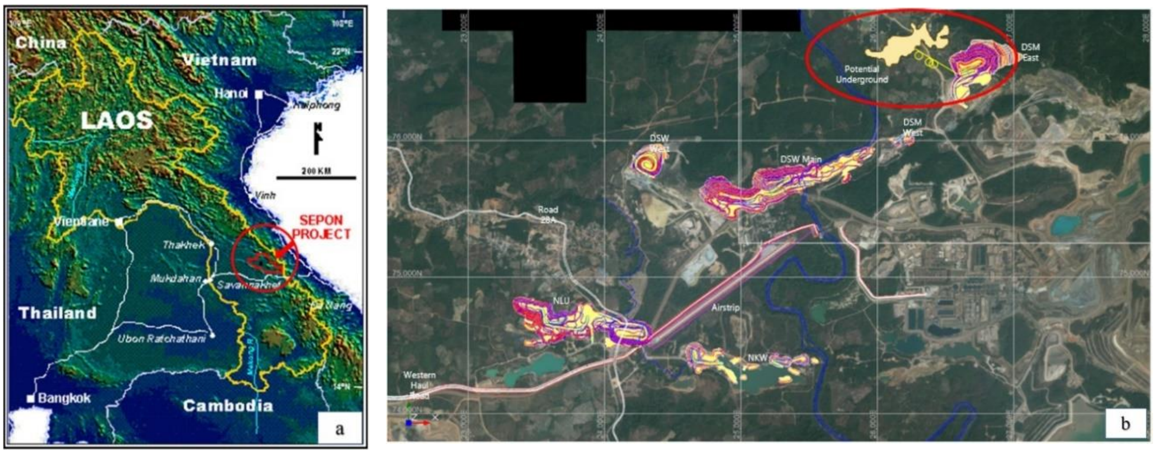

Figure 2. 1 The location of mine site (a) and pit layout for underground (b)

2.3. Mineralogy of the research area

The geological composition of the region comprises a variety of rock units, encompassing clay, sandstone, siltstone, limestone, dolomite, intrusive rhyodacite copper (RDP), claystone, and conglomerate. These rock formations have evolved over millions of years, with their origins dating back to the Ordovician period through to the Cretaceous era. Each of these geological units has unique characteristics and properties that influence the mining and exploration processes in the area.

Moreover, the mine site is situated within a fault zone, which is a distinctive geological feature. This fault zone is characterized by a network of both major and minor faults, all oriented in a northeast to southwest direction. These fault structures have played a significant role in shaping the geological landscape of the region and have influenced the distribution and orientation of mineral deposits within the area. Understanding and mapping these fault zones is crucial for the safe and efficient extraction of resources from the mine. The Figure 2.2 as illustrated the geological map of Sepon Gold-Copper Mine Deposit.

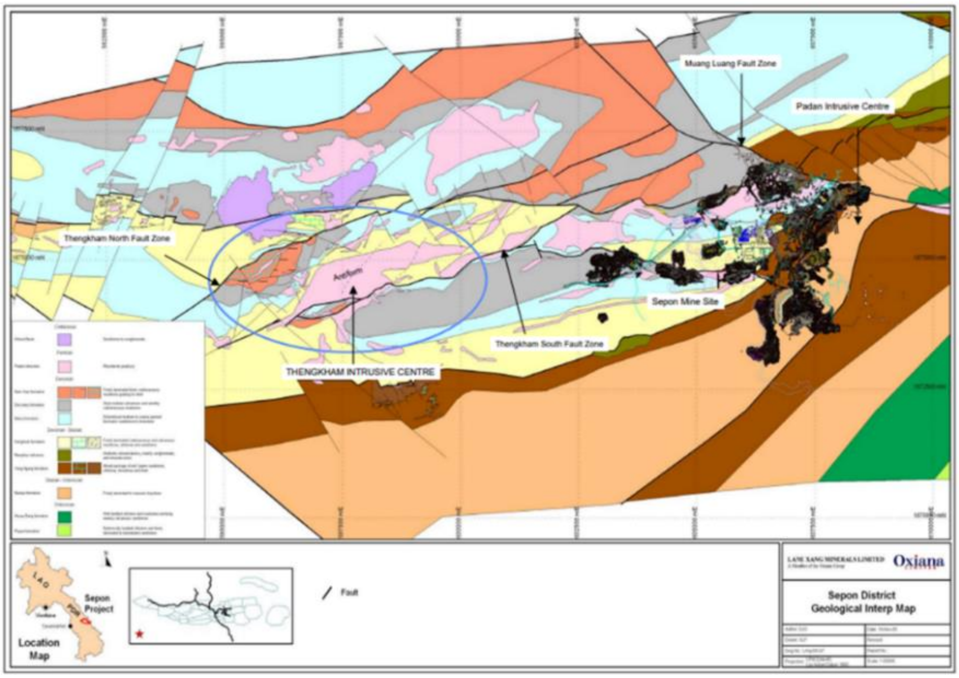

Figure 2. 2 Geological map of Sepon Gold-Copper Mine Deposit

2.4. Current mining method in the study area

During this period, the open stoping method has become a well-established mining technique at the Sepon Gold-Copper Mine Deposit. This development is primarily driven by economic considerations and the specific nature of the orebody. However, the open-pit method has been discontinued due to the depletion of easily accessible shallow ore reserves. In response, the transition to underground mining using the open stope method has been selected as mentioned in chapter 1. Additionally, an access road needs to be excavated to connect with the orebody within the underground Discovery East Mine, as illustrated in Figure 2.3. This shift in mining strategy reflects the evolving needs and challenges of resource extraction at the Sepon Gold-Copper Mine Deposit. The access road to the orebody provides a crucial transportation link that allows personnel, equipment, and materials to reach and navigate within the underground Discovery East Mine. This road is essential for efficient mining operations and ensures safe and effective access to the valuable mineral deposits deep within the mine.

Figure 2. 3 The access road to the orebody

2.5. Problem statement of the research area

The study area grapples with a spectrum of geological and environmental challenges significantly affecting mining operations. These challenges, encompassing weathered rocks, fault lines, and joint interfaces, exert varying impacts on the strength of different rock and soil types, illustrated in Figure 2.4. Geological defects, including planar and wedge failures, compound these issues.

Furthermore, the hydrological impact introduces distinct challenges demanding meticulous investigation and effective mitigation strategies to uphold the safety and efficiency of mining operations. In underground mining, prevalent disasters often stem from incidents like rock falls from the roof, rock sliding from the walls, or, in extreme cases, tunnel collapses.

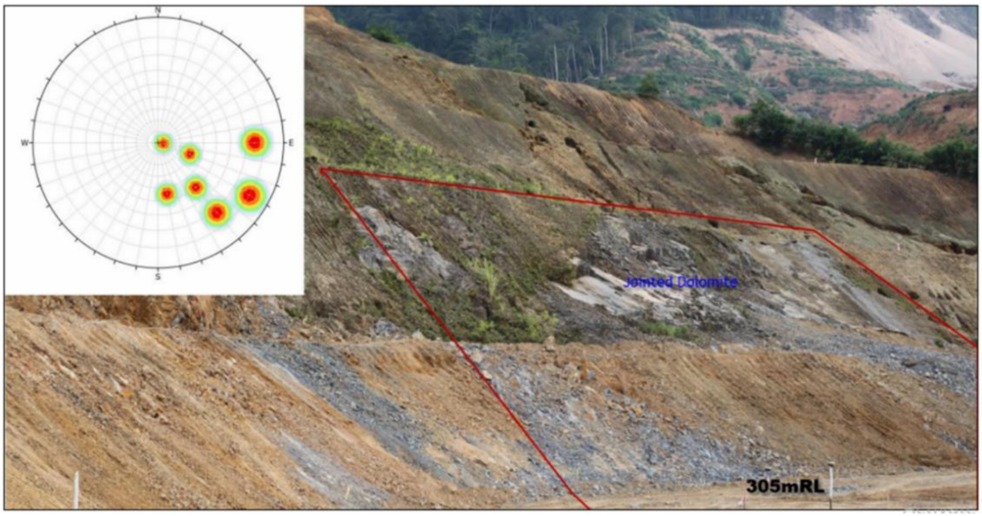

Figure 2. 4 weather rock and join contact

2.6. Research Methodology

The methodology of this dissertation is visually represented in the form of a flowchart shown in Figure 2.5. This flowchart outlines the sequential steps involved in processing input data and generating output data through numerical simulation analysis or stope design. The ultimate objective of this process is to leverage the quality of the rock mass as a controlling factor in determining stope dimensions. This structured approach ensures a systematic and data-driven methodology in achieving the research goals and effectively utilizing rock mass quality in optimizing stope design.

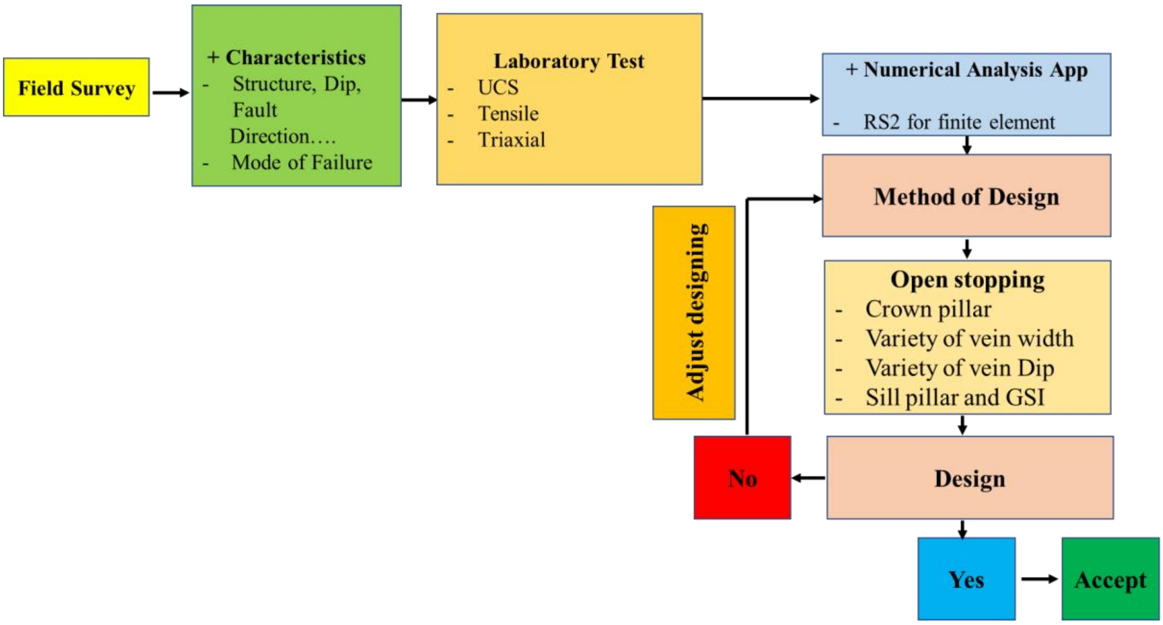

Figure 2. 5 Configuration of the flow chart for the research methodology

2.6.1. Field work

Field studies are crucial for gaining insight into the challenges faced within the mine, including its structural, geological, geotechnical conditions, and mining methods. As a result, the dominant structural orientations at Sepon are primarily determined by the bedding patterns within the rock mass. These bedding orientations serve as critical planes of weakness for the rock, with spacing that can range from a few centimeters to over 5 meters.

This information is vital for mining operations, geotechnical assessments, and assessing geological hazards in the area. Investigating the current mining conditions and the associated challenges at the site depicted in Figure 2.6 revealed the presence of geological features, including faults, joints, and bedding planes, near the mining excavations. Additionally, the mining methods employed in the underground Sepon Mine were thoroughly examined. The research area showcased a mining approach and design characterized by open stoping, with development progressing from the interior and moving outward without internal support.

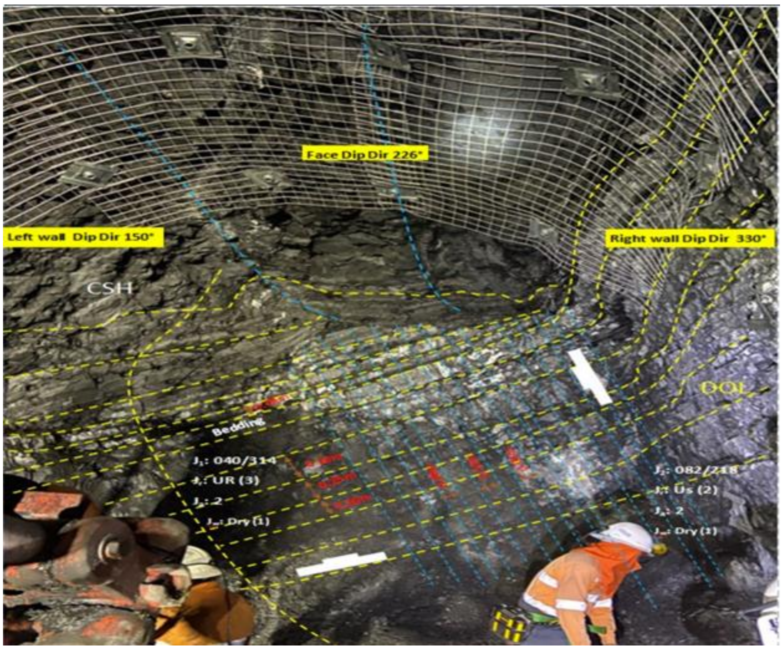

Figure 2. 6 An underground geotechnical face mapping

2.6.2. Laboratory work

In a preceding field study, laboratory tests were conducted to assess the geological properties, including compressive strength, tensile strength, compressive strain, cohesion (c), friction (Ø), Young's modulus, unit weight of collected rock samples, and Poisson's ratio. The results of these tests were supplied by Lanxang Mineral Limited company. Based on the test findings, it can be concluded that the rock exhibits favorable qualities, as the uniaxial compressive strength (UCS) exceeded 25 MPa, classifying it as a hard rock, as shown in Figure 2.7, (a,b,c).

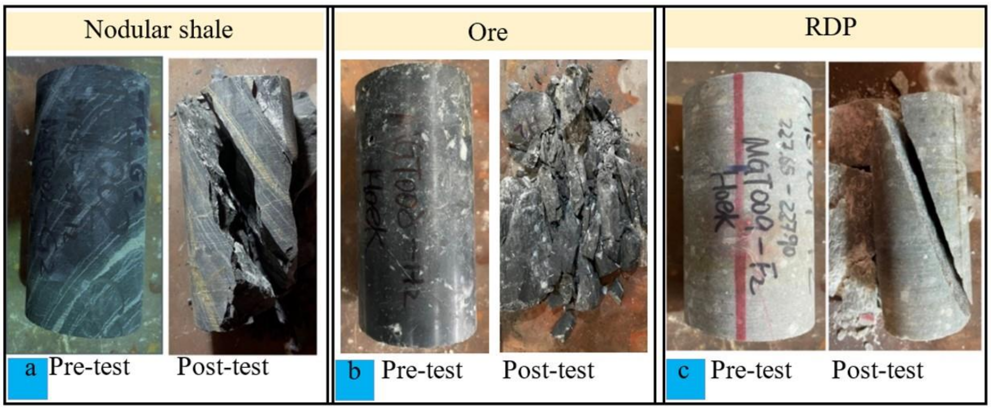

Figure 2. 7 The pre-test and post-test by using triaxial compressive strength test

Figures 2.8(a)-(c) illustrate the results of the triaxial tests. The findings reveal that the ore sample exhibited the highest uniaxial compressive strength (UCS) at an impressive 224.92 MPa, followed by Ryodacite Porphyry (RDP) at 82.58 MPa and Nodular Shale at 66.59 MPa. It's worth noting that the core sample displayed the highest strength values. Furthermore, the test results include Young's modulus values, calculated in gigapascals (GPa). Interestingly, despite the differences in strength, the overall density of all three rock types is nearly identical.

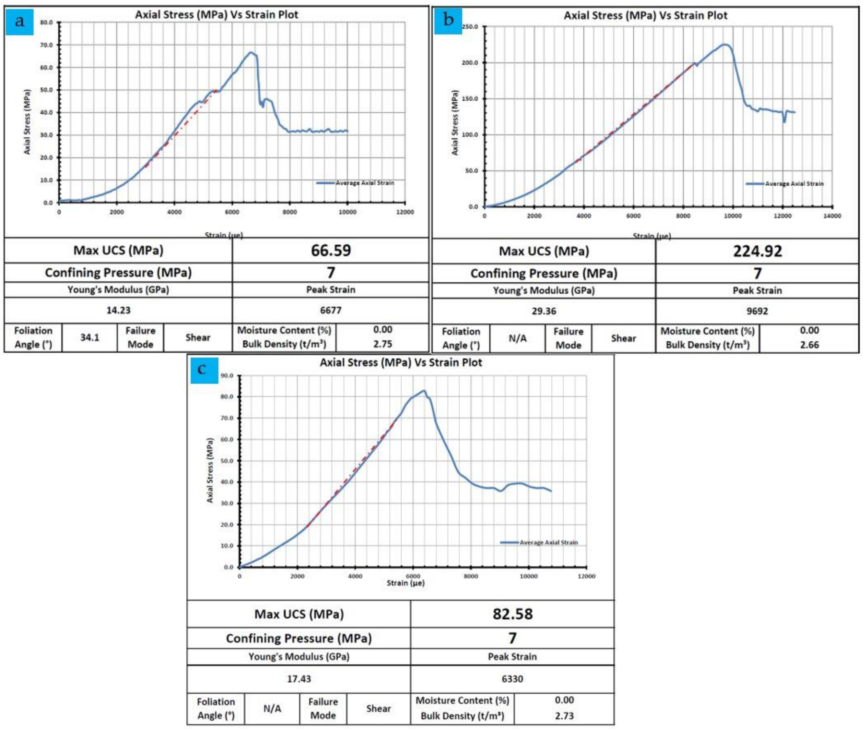

Figure 2. 8 The result for the lab test of triaxial compressive strength (a) Nodular shale, (b) Ore, (c) RDP

2.6.3. Geological rock mass classification in research area

2.6.3.1. Rock quality designation, RQD

Figure 2.9 shows Rock Quality Designation (RQD) is a crucial metric used to evaluate the quality of rock core samples extracted from boreholes. It quantifies the degree of jointing or fractures within a rock mass and is expressed as a percentage. An RQD value of 75% or higher indicates good-quality hard rock, while values less than 50% suggest low-quality, weathered rock (Deere & Deere, 1988).

To calculate RQD, you take a rock core sample from a borehole, sum the lengths of all sound rock pieces that are at least 100 mm in length, and then divide this total by the length of the core run. Only those rock pieces that are considered hard and of good quality are included in the calculation. Weathered rocks that do not meet soundness requirements and have lengths less than 100 mm are excluded from the RQD calculation. The measurement of the length of core pieces is typically taken along the centerline of each piece as it is shown in the general question below.

The RQD test offers valuable insights into the rock's integrity and the extent of damage caused by weathering, helping geologists and engineers assess the suitability of the rock for various purposes, such as construction or mining.

$$\text{Core Recovery, CR} = \frac{\text{Total length of rock recovery}}{\text{Total core run length}} \times 100\% \qquad (2.1)$$

$$\text{RQD} = \frac{\sum \text{Length of sound pieces} > 100\text{ mm}}{\text{Total core run length}} \times 100\% \qquad (2.2)$$

In the mine site, the presence of highly jointed conditions and unconformities can lead to underground collapses and the floating of rock masses. Based on borehole samples and visual structural analysis, it has been determined that the rock mass condition is within the weak zone, and its structures are complex. Referring to Table 2.1, the Rock Quality Designation (RQD) results indicate that the RQD values fall within the range of 20-50%. This suggests that the rock mass at Sepon Underground Mine is categorized as fair to poor quality rock.

However, when investigating deeper into the rock mass, the conditions improve significantly. At greater depths, RQD values of ≥ 90% have been observed, as illustrated in Figure 2.10, indicating a strong and well-consolidated rock mass. This information is critical for assessing the stability and suitability of the rock for mining or construction purposes at different depths within the mine.

Figure 2. 9 Evaluation of the rock mass's geotechnical characteristics in Sepon Mine

Before commencing any mining operations, it is of utmost importance to gain a thorough understanding of the geological strength of the rock mass. In this study, the Geological Strength Index (GSI) was employed for characterizing the rock mass. This choice was made due to the wide range of applications of GSI in studies related to underground mining. The GSI system, developed by Hoek (Hoek, 1994), is a commonly used method known for its accuracy, efficiency, and simplicity in assessing the characteristics of the rock mass.

This approach was formulated by integrating observations of rock mass conditions, drawing from Terzaghi's descriptions, and incorporating insights gained from the extensive experience of the Rock Mass Rating (RMR) system. The goal is to establish a connection between the structure of the rock mass and the circumstances of rock discontinuities. By analyzing core log samples, it can be inferred that the Rock Quality Designation (RQD%) averages between 80% to 100% at depths ranging from over 100 to 500 m. This indicates that the rock mass exhibits favorable qualities at these depths, which is valuable information for mining and engineering considerations.

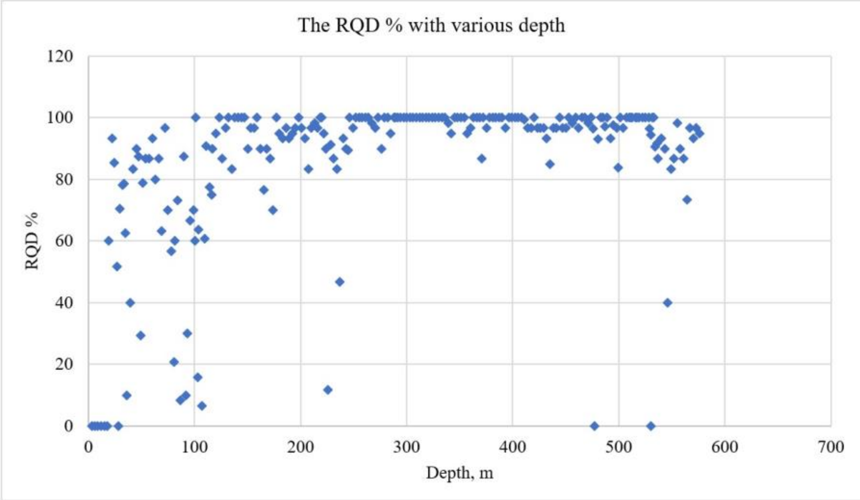

Figure 2. 10 Evaluated RQD in the research area the RQD in the research area

Table 2. 1 Rock Quality and RQD by (Lucian & Wangwe, 2013)

Rock Quality	RQD (%)
Very poor (Completely weathered rock)	< 25%
Poor (weathered rocks)	25% to 50%
Fair (Moderately weathered rocks)	51% to 75%
Good (Hard Rock)	76% to 90%
Very Good (Fresh rocks)	91% to 100%

2.6.3.2. Q-system and rock mass rating, RMR

The Q-system was developed in 1974 by (Barton et al., 1974) Since its introduction in 1974, there has been significant progress in support philosophy and technology in underground excavations. Various new types of rock bolts have been introduced, and the continuous development of fiber-reinforced technology has significantly altered support procedures in many ways. The use of sprayed concrete has been embraced, even for high-quality rock masses, driven by increased safety requirements in recent years. Reinforced ribs made of sprayed concrete have largely supplanted cast concrete structures. The formula for the Q-system can be defined as follows:

$$Q = RQD \frac{J_r \times J_w}{J_a \times J_n} \frac{1}{SRF} \qquad (2.3)$$

where

RQD = Degree of jointing (Rock Quality Designation)

J_a = Joint alteration number

J_n = Joint set number

J_r = Joint roughness number

J_w = Joint water reduction factor

SRF = Stress Reduction Factor (e.g., due to faulting).

Bieniawski (Bieniawski, 1989) introduced a rock classification system known as the Rock Mass Rating (RMR). This system employs six parameters for categorizing a rock mass: uniaxial compression strength, Rock Quality Designation (RQD), spacing of discontinuities, condition of discontinuities, orientation of discontinuities, and groundwater condition.

2.6.3.3 Geological strength index, GSI

In this research, GSI values play a crucial role in determining the properties of the rock mass that will be used in numerical simulations. The strength of a jointed rock mass is influenced by both the characteristics of the intact rock pieces and the ability of broken pieces to move and rotate under various stress conditions. This mobility is governed by the geometrical shape of the intact rock pieces and the condition of the surfaces that separate them. Rock pieces with angular shapes and clean, rough discontinuity surfaces will contribute to a much stronger rock mass compared to rock masses containing rounded particles surrounded by weathered and altered materials. The impact of blast damage on the properties of the near-surface rock mass has also been considered in the 2002 version of the Hoek-Brown criterion, as discussed by (Hoek et al., 2002) as follows:

$$m_b = m_i \exp\left(\frac{GSI-100}{28-14D}\right) \tag{2.4}$$

$$S = \exp\left(\frac{GSI-100}{9-3D}\right) \tag{2.5}$$

$$a = \frac{1}{2} + \frac{1}{2}\left(e^{-GIS/15} - e^{-20/3}\right) \tag{2.6}$$

The Geomechanical Strength Index (GSI), as introduced by Hoek in 1994 and further developed by Hoek et al. in 1995, offers a comprehensive classification system for assessing various geological conditions and their impact on rock mass strength reduction. This classification is presented in Table 2.2 for blocky rock masses and in Table 2.3 for heterogeneous rock masses.

In the early years of applying the GSI system, attempts were made to estimate the GSI value directly from the Rock Mass Rating (RMR) system. However, this correlation was found to be unreliable, especially when dealing with poor quality rock masses or rocks with unique lithological characteristics that did not align with the RMR classification. Consequently, it is recommended that GSI values should be directly estimated using the charts provided in Table 2.2 and Table 2.3, rather than relying on the RMR classification system.

Table 2. 2 Characterization of blocky rock masses on the basis of interlocking and joint conditions.

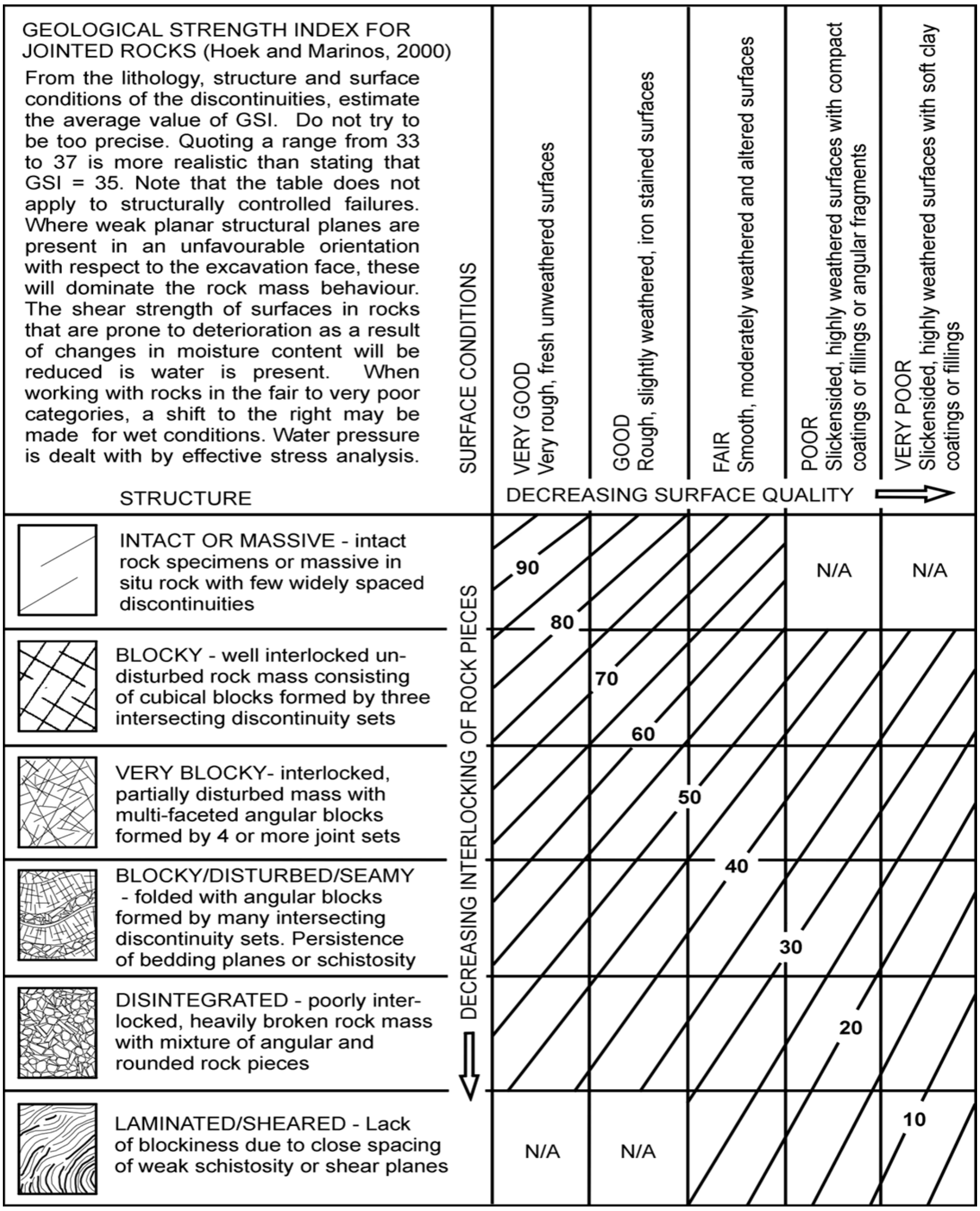

Table 2. 3 Estimate of Geological Strength Index GSI for heterogeneous rock masses such as flysch. (After (Marinos & Hoek, 2001)

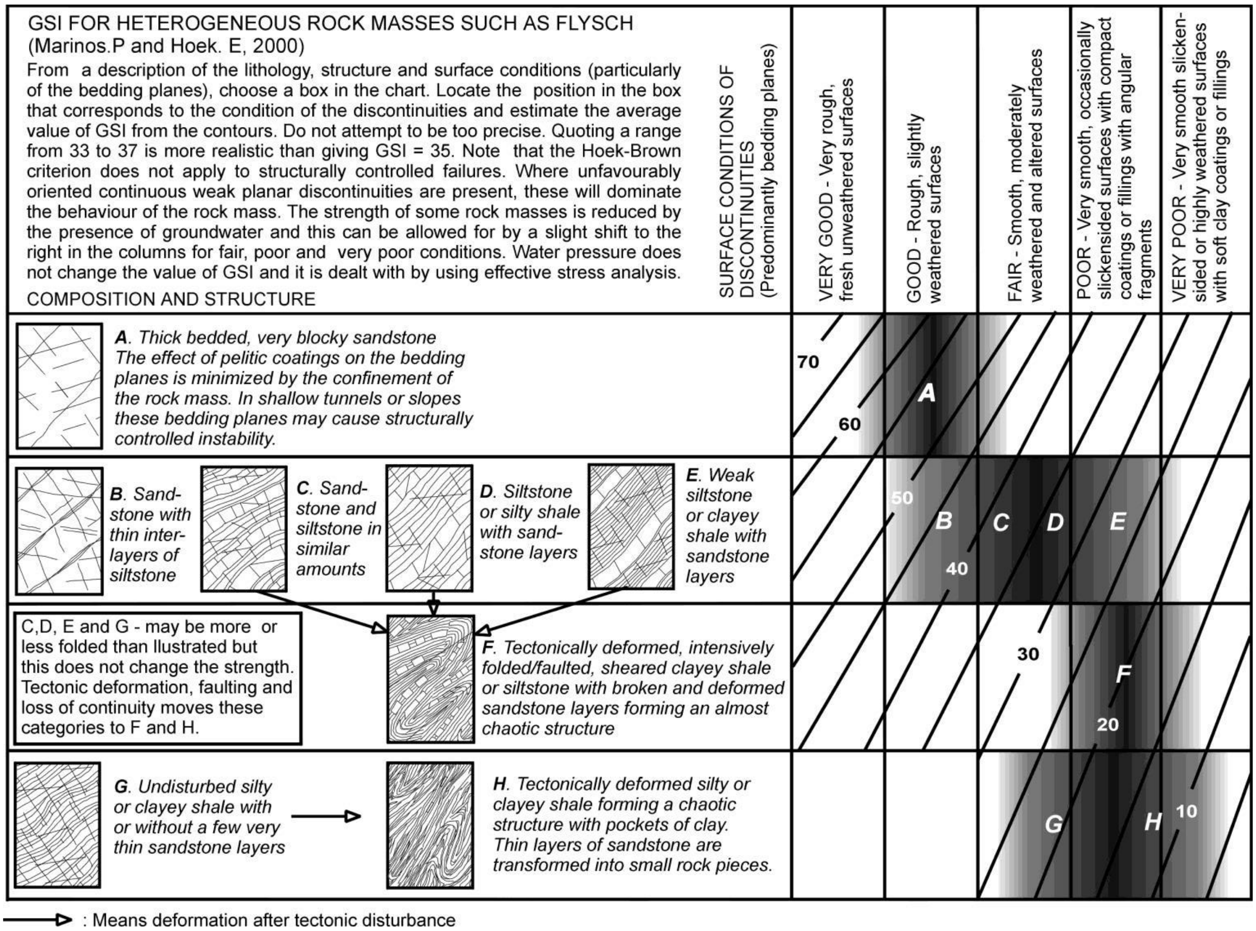

D represents a critical factor that considers the extent of disturbance attributed to blast damage and stress relaxation. Its value is on a scale from 0, signifying minimal disturbance in in-situ rock masses, to 1, indicating significant disturbance in rock masses. Detailed guidelines for selecting the appropriate D value can be found in Table 2.4. It's important to emphasize that the D factor pertains solely to the zone affected by blast damage and should not be applied to the entire rock mass. To illustrate, in tunnels, the blast damage typically affects a zone about 1 to 2 meters thick surrounding the tunnel. This zone should be considered separately when creating numerical models, distinct from the surrounding rock mass. At Sepon Gold Mine, overbreak in tunnels after blasting can vary between 0.5 to 2 meters, yielding a D factor of approximately 0.7. It is essential to avoid applying the D factor to the entire rock mass, as it can lead to unnecessarily pessimistic results.

Table 2. 4 Guidelines for estimating disturbance factor D

Appearance of rock mass	Description of rock mass	Suggested value of D
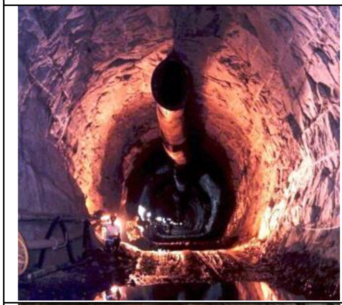	Excellent quality controlled blasting or excavation by Tunnel Boring Machine results in minimal disturbance to the confined rock mass surrounding a tunnel.	D = 0
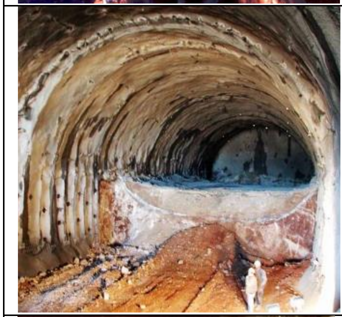	Mechanical or hand excavation in poor quality rock masses (no blasting) results in minimal disturbance to the surrounding rock mass. Where squeezing problems result in significant floor heave, disturbance can be severe unless a temporary invert, as shown in the photograph, is placed.	D = 0 D = 0.5 No invert
	Very poor quality blasting in a hard rock tunnel results in severe local damage, extending 2 or 3 m, in the surrounding rock mass.	D = 0.8
	Small scale blasting in civil engineering slopes results in modest rock mass damage, particularly if controlled blasting is used as shown on the left hand side of the photograph. However, stress relief results in some disturbance.	D = 0.7 Good blasting D = 1.0 Poor blasting
	Very large open pit mine slopes suffer significant disturbance due to heavy production blasting and also due to stress relief from overburden removal. In some softer rocks excavation can be carried out by ripping and dozing and the degree of damage to the slopes is less.	D = 1.0 Production blasting D = 0.7 Mechanical excavation

In conclusion, when assessing the RQD result and the RMR classification of Sepon Gold-Copper Mine Deposit, the GSI values are notably favorable, exceeding 32. This suggests a promising scenario for this mining area. Nonetheless, it's crucial to emphasize that the condition of the rock mass remains a vital consideration for mine stability. Notably, in the actual mine site, a D factor of 0.7 is applied, indicating effective blasting practices.

2.7. Conclusions

In this chapter, we present a brief explanation of the research background and plan. The Sepon Gold Copper Deposits, discovered in 1998, represent one of Laos's most significant gold copper deposits, making a substantial contribution to the country's economic development. Ensuring a sound and effective mining method is crucial for the stability of excavated areas. Currently, instability issues in the open stoping method from regional geological conditions and structures. To address this, we utilize Rock Mass Classification (RQD) alongside the Q-system and RMR to assess the geological properties.

To achieve the research objectives, simulations were employed to assess the stability of underground mines. Specifically, RS2 simulations were utilized to generate the research findings. RS2 simulation is widely adopted within the mining industry due to its efficacy in assessing underground mine stability on a global scale. Developed by Rocscience, this simulation software caters to the unique needs of the mining sector. Additionally, another key simulation employed is RS2, a two-dimensional plastic finite element grid used for stress and displacement calculations around underground openings. It's a versatile tool capable of addressing a broad spectrum of mining and civil engineering challenges. In this dissertation, both simulations were put to use to evaluate the stability of open stope mining at Sepon Underground Mine.

Based on the perspective outlined in the problem statement, next chapter were discuss the following objectives:

1. To understand stress conditions around the stope, crown pillar, and sill pillar areas within the shallow open stope mining method, considering various factors such as geology, excavation sequence, vein geometry, and stress ratios.
2. To investigate the effectiveness of vein excavation techniques under different mine environment conditions, including stress ratios, geology, excavation steps, vein dipping, sill pillar thickness, and vein width.
3. To implement measures to control induced stresses in the crown pillar within shallow underground settings, adjusting crown pillar thickness based on varying geological conditions and vein geometries.

4. To develop underground mine design guidelines for gold deposits after a comprehensive analysis of the research study's results.

2.8. Reference

Barton, N., Lien, R., & Lunde, J. (1974). Engineering classification of rock masses for the design of tunnel support. *Rock Mechanics, 6*, 189–236.

Bieniawski, Z. T. (1989). Engineering rock mass classifications: a complete manual for engineers and geologists in mining, civil, and petroleum engineering. John Wiley & Sons.

Deere, D. U., & Deere, D. W. (1988). The Rock Quality Designation (RQD) Index in Practice. In *ASTM Special Technical Publication: Vol. STP 984* (pp. 91–101). https://doi.org/10.1520/STP48465S.

Hoek, E. (1994). Strength of rock and rock masses, ISRM News Journal, Vol. 2. *Hoek, E.(2000) Rock Engineering, A Course Notes, Http://Www. Rocscience. Com*, 31–38.

Hoek, E., Carranza, C., & Corkum, B. (2002). Hoek-brown failure criterion – 2002 edition. Narms-Tac, 267–273.

Lucian, C., & Wangwe, E. M. (2013). The usefulness of rock quality designation (RQD) in determining strength of the rock. *International Refereed Journal of Engineering and Science*, *2*(9), 36–40.

Marinos, P., & Hoek, E. (2001). Estimating the geotechnical properties of heterogeneous rock masses such as Flysch Estimating the geotechnical properties of heterogeneous rock masses such as Flysch Estimation des propriétés géotechniques des masses rocheuses hétérogènes, comme le flysch. *Bull. Engg. Geol. Env*, *60*, 85–92

CHAPTER 3
ASSESSMENT OF THE STABILITY OF SEPON UNDERGROUND GOLD MINE DEPOSITS

3.1. Introduction

The rock mass strength was assessed in the previous chapter using rock mass classification methods such as Rock Quality Designation (RQD) and Geological Strength Index (GSI). The results revealed that the geological strength index of the rock mass is characterized by a GSI value of 32. The ore, hosted within the vein, is nearly vertically inclined in the Sepon Gold Mine Deposit, as depicted in Figure 3.1. The mineralized veins have a North-South strike with dips ranging from 62° to 75°. These veins vary in thickness, ranging from 5 to 50 meters, and some can extend over 100 meters in length. This chapter primarily focuses on the excavated vein highlighted in yellow, as shown in Figure 3.1. Laboratory tests for geological strength revealed that the rock strength is weak in the hanging wall domain. Furthermore, the results indicated that the vein is stronger than both the hanging wall and footwall. Given the geological conditions, the hanging wall is susceptible to environmental impacts like ground subsidence if the underground mine is developed at a shallow depth. Figure 3.2 illustrates failures surrounding the excavated stope in the study area. However, this chapter discusses vein extraction and explores the stability conditions of vein stope excavation under various regional stress regimes, varying geological and structural conditions, and excavation sequences. In response to the instability issues currently encountered in the mine, this chapter aims to offer practical solutions by understanding the key parameters that contribute to such instabilities using RS2 simulation.

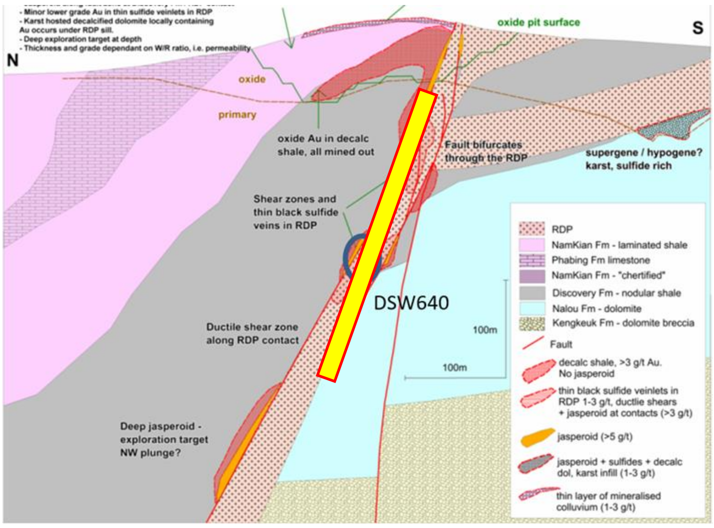

Figure 3. 1 Shows the analyzed vein location of mine at the cross-section map

Figure 3. 2 Current open stope in the host rock

3.2 Numerical Analysis

3.2.1. The input parameters

To assess the value of whole rock samples, including core specimens representing unweathered rock, essential input parameters were defined using a rock laboratory application. These parameters are detailed in Table 3.1 below. The Geological Strength Index (GIS), as introduced by (Hoek et al., 2013; Marinos & Hoek, 2018), was employed to characterize the rock's properties. Various GIS values falling within the range of 35 to 55 were calculated. These values correspond to different rock mass conditions, with 35 indicating blocky rock masses with moderately fair joint surface quality, and 55 representing extremely blocky rock masses with good joint surface quality.

Table 3. 1 The geotechnical properties of rock at Sepon gold mine deposit

Geological Strength Index (GSI)	**Zone/Rock type**	**Density (MN/m^3)**	**σ_{ci} (MPa)**	**Tensile σ_t (MPa)**	**E_{rm} GPa**	**v**	**Hoek Brown Parameter**		
							mb	**s**	**a**
72	Footwall RDP	0.0275	82.5	15.5	17.4	0.3	6.167	0.031	0.50
62	Ore body	0.0266	224.9	13.8	29.3	0.3	2.656	0.01	0.50
51	Hanging wall Nodular shale	0.0279	66.5	11.6	14.2	0.35	0.898	0.001	0.50

Notes: σ_{ci} = uniaxial compressive strength of intact rock material; mb, s, a = material constant for Hoek-Brown Failure Criterion; σ_t = uniaxial tensile strength ; E_{rm} = Young's modulus of rock mass; v = Poisson's Ratio.

Poisson's ratio can be estimated using the following relationship, which has been derived from a best-fit regression of suggested values found within the GSI classification system (as documented by Hoek et al. in 1995)

$$V_{rm} = 0.32 - 0.0015 \times GSI \qquad (3.1)$$

3.2.2. Model construction

To comprehensively assess stope stability at the Sepon Gold Mine Deposit, a series of numerical models were developed using RS2 for a finite element plastic numerical analysis utilizing the Generalized Hoek-Brown criterion was performed to assess the stability of the surface slopes and underground stopes in a simplified model. These models incorporated varying inclined vein angles, different excavation depths, and diverse mining sequences. The initial model was established with dimensions of 520 m in width and 700 m in length, with the x, y. The top portion of the model was left unconstrained, as depicted in Figure 3.3, and was based on the current mine cross-section plan shown in Figure 3.1. Stopes were initiated at around 100 m, and a crown pillar was retained to ensure stability. Each stope was equipped with sill pillars to maintain stability during ore extraction. For mining purposes, the focus was on a vein with dimensions of 10 m in width and 25 m in height, which was subdivided into four excavation sections. Each section underwent excavation in five steps, with the stopes being excavated in dimensions of 10 m by 5 m up to a height of 25 m. The initial mining sequence started from the upper part of the mining area and progressed to the lower part. Monitoring points were strategically positioned at the top of each stope. Modified parameters included adjustments to geological conditions, alterations in the mining sequence, variations in vein width, and stress ratio assessments when compared to the currently employed open stoping method. To optimize mine stability, a variety of supporting systems were evaluated to determine their effectiveness and economic feasibility. The analysis encompassed the rock failure mechanisms, factor of safety, and displacement of the rock mass, providing valuable insights for the mine stability guidelines.

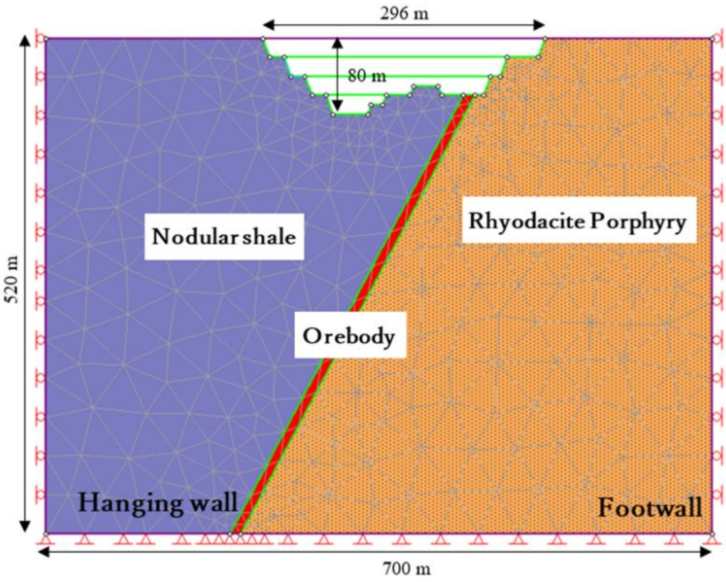

Figure 3. 3 Model set up showing dimensions

3.2.3. Mining Sequence

Given the orebody's favorable Geologic Strength Index (GSI) of 62 and a vein dip of 62°, the overhand cut mining method is typically employed in mining operations. In contrast to conventional mining sequences that progress from the bottom upward, leaving a 5 m-thick sill pillar after each excavation step, the overhand cut method starts at the base and advances upward. This is depicted in the first group of excavations, consisting of five steps as illustrated in Figure 3.4. Once the initial excavation group is completed, the method is then applied in a similar manner to subsequent excavations further below. This mining sequence continues until the final excavation. However, it's important to note that surface subsidence is inevitable in this process (Guggari et al., 2023; Sasaoka et al., 2015), and a substantial crown pillar with a thickness of approximately 40-50 meters is required.

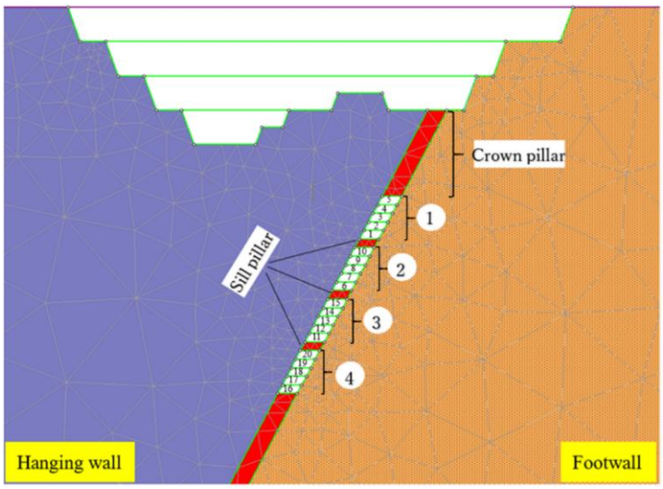

Figure 3. 4 The mining consequence

3.2.3.1. Surface and slope deformation

The stability of the slopes was assessed through the use of monitoring points located near the surface of the pit. This assessment revealed a factor of safety (FoS) of approximately 2.46, as illustrated in Figure 3.5. Once the surface slopes were completed, it became crucial to maintain continuous monitoring of the underground mining operations. Figure 3.5 displays the displacement, stress, and yielding zones within this section.

The results, depicted in Figure 3.6, highlight significant displacement predominantly occurring on the hanging wall side, as shown by the monitoring points along the surface. Displacement monitoring pins were strategically placed at 10 m intervals along the surface, and their corresponding data is presented here. Notably, the footwall remained unaffected, while the bench on the hanging wall side exhibited substantial displacement, extending down to the pit bottom.

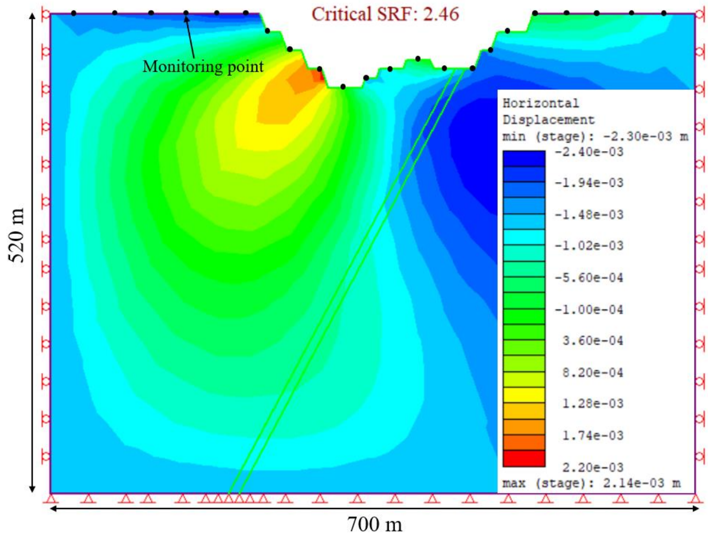

Figure 3. 5 Slope stability before beginning an underground mining operation

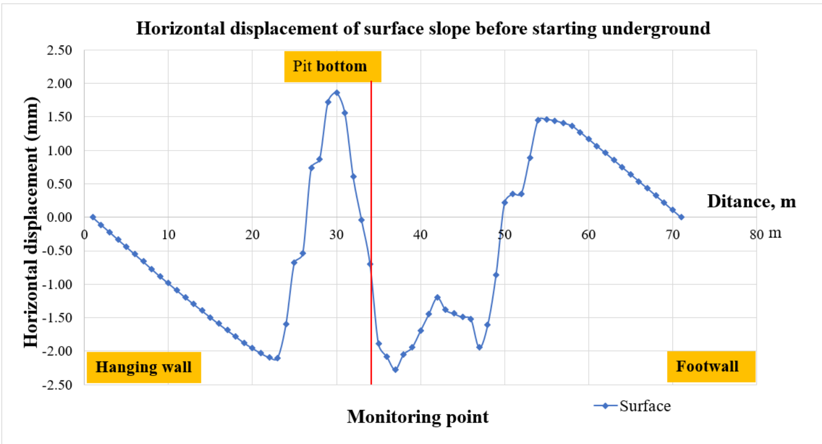

Figure 3. 6 The monitoring point along the surface displaying displacement

3.2.3.2. Impacts of Instability in a Vein Stopes Under Different Mine Conditions

When project-related stress risks reach a certain threshold, it becomes necessary to measure in-situ stress. As stress-induced risks escalate, they can impact the stability of the rock mass. To investigate this phenomenon, this section utilizes RS2 simulation. In this study, a range of stress ratios (0.5, 1.0, 1.5, 2, 2.5, and 3), GSI values spanning from 20 to 65, vein inclinations varying from 62° to 90°, and stope widths equal to or greater than 5 meters are applied in the model. However, in the actual mine conditions, the geological characteristics are represented by a GSI value of 32 and an inclined vein with a dip angle of 62°.

3.2.3.3. Stress Condition and Ground Behavior around Stope and Crown Pillar in Underhand Variant

To simulate the underhand variant, the stope in the numerical model is excavated from the upper slice, following the sequence depicted in Figure 3.7(a). This excavation process leaves a 20-meter vein as the crown pillar. The excavated stope is left as an open stope. Differential stress, defined as the difference between major and minor in-plane principal stresses ($\sigma_1 - \sigma_3$), is recorded at the center of the crown pillar, denoted by the yellow dot in Figure 3.7(a). This differential stress is continuously monitored as the stope progresses downward. Figure 3.7(b) displays the changes in differential stress at the monitored point throughout the stope's excavation progress.

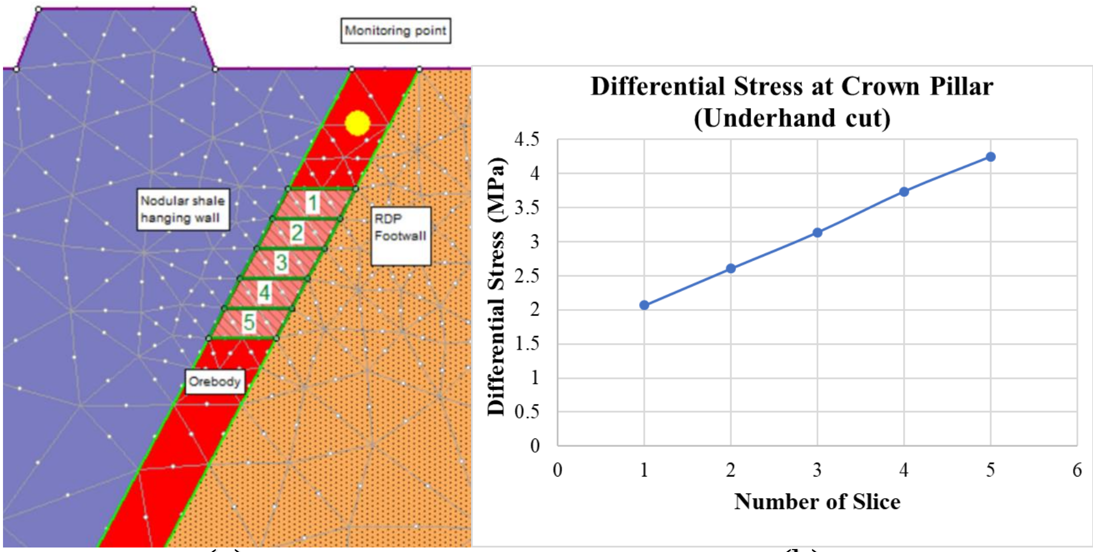

(a) (b)

Figure 3. 7 (a) Sequence of stopping and location of monitored point (b) Differential stress at monitored point as the stope progressing downward

Based on the simulation results, it is evident that the differential stress at the center of the crown pillar steadily increases as the stope moves away from the crown pillar. This observation suggests that the stress induced by the stope's excavation accumulates within the crown pillar area, even as the stope progresses away downward from it. The gradient of the curve indicates that the accumulation of induced stress in the crown pillar becomes less pronounced as the stope descends further. The implications of this effect on crown pillar and stope stability are illustrated in Figure 3.8. In Figure 3.8, the colors represent the contour of yielded elements in the simulation results. Zones where the stress satisfies the yield criterion are considered as yielded elements. By examining the overall pattern of these yielded elements, we can determine whether stope or crown pillar failure has occurred. A crown pillar is assumed to have failed when yielded elements propagate from the stope to the surface area. However, if the yielded elements are confined to the vicinity of the stope without extending to the surface, it suggests that failure is limited to the stope itself.

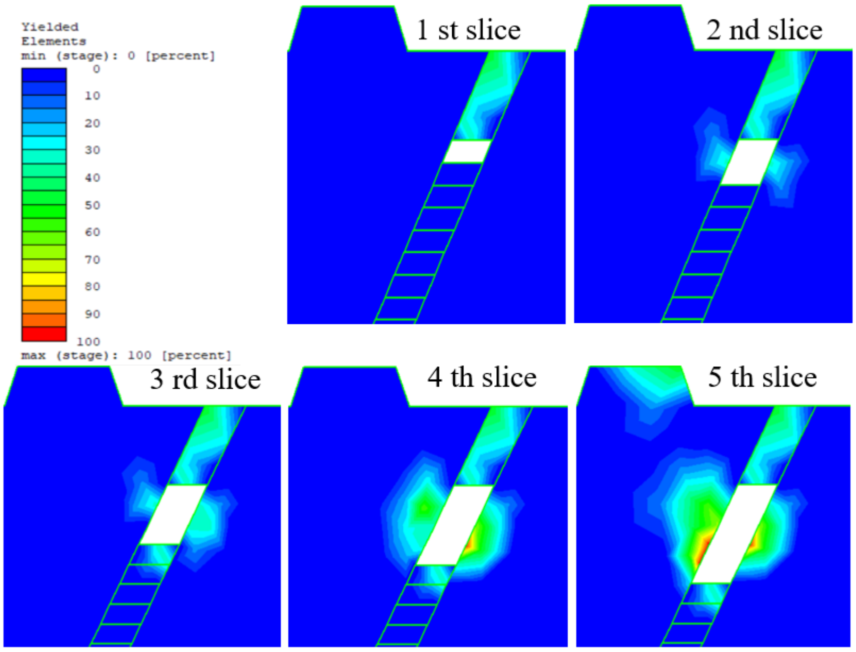

Figure 3. 8 Crown pillar and stope stability in underhand variant

3.2.3.4. Stress Condition and Ground Behavior around Stope and Crown Pillar in Overhand Varian

Since the open stoping direction in the overhand method differs from the underhand approach, the stress conditions around the stope and crown pillar exhibit variations. The simulation for the overhand cut is conducted using the stoping sequence illustrated in Figure 3.9(a). Similar to the previous simulation, the differential stress is recorded at the same location as the stope progresses upward. The results are presented in Figure 3.9(b). However, when comparing the differential stress between the underhand cut method and the overhand cut method, it is evident that the overhand cut method exhibits lower values, approximately around

3.8 MPa, whereas the underhand cut method demonstrates higher values, reaching approximately 4.3 MPa.

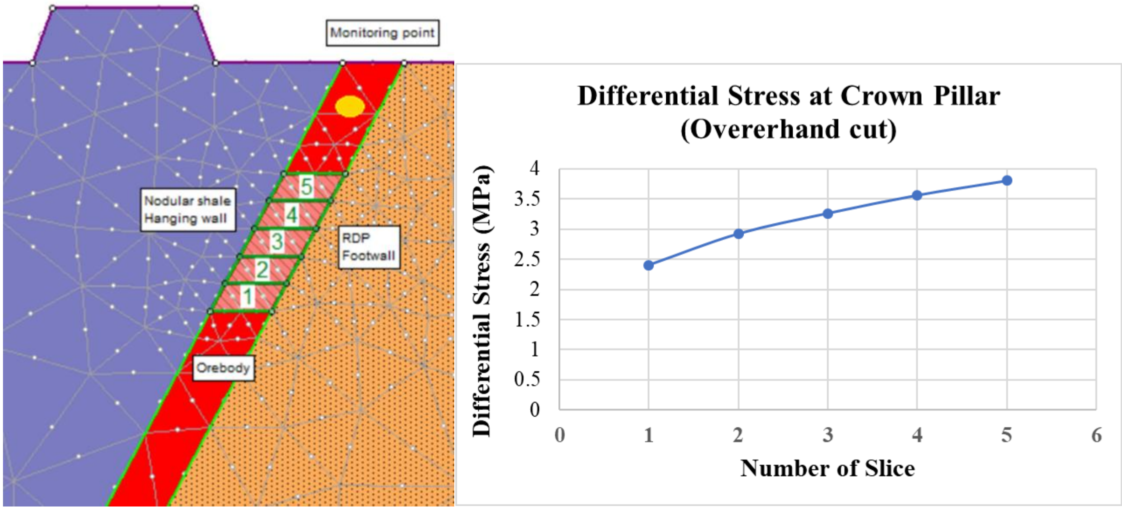

(a) (b)

Figure 3. 9 (a) Sequence of stopping and location of monitored point (b) Differential stress at monitored point as the stope progressing upward.

In Figure 3.9(b), it is evident that the differential stress at the crown pillar in the overhand variant increases as the stope progresses upward. The induced stress from the initial stope opening already has an impact on the differential stress within the crown pillar. This influence becomes more pronounced as the stope approaches the monitored point. Consequently, the likelihood of crown pillar failure increases as the stope progresses upward. The implications for crown pillar and stope stability, as derived from the numerical simulation results, are illustrated in Figure 3.10.

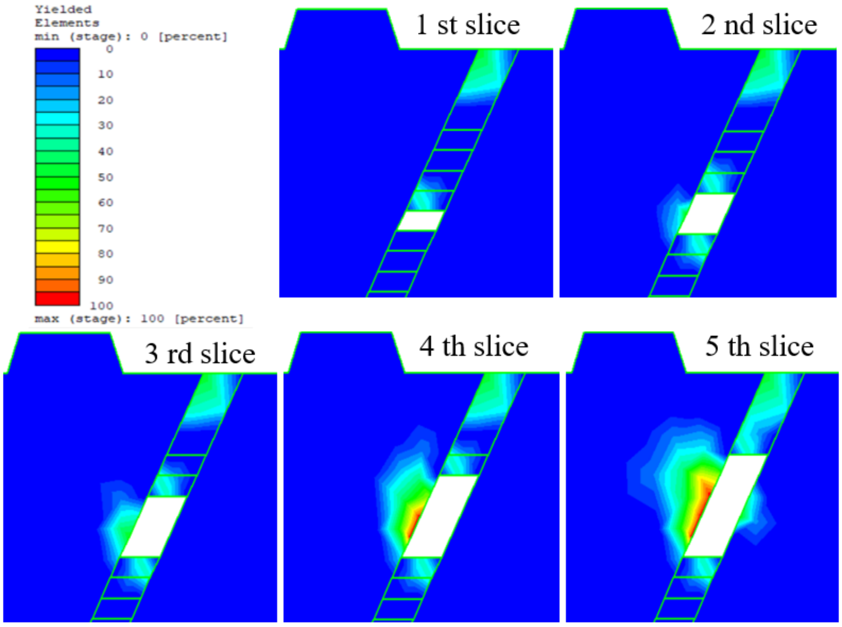

Figure 3. 10 Crown pillar and stope stability in overhand variant

The simulation results reveal instability occurring in both the stope and crown pillar areas. When the first slice is excavated, a fully yielded zone, indicated by the red color, forms more prominently on the stope's roof and hanging wall compared to the footwall. Furthermore, this failure propagates to the surface, as observed in the yielded zone pattern above the stope in the overhand cut method. At this level, the failure is limited to the stope and crown pillar area, with no broader surface impact. As the stope progresses to higher levels, with increasing differential stress, crown pillar failure becomes evident, occurring precisely during the excavation of the 4th slice. The fully yielded zone extends to the surface, raising concerns of potential sinkhole subsidence. The failure pattern in the 5th slice indicates that sinkhole subsidence has expanded into the hanging wall area. It is anticipated that if crown pillar failure occurs during the excavation of the 5th slice, subsidence may affect a larger area. In comparison to stope and crown pillar stability in the underhand variant, the overhand variant appears to be more stable. Stope roofs during underhand stoping remain slightly unstable stable, with yield zone occurrence. These findings suggest that the overhand cut method provides better stability conditions for both the stope and crown pillar.

3.2.4. Determined of the Various Stress Ratio

Analysis of the results reveals the varying degrees of instability around the open stope, dependent on the K ratio (stress ratio). The findings, as illustrated in Figure 3.11a, indicate that at a K ratio of 0.5, the instability is relatively low compared to other stress ratios. Figure 3.11b illustrates that predominant failure initiates around the open stope with a K ratio of 1. Notably, the failure zone is more pronounced on the hanging wall side due to the weak rock mass characterized by a GSI of 51. As the K ratio increases to 1.5, Figure 3.11c shows that additional failure zones begin to develop. Furthermore, Figures 3.11d to 3.11f reveal a significant increase in instability when the K ratio is raised from 2 to 3. The most extensive failure zone occurs at the highest K ratio of 3, surpassing the failure zones observed at K ratios of 2 and 2.5. However, it's worth noting that the sill pillar remains stable for K ratios of 0.5 and 1. At a K ratio of 1.5, the sill pillar is affected, along with the crown pillar. For K ratios of 2 to 3, both the sill pillar and crown pillar are significantly affected. At the mine site, the stress ratio currently ranges from 1.3 to 1.7. Whether the open stope will fail or not depends on several factors, including the size of the stope, the Geological Strength Index (GSI), vein angle, and the characteristics of the rock mass surrounding the open stope. In the Sepon Gold-Copper Mine Deposit, the GSI for the ore vein is 62, for the hanging wall is 51, and for the footwall is 72. These values suggest that the GSI is favorable enough to maintain stability.

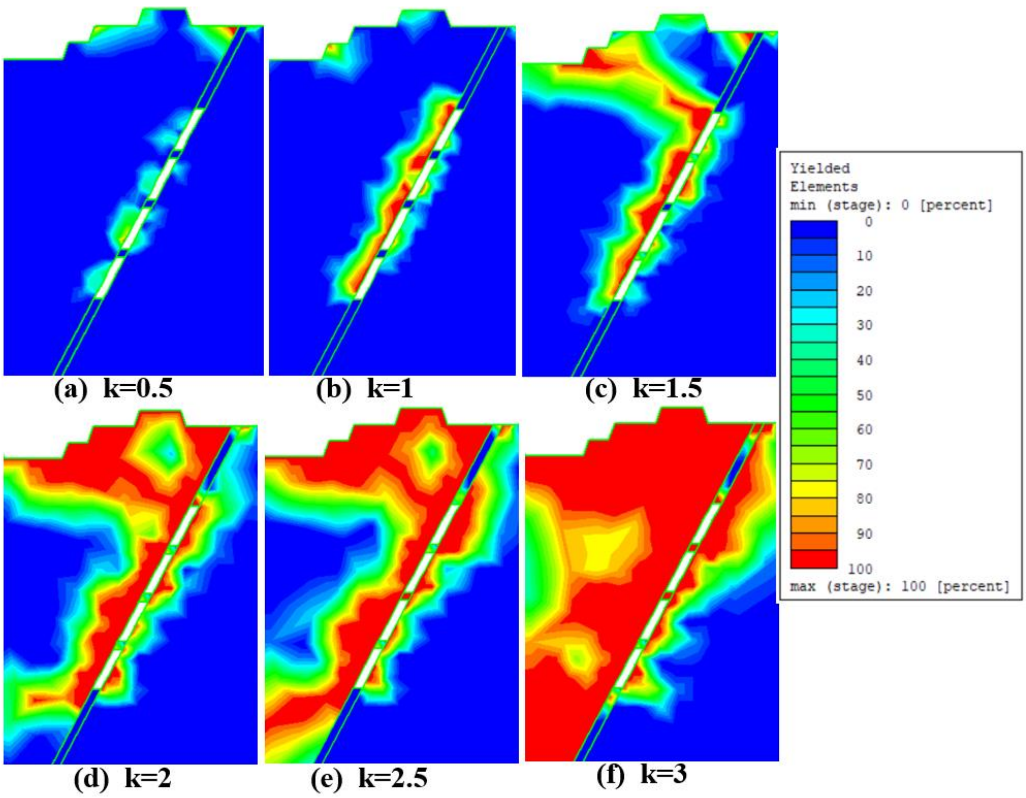

Figure 3. 11 Depict the result of the study area under different stress ratios under yielded element

The horizontal displacement graph in Figure 3.12 demonstrates that low displacement is associated with a lower stress ratio. Specifically, a K ratio of 0.5 results in a displacement of 8.32 mm, which doubles to 16.7 mm at a K ratio of 1. The displacement increases to 35.4 mm at a K ratio of 1.5 and nearly doubles again to 62.8 mm at a K ratio of 2. However, when the K ratio is raised to 2.5, the displacement increases slightly to 87.9 mm, and it surges to 135 mm at a K ratio of 3. Hence, the highest displacement is observed at the highest stress ratio, while the lowest displacement occurs with the lowest stress ratio (Kaiser et al., 2001; Sepehri et al., 2017; Thae et al., 2022).

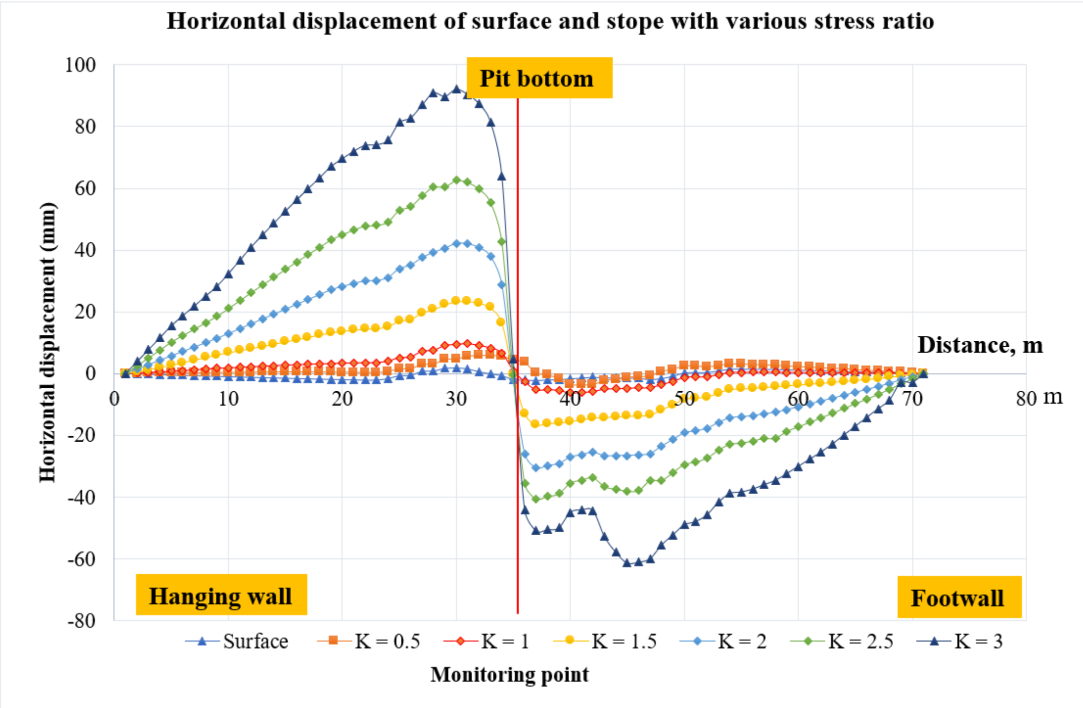

Figure 3. 12 The horizontal displacement with various stress ratios

3.2.5. Geological Strength Index (GSI)

The performance of stope stability was further evaluated in relation to rock mass properties, which were determined based on the Geological Strength Index (GSI) parameters. Different GSI values were simulated, ranging from 20, representing a disintegrated rock mass with poor joint surface quality, to 55, indicating a blocky rock mass with good joint surface quality. Rock mass properties for each GSI value were determined using the Hoek and Brown Failure Criterion, summarizing the characteristics of the rock mass. The primary dataset, including Uniaxial Compressive Strength (UCS) and tensile properties, was obtained from laboratory test results. An additional dataset was generated using RocLab software, incorporating the GSI values. Parametric analyses were then conducted for various geological conditions, and a comparison of the open stoping method was performed.

According to the results presented in Figure 3.13, the Geological Strength Index (GSI) significantly influences the safety factor. As demonstrated, underground mining operations adhering to a GSI of 35 achieve a safety factor of 1.3 or higher, ensuring safety. However, when the GSI falls below 35, the safety factor drops below 1.3, falling short of the safety requirements

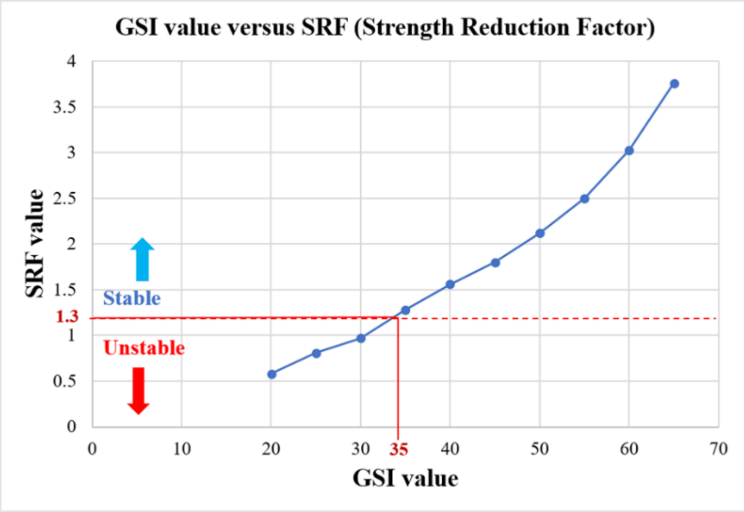

Figure 3. 13 Strength reduction factor with various GSI values

However, it was evident from the horizontal displacement on Figure 3.14 that the lowest GSI value produced displacements up to 15 cm, which was illustrated by the highest displacement on GSI 30. On the other side, when the GIS values rise, the higher GSI value illustrates the smaller horizontal displacement. Since it confirms that a high value of GSI results in a high level of stability, particularly in surface mining and open stopes, the GSI value plays an important role in this condition of the numerical simulation for the safety of factors and horizontal displacements.

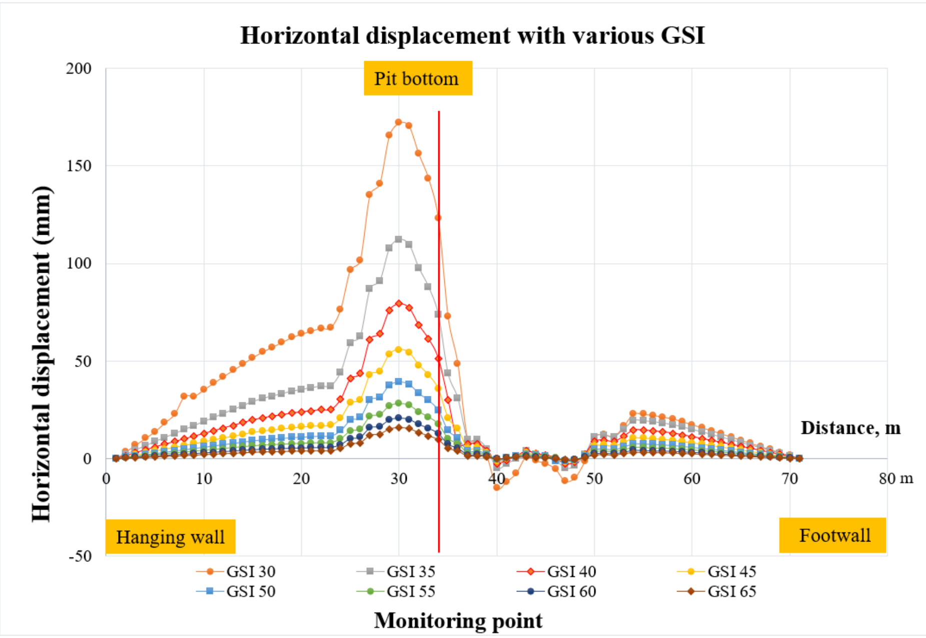

Figure 3. 14 Horizontal displacement with various GSI values

The results obtained from the simulation, as depicted in Figure 3.15, offer valuable insights into the behavior of the open stope under varying GSI conditions. In Figure 3.15(a), the lowest GSI value of 25 results in a substantial failure zone, primarily affecting the hanging wall side while having a relatively minor impact on the crown pillar. This implies that the stability of the open stope is significantly compromised at this GSI level.

Moving on to Figure 3.15(b), an increase in the GSI to 30 leads to a slight improvement in the extent of the failure zone. Although there is a marginal reduction in the size of the failure zone, the hanging wall region continues to exhibit dominant failure behavior. Notably, even a moderate increase in GSI has limited effectiveness in stabilizing the open stope. However, as the GSI values continue to rise, the situation changes significantly. From GSI values of 35 to 50, there is a noticeable decrease in the size and extent of the failure zone. Figures 3.15(e) and 3.15(f) illustrate that when the GSI reaches 45 and 50, respectively, the impact on the failure zone is least pronounced. These figures indicate that the open stope demonstrates improved stability with a considerable reduction in the occurrence of failures, particularly in the hanging wall section.

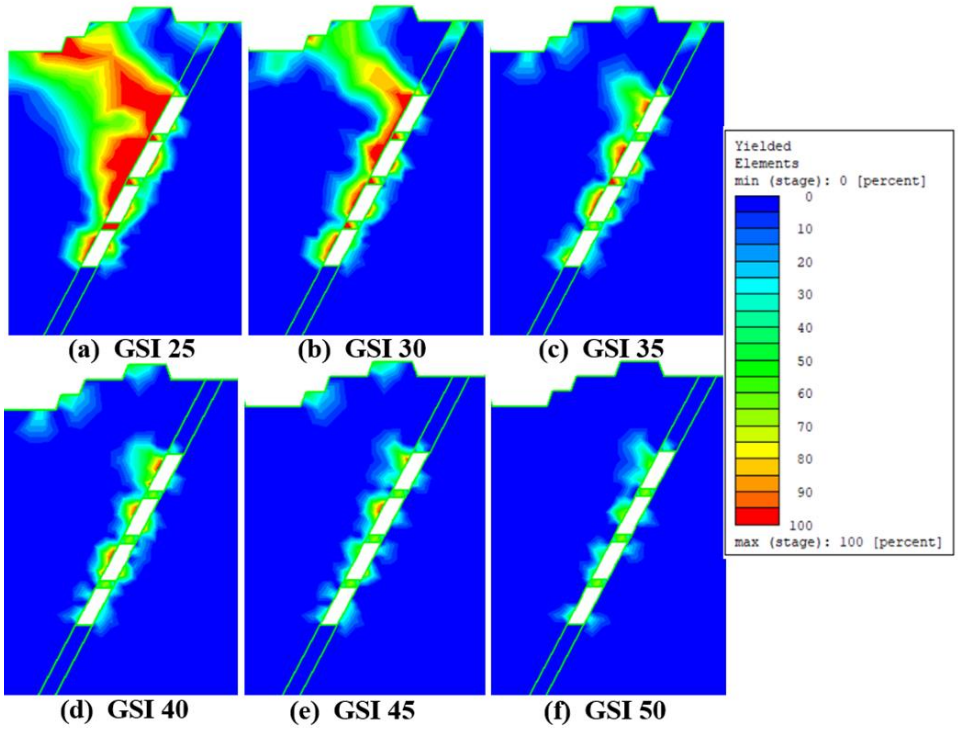

Figure 3. 15 The effect of various GSI values to open stope

Overall, the simulation results shown in Figure 3.15 emphasize the crucial role of the Geological Strength Index (GSI) in determining the stability of the open stope. A lower GSI, as seen with a value of 25, led to a significant failure zone, primarily affecting the hanging wall side. In contrast, higher GSI values, such as 45 and 50, resulted in improved stability and a substantial reduction in the extent of the failure zone. These findings underscore the significance of considering GSI as a critical factor in the design and management of open stopes to ensure their long-term stability and safety. However, in the Sepon Gold-Copper Mine Deposit, the GSI value for the ore vein is 62, while the footwall and hanging wall have values of 72 and 51, respectively. These values are sufficiently high to maintain stability, as discussed in the results above.

3.2.6. Comparison of Different Vein Widths

To assess and select the most suitable design based on geological conditions and ore recovery, six different design factors were examined with varying sizes for open stope dimensions. These design elements have been utilized by several researchers to evaluate potential failure zones (Dintwe et al., 2021; Purwanto et al., 2013; Thae et al., 2022). In this study, the yield zone was analyzed to assess the likelihood of failure zones.

The results reveal that the failure zone is confined to a relatively small area, as indicated by the yielded elements. The initial excavation measures 3×15 m and consists of five minor steps. Figure 3.16(a) illustrates the limited-scale propagation surrounding an open stope with dimensions of 3×15 m (width and height). Each small step in the mining sequence measures 33 m, using an overhand cut method tailored to the rock mass while considering the orebody's Geological Strength Index (GSI) value of 62. Although the ore recovery is somewhat reduced, the first design is relatively narrow, ensuring great stability around the open stope without affecting the crown pillar. The results in Figure 3.16(b) also show small-scale propagation around the open stopes, but the stope size is slightly different, measuring 3×25 m for the initial excavation step, consisting of five smaller steps, each measuring 3×5 m in height. In this case, the failure zone extends further compared to the design in Figure 3.16(a). However, despite the improved stability, the crown pillar remains unaffected, and ore recovery is enhanced.

In Figure 3.16(c), the design employs an initial excavation size of 5×25 m. The results indicate that the failure zone primarily forms between the first and fourth excavations, more extensive than the previous two designs. Similar to Figure 3.16(b), the failure zone increases, but the crown pillar remains unharmed. However, ore recovery is enhanced. Figures 3.16(d) to 3.16(f) largely exhibit the same failure zone, with a noticeable growth from Figure 3.16(e) to Figure 3.16(f). These findings demonstrate that larger open stopes can lead to significant failure zones, especially involving the hanging wall and crown pillar failures in designs as large as 20×25 m.

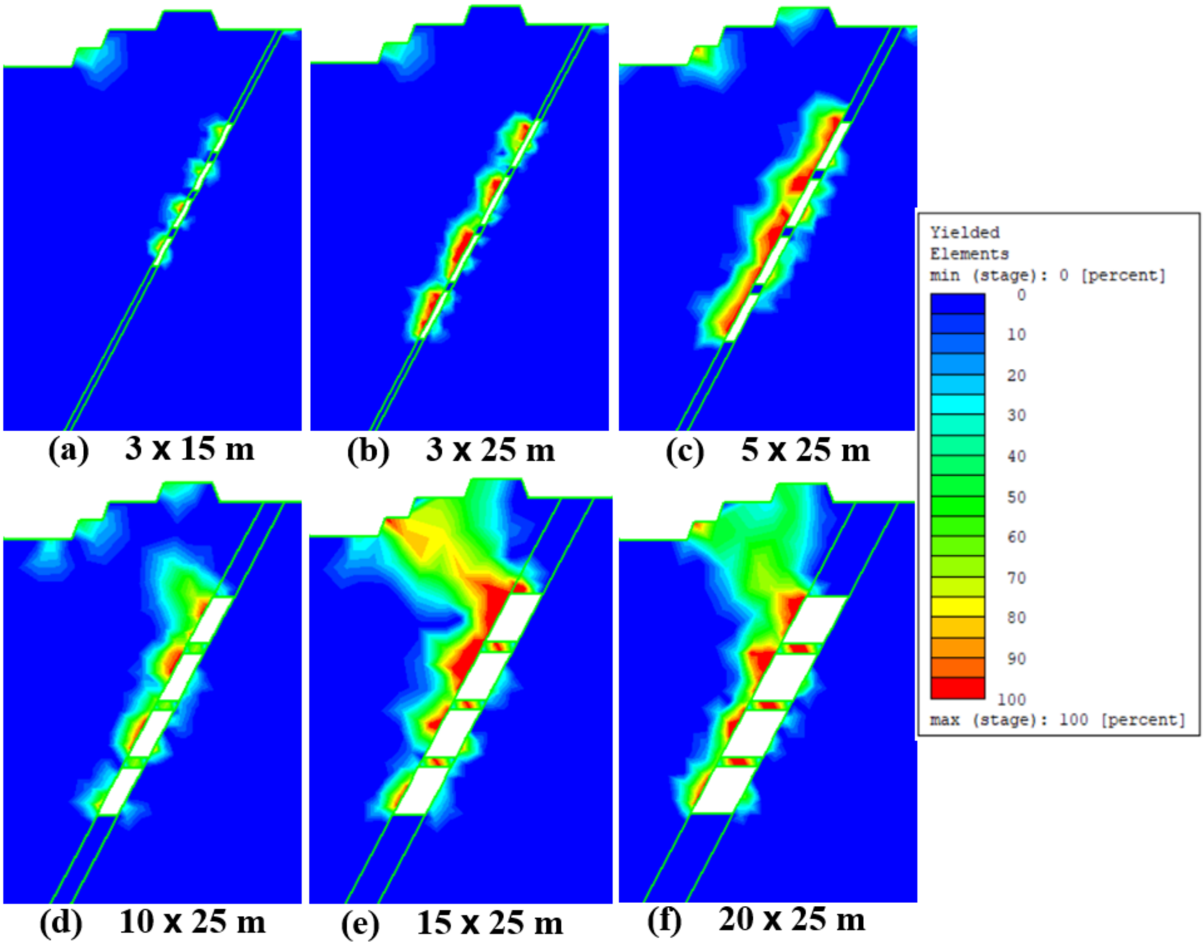

Figure 3. 16 Various designs of open stop dimension

Based on the evaluation of six distinct designs, taking into account the stope geometry and geological characteristics, it can be concluded that Figure 3.16(d) presents a well-suited stope design for the Sepon Gold-Copper Mine Deposit. The results indicate that the extent of the failure zone in this design falls within an acceptable range, striking a balance between excessive failure and overly conservative design. This suggests that Figure 3.16(d) offers a practical and balanced stope design tailored to the specific conditions at the Sepon Gold-Copper Mine Deposit.

Mining operations induce volumetric and stress-strain changes in rock masses. As the deformation exceeds the limits set by the rock's strength, instability develops around the excavation area. It is crucial to monitor the stability of the surrounding rocks to prevent unforeseen failures. Therefore, careful observation and monitoring of the stability of rocks encircling stopes are essential. In contrast to real-time monitoring during active mining operations, where automatic monitoring occurs intermittently and occasionally using reference points, in this simulation, the monitoring points were strategically placed at critical locations in the model. Evaluating displacements in the ongoing underground Sepon Mine revealed significant deformation conditions that could lead to failure. Based on these results, it can be observed that the displacements along the surface were pinned every 10 m, as shown in Figure 3.17. The highest displacement occurred on the hanging wall, predominantly on the crest, whereas the footwall side exhibited relatively lower displacements. This can be attributed to the stronger rock mass on the footwall side and the weaker rock mass on the hanging wall. This study examined six different designs for an open stope. The wider open stope design of 20×25 m resulted in a larger failure zone and higher displacement. Conversely, a stope with 3×15 m dimensions exhibited the lowest potential failure zone. The results indicated that the displacement gradually increased with increasing stope size.

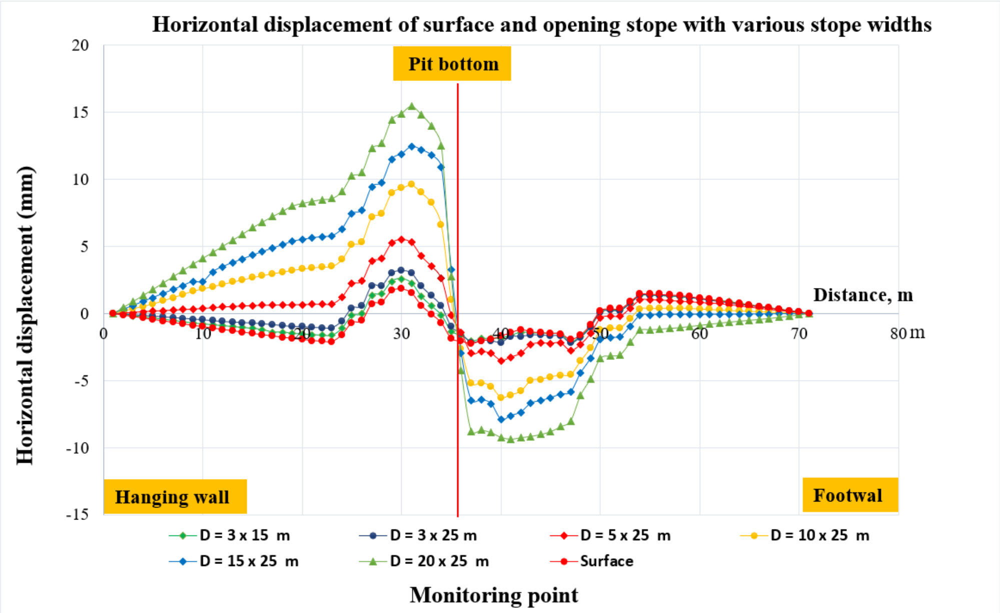

Figure 3. 17 Comparison of the displacement of six different stope sizes

Figure 3.18 provides a visual representation of the displacements, revealing that the most significant displacement occurred during the third and fourth excavation steps, notably on the hanging wall side. In contrast, the displacement on the footwall side remained relatively low. Throughout the excavation process, the safety factor remained relatively stable, with an approximate value of 1.67.

The results show that the first excavation step exhibited the lowest displacement, with a value of 2.37 mm. In the second open-stope excavation, there was a gradual increase in displacement to 2.63 mm. Similarly, the third and fourth excavation steps witnessed further increases in displacement, measuring 3.25 mm and 3.78 mm, respectively. Notably, it is observed that as the excavation depth increases, the predominant displacement also increases (Dintwe et al., 2021; Thae et al., 2022).

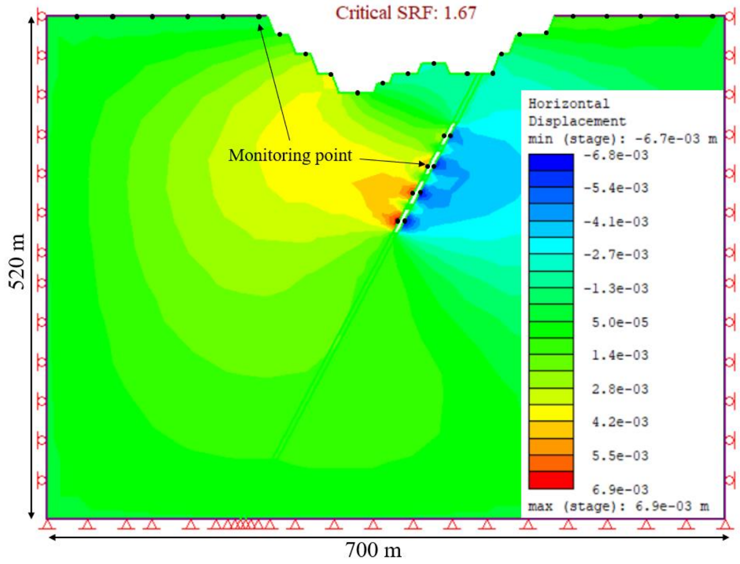

Figure 3. 18 The displaying displacement in the open stope

Furthermore, the highest displacement was predominantly located on the hanging wall side, while the footwall side displayed a slightly higher displacement, especially along the crest, as depicted in Figure 3.19.

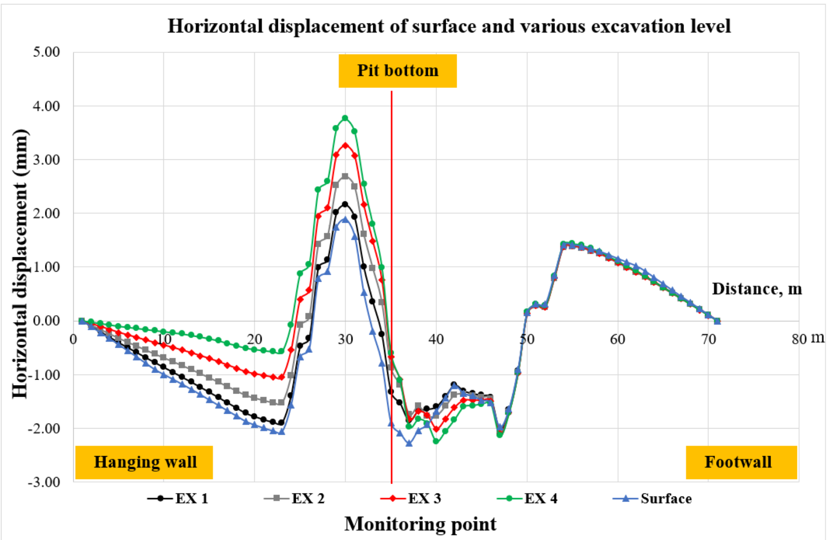

Figure 3. 19 Horizontal displacement of surface and various excavation levels

Based on the data presented in Figure 3.20, the monitoring sites were strategically placed along the side of the open stope. The results consistently indicated higher displacements on the hanging wall side, which can be attributed to the comparatively lower strength of the rock mass in comparison to the footwall side. Specifically, the hanging wall side exhibited a

Geological Strength Index (GSI) of 51, signifying a relatively weaker rock mass. In contrast, the footwall side boasted a GSI of 72, denoting a stronger rock mass. Consequently, this, along with the favorable geometry, contributed to the lower displacements recorded on the footwall side in this particular scenario.

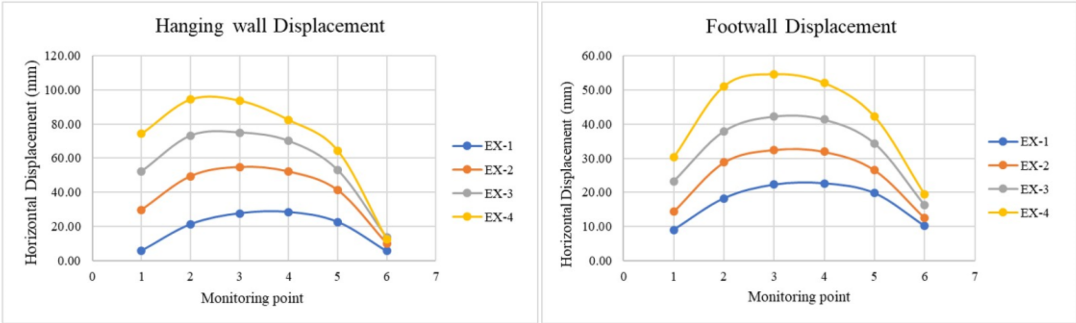

Figure 3. 20 The horizontal displacement in each stope excavation.

3.2.7. Various inclined vein angles

The Sepon Gold Mine is situated in a geologically complex region, characterized by the presence of inclined mineral veins. These veins contain valuable resources, but their orientation can significantly affect the stability of the underground mining operations. The geological and geotechnical team at the mine initiated a comprehensive study to understand and address this challenge. The study began with an assessment of the Geological Strength Index (GSI) of the rocks within the mine. GSI provides vital information about the quality and mechanical properties of geological materials. In this context, it helped in characterizing the specific rock formations and predicting their behavior under varying conditions.

One of the key objectives of this study was to analyze the orientation of the inclined mineral veins at the Sepon Gold Mine. These veins were found to range from nearly vertical (with angles between 62° and 75°) in their natural state. The study recognized the importance of understanding how variations in vein inclination could impact the stability of the underground workings. The study incorporated an array of dipping angles for the models, including 46°, 52°, 62°, 72°, 82°, and 90°. These angles were carefully selected to represent the diversity of vein orientations encountered at the Sepon Gold Mine. By simulating conditions at these angles, the study aimed to provide a holistic view of the mine's stability under different geological scenarios.

A comprehensive comparative analysis of open stoping methods was conducted, examining stope stability under varying vein dipping angles. The simulation results highlighted a significant trend: the potential for failure is notably higher when the vein is inclined at 46°

compared to other vein orientations in the open stoping method. In such cases, the simulation predicted the highest potential displacement, approximately 74 mm. Conversely, at 52°, displacement reduced to 26.5 mm, while a 62° vein dip resulted in 16.5 mm of displacement. Vein inclinations at 72°, 82°, and 90° exhibited significantly lower potential displacements, measuring 14.3 mm, 12.9 mm, and 12 mm, respectively. In conclusion, highly inclined veins, like those at 46°, are associated with a greater risk of displacement and larger failure zones, whereas near-vertical angles, such as 82° and 90°, result in minimal displacement and smaller failure areas. These findings have critical implications for decision-making in selecting open stoping methods and implementing appropriate safety measures in mining operations.

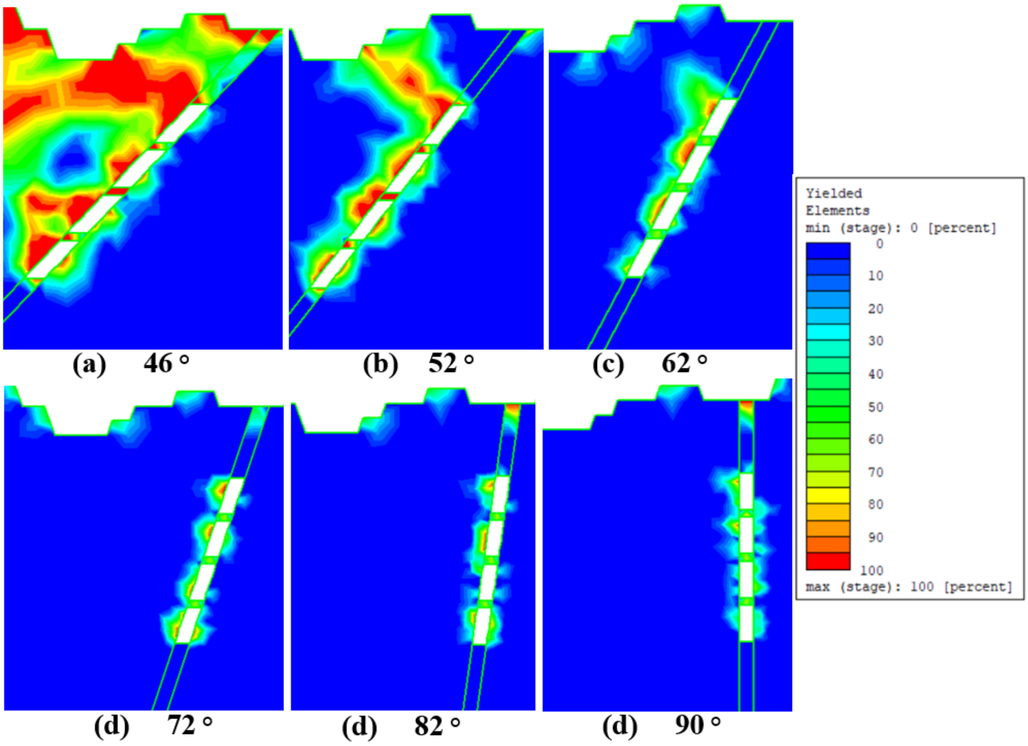

Figure 3. 21 The variety of vein angle

3.2.8. The effect of crown pillar in various thickness

The stability of the crown pillar in underground mining operations holds immense significance in preventing surface subsidence. The crown pillar, situated between the underground workings and the surface, acts as a crucial structural support, bearing the immense weight and pressure from the overlying rock mass. Ensuring the stability of this pillar is paramount, as any failure or compromise in its structural integrity could result in surface subsidence.

Maintaining the crown pillar's stability involves comprehensive assessments of geological factors, mining methods, and the surrounding rock mass properties. Engineers and geologists employ various techniques such as numerical modeling, geotechnical analysis, and ground support systems to reinforce and safeguard the integrity of the crown pillar as shown in Figure 3.22. Additionally, monitoring systems are often implemented to continuously assess any changes in stress distribution or structural weaknesses that might compromise its stability.

The comparison of various crown pillar thicknesses revealed significant insights. Figure 3.22(a) illustrates that a 10 m thick crown pillar exerts a substantial impact, leading to surface collapse. In Figure 3.22(b), a 20 m thickness showed an unstable outcome, although with slight improvement. Figure 3.22(c) with a 30 m thickness exhibited some stability enhancement, yet it remains at a precarious level, deemed unacceptable based on the results. Conversely, Figures 3.22(d) and (e) depicting 40-50 m thicknesses demonstrated a notable increase in stability. In this simulation, the sill pillar has a thickness of only 5 m, which proves to be stable when applied to small vein widths. However, based on the results, it's evident that a 5 m thickness for the sill pillar is insufficient to maintain stability in this particular situation. Therefore, it is suggested that for a vein width of 10 m, the sill pillar should have a thickness of 10 m to ensure stability. Understanding crown pillar failure involves considering multiple factors, notably the Geological Strength Index (GSI) of the ore vein, footwall, and hanging wall. Additionally, the presence of discontinuities, fractures, and faults significantly influences crown pillar stability. The analysis underscores the crucial role of crown pillar thickness in mitigating potential failures and surface collapses. Factors such as GSI values and geological discontinuities necessitate careful consideration in ensuring the stability of crown pillars in underground mining operations.

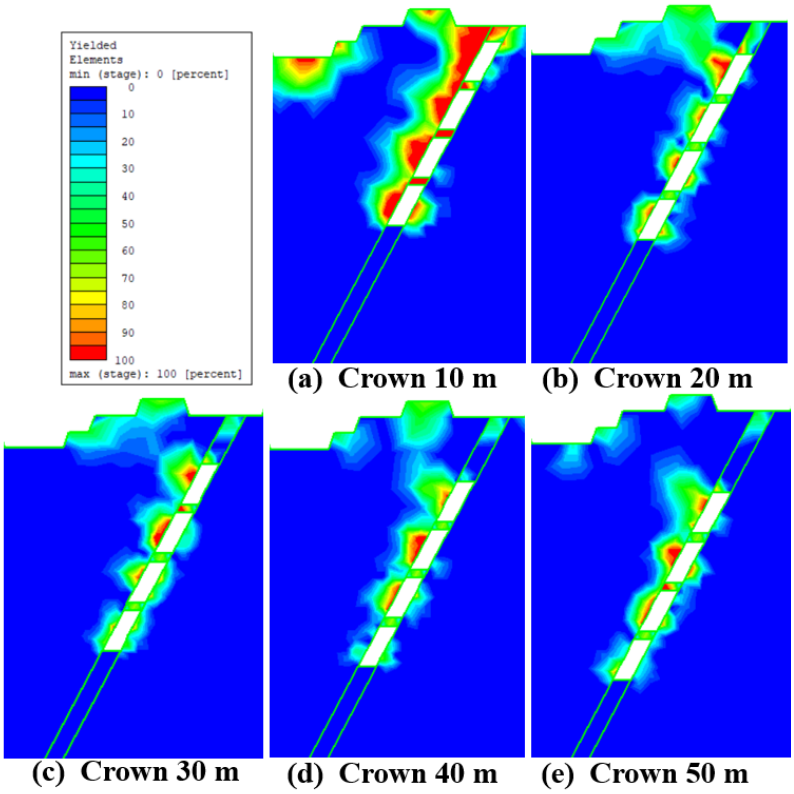

Figure 3. 22 The effect of crown pillar in various thickness

3.3. conclusion

In summary, this chapter provides a comprehensive assessment of stope instability in excavated inclined veins under various conditions at the Sepon Gold Mine. The current mining method employed at the Sepon Gold Mine is the open stoping method, and the findings of this investigation offer valuable insights applicable to different mining regions.

- Firstly, the study underscores the significance of geological conditions in rock mass stability. Weak rock masses with a Geological Strength Index (GSI) value of ≤ 35 are identified as particularly susceptible to instability, necessitating the implementation of artificial support mechanisms. Secondly, the research reveals that in shallow underground mines like the Sepon Gold Mine, high vertical stress plays a pivotal role in stope stability. However, at depths of ≥ 130 meters, it becomes evident that horizontal stress becomes a more influential factor. Thirdly, the inclination of veins is identified as a critical determinant of stope stability, especially in the hanging wall section. It is demonstrated that inclined veins with dips of ≤ 46°, particularly in weak rock mass conditions, pose a higher risk of instability and potential collapse. The fourth aspect addresses the importance of carefully designing sill pillar thickness for underground mine stability. For underground mines planning to develop large excavated stopes of ≥ 10 meters in width, a sill pillar thickness of ≥ 10 meters is recommended. In contrast, excavated stopes with a width of ≤ 5 meters can maintain stability with a sill pillar thickness of 5 meters, ensuring safety and stability in the context of underground open stoping. These findings provide crucial guidance for mining operations and safety measures, offering insights into stope stability and support design for different geological and depth conditions.

- The comparison between overhand and underhand cuts indicates that the overhand cut yielded superior results compared to the underhand cut. This outcome aligns with the characteristics of the ore vein, particularly its high Geological Strength Index (GSI), making it suitable and more favorable for overhand cut operations.

- In assessing the stress ratio within the simulation, a low K ratio of 0.5 demonstrated excellent stability within the open stope, while a K ratio of 1 also yielded favorable results. However, as the K ratio exceeded 1.5, failure instances notably increased on a larger scale. At the mine site, the K ratio typically ranges between 1.3 and 1.7. Therefore, if the K ratio increases beyond this range, it is recommended to conduct a thorough evaluation of the Geological Strength Index (GSI) conditions and reassess the dimensions of the open stope.

- The analysis of crown pillar stability suggests a dependency on both the width of the vein and the Geological Strength Index (GSI). It is recommended that the thickness of the crown pillar should not fall below 40-50 meters, especially with a vein angle of 62°, to ensure sufficient stability.

3.4. Reference

Dintwe, T. K. M., Sasaoka, T., Shimada, H., Hamanaka, A., Moses, D., Liu, S., & Meng, F. (2021). Effects of Sublevel Open Stope Underground Mining on Surface and Open Pit Slopes. *Journal of Geoscience and Environment Protection*, *09*(01), 121–131. https://doi.org/10.4236/gep.2021.91010

Guggari, V. B., Kumar, H., & Budi, G. (2023). Numerical analysis for assessing the effects of crown pillar thickness on ore dilution around the sub-level open stopes. *Ain Shams Engineering Journal*, *xxxx*, 102301. https://doi.org/10.1016/j.asej.2023.102301

Hoek, E., Carter, T. G., & Diederichs, M. S. (2013). Quantification of the geological strength index chart. *47th US Rock Mechanics / Geomechanics Symposium 2013*, *3*, 1757–1764.

Hoek, E., Kaiser, P.K. and Bawden, W.F. (1995) Support of underground excavations in hard rock, Balkema, Rotterdam.

Kaiser, P. K., Yazici, S., & Maloney, S. (2001). Mining-induced stress change and consequences of stress path on excavation stability - A case study. *International Journal of Rock Mechanics*

Marinos, P., & Hoek, E. (2018). GSI: A geologically friendly tool for rock mass strength estimation. *ISRM International Symposium 2000, IS 2000*.

Purwanto, , Shimada, H., Sasaoka, T., Wattimena, R. K., & Matsui, K. (2013). Influence of Stope Design on Stability of Hanging Wall Decline in Cibaliung Underground Gold Mine. *International Journal of Geosciences*, *04*(10), 1–8. https://doi.org/10.4236/ijg.2013.410a001

Sasaoka, T., Takamoto, H., Shimada, H., Oya, J., Hamanaka, A., & Matsui, K. (2015). Surface subsidence due to underground mining operation under weak geological condition in Indonesia. *Journal of Rock Mechanics and Geotechnical Engineering*, *7*(3), 337–344. https://doi.org/10.1016/j.jrmge.2015.01.007

Sepehri, M., Apel, D., & Liu, W. (2017). Stope Stability Assessment and Effect of Horizontal to Vertical Stress Ratio on the Yielding and Relaxation Zones Around Underground Open Stopes Using Empirical and Finite Element Methods. *Archives of Mining Sciences*, *62*(3), 653–669. https://doi.org/10.1515/amsc-2017-0047

Thae, C., Dyson, O., Takashi, M., & Hideki, S. (2022). Design and Stope Stability Analysis of Multiple Concurrent Excavated Veins in Underground Mine ; Case Study of Hermyingyi Tin - Tungsten (W - Sn) Mine. *Geotechnical and Geological Engineering*, *0123456789*. https://doi.org/10.1007/s10706-022-02322-

CHAPTER 4
THE STABILITY OF GENTLE ORE BODY WITH SEVERE CONDITION IN OPEN STOPES

4.1. Introduction

In the preceding chapter, the discussion revolved around the instability of the stope in a vein, with a focus on comparing the dimensions of open stoping. The findings illuminated the substantial influence of the open stoping method on the stability of the surrounding rock mass, extending beyond the crown pillar to encompass the entire excavated stope area. Consequently, the evaluation of crown pillar safety in open stoping becomes imperative to pinpoint key factors that may trigger failure. These factors encompass aspects like rock strength, the instability attributed to geological conditions, and the ratio of the crown pillar's span, among others. The significance of this evaluation is underscored by the Sepon Gold Mine's need to extend its extraction operations to greater depths, driven by the depletion of resources in the shallower strata, as depicted in Figure 4.1.(Dintwe et al., 2022)

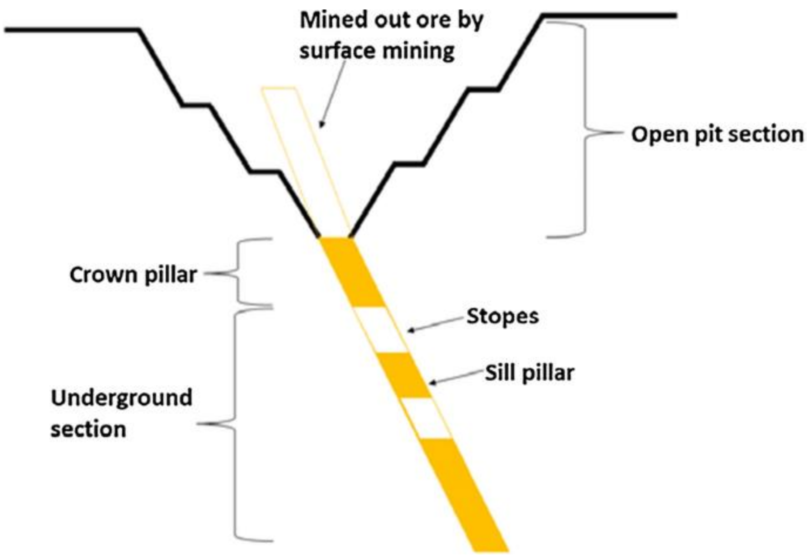

Figure 4. 1 The crown pillar behavior in transition from open pit to the underground

Furthermore, the condition of the crown pillar within the mine can be influenced by a variety of factors, including weathering conditions like weak rock, joint spacing, the environmental impact, the orientation of major discontinuities, and other rock mass properties, as documented by (Tavakoli, 1994). It is evident that in-situ stresses, structural geology, and the geometry of the crown pillar all assume pivotal roles in the stability equation. Each of these parameters can contribute to understanding the potential modes of failure, underlining the complexity and multifaceted nature of crown pillar stability assessments.

Figure 4.2 illustrates examples of crown pillar failures derived from case studies within the research area. In potential low-stress environments, such as those where crown pillars are anticipated to be controlled more by structural factors than stress, various geological features become infuence. Faults, shear zones, and schistosity can influence the stability of the crown pillar. The Figures in 4.2 showcase five distinct types of crown pillar failure in cases involving altered rock (Trevor, 2014). These encompass localized shear failures like chimneying and crown degradation. In settings where sound rock conditions prevail, the presence of discontinuities becomes the most critical parameter, often indicating the potential for large-scale movements. In these five cases, it is crucial to assess stress redistribution around the excavation to determine whether this stress is sufficient to prevent direct gravity failure or sliding block failure, a concept discussed by (Bétournay, 1989).

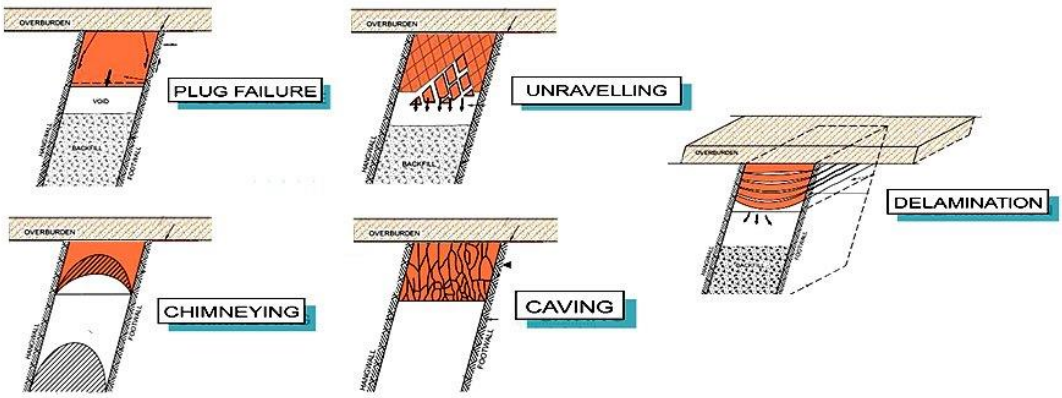

Figure 4. 2 Principal Surface Crown Pillar Failure Mechanisms

Crown pillar failures most frequently occur as a result of sliding along adversely oriented joints in the rock mass, typically at the hanging wall or footwall contact. This issue is particularly pronounced in shallow underground mines, where high vertical stress can lead to the collapse of hanging wall and footwall rock. Therefore, it is essential to design a suitable crown pillar to ensure the overall safety of the stope. Additionally, the importance of implementing appropriate supports and ground control mechanisms for safe mining operations cannot be overstated, which necessitates the careful selection of pillar supporting technologies within the stope opening. To gain a deeper understanding of crown pillar behavior under various conditions, such as thickness, depth, span, and width, simulations were carried out using RS2 software. These simulations were instrumental in identifying yielding elements, determining displacement extents, and calculating safety factors, all of which contribute to comprehending crown pillar failure mechanisms in the context of the open stoping method.

4.2. The characteristic of orebody

The underground deposit encompasses three distinct lithologies: Discovery, Padan, and Nalou. Each of these lithologies is characterized by specific predominant rock types. Within the Discovery lithology, calcareous shales stand out as the primary rock type, as depicted in Figure 4.3. Contrarily, the Padan lithology showcases dolomites and limestones as its primary rock types. Notably, the Padan formation also includes rhyodacite porphyry units, adding significant geological diversity to the deposit. Understanding these geological compositions is pivotal in comprehending the makeup and features of the underground deposit. The development of this deposit presents considerable challenges due to the gentle dip of the vein and the presence of heavily fractured rock mass, among

other factors.

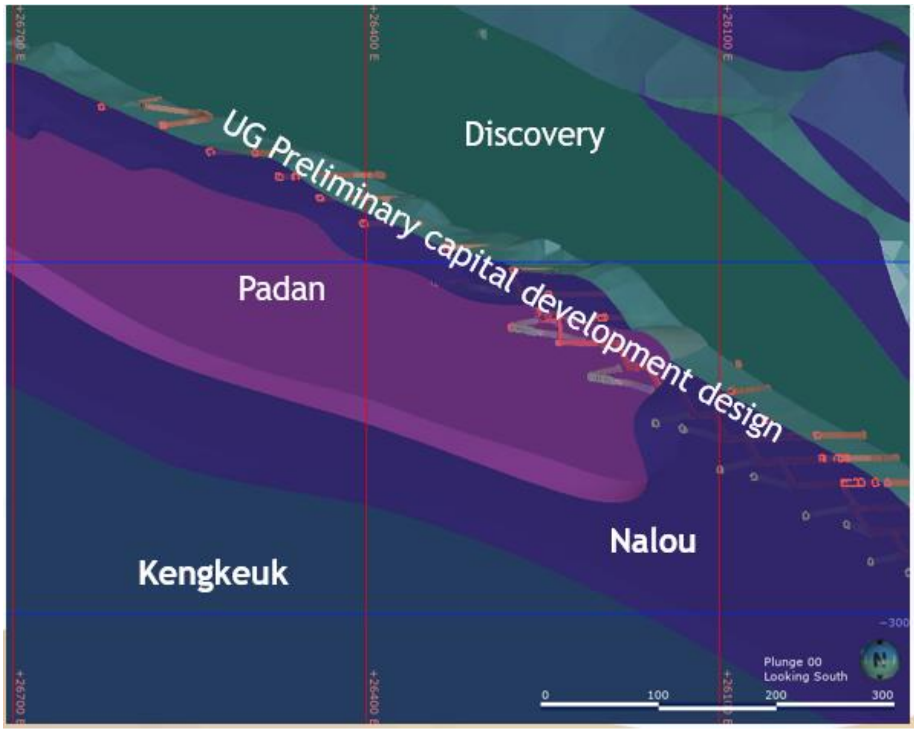

Figure 4. 3 Sepon Lithological Interpretation

4.3. Data collection

The initial geotechnical investigation program involved the drilling of 10 diamond drill holes from the surface as shown in Figure 4.4. Subsequently, the following steps were carried out. The drill holes were geotechnically logged to gather information on various parameters, including Q (Rock Quality Designation), RMR (Rock Mass Rating), GSI (Geological Strength Index), and weathering. These parameters help assess the geological and geotechnical characteristics of the rock formations encountered during drilling. In addition to geotechnical logging, the holes were also structurally logged. This step involved recording details about the structural features of the rock, such as fault lines, joint patterns, and fractures, which can significantly impact the stability of the rock mass. Core samples from the drill holes were sent to a laboratory for testing. These tests aimed to establish intact rock strength failure envelopes, providing valuable data on the mechanical properties of the rock samples and strength under various conditions.

Importantly, the geotechnical logging process is an ongoing and continuous effort, with collaboration between the geotechnical team and the resource geology team. This collaboration ensures that available diamond drilling programs are adequately logged and assessed in a way that is relevant to the project's geological and geotechnical objectives. This comprehensive geotechnical investigation program is essential for understanding the geological and geotechnical aspects of the site, which, in turn, supports informed decision-making in mining and engineering activities.

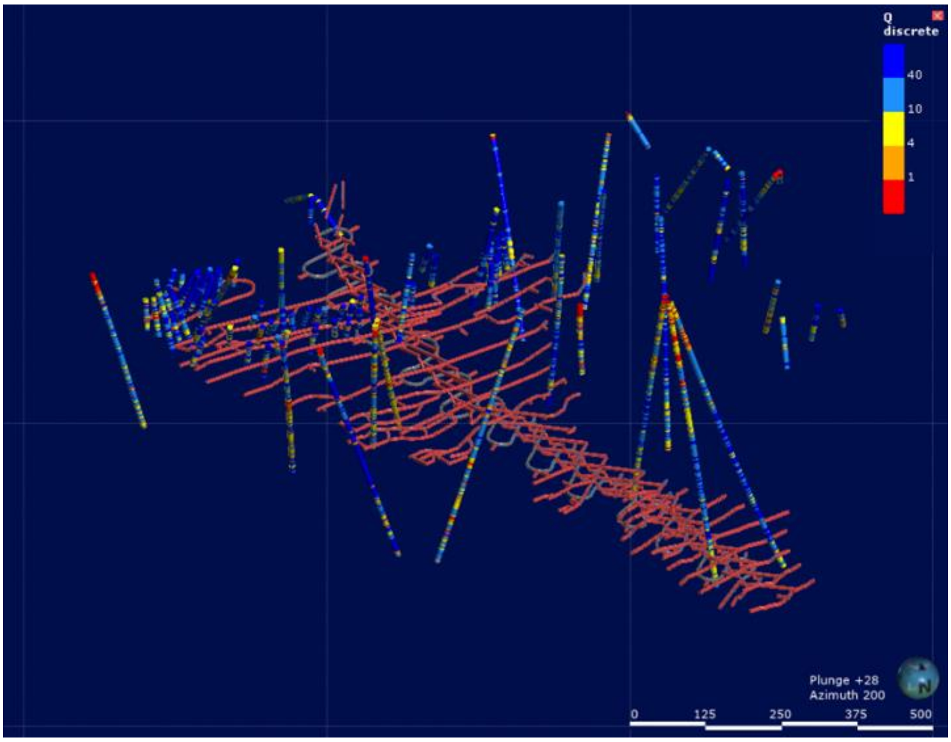

Figure 4. 4 Sepon current geotechnical drill hole database

4.4. Geotechnical rock mass characteristics

Variability is a notable characteristic of the rock mass at the Sepon Gold-Copper Mine Deposit. The quality of the rock mass can vary significantly, spanning from "Very Good" to "Very Poor," in accordance with the criteria set by major rock mass rating systems. However, the averages tend to fall within the "Fair" to "Good" range. This variability in rock mass quality underscores the importance of careful geological and geotechnical assessments to understand and address the challenges posed by different rock conditions within the mine as shown in Figure 4.5. It also emphasizes the need for tailored engineering and support measures to ensure the safe and efficient extraction of resources.

Figure 4. 5 Nalou formation dolomite (DOL) and discovery formation calcareous shales (CSH)

4.5. The plane view and the cross-section

As the Sepon Gold-Copper Mine Deposit has numerous open pits in proximity to underground mining, the orebody is interconnected with many of these open pits. However, due to the high cost of removing waste material and the stripping ratio exceeding the profitability criteria, several open pits cannot continue surface operations. Therefore, underground mining becomes essential to maintain productivity. Figure 4.6 illustrates the plan view and cross-section of the current underground mine, with stope depth reaching 150 meters from the surface in this section.

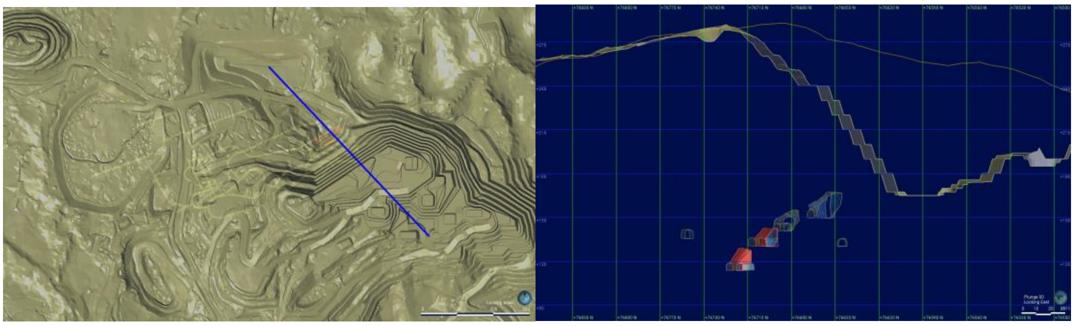

Figure 4. 6 Plane view and cross-section of the Sepon underground mine

Considering the orebody characteristics within the Sepon Gold-Copper Mine Deposit reveal a relatively gentle dip angle, averaging around 32° to 37°, with a depth of 500 meters from the surface, posing challenging conditions for underground design. Employing the open stope method was the chosen design approach. However, the underground mine's steepness presents difficulties for room and pillar design while the inclination challenges the open stope method. To enhance the stability of the open stope, efforts are directed towards making the angle more vertical by blasting the waste material, albeit with the potential risk of dilution during operational phases. Figure 4.7 provides an illustrative layout design for the underground pit operations. The projected mine life for this underground operation spans approximately 6 years, with an annual production target of 78,000 T.

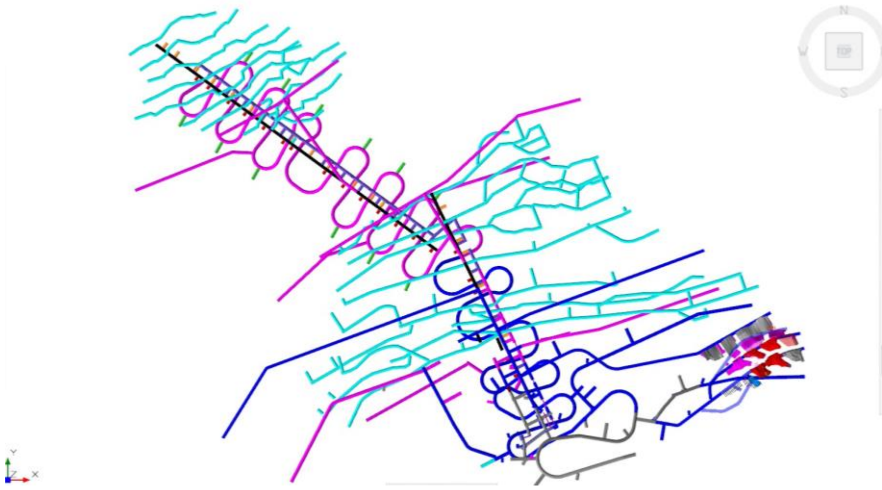

Figure 4. 7 The layout design for the underground pit operations

4.6. Model Simulation

To assess the potential failure of the crown pillar, a series of numerical analyses were conducted using two-dimensional finite element modelling in the RS2 simulation software. The constructed model had dimensions of 700 m by 350 m, with open stoping areas measuring 10 m by 5 m. The excavated region was situated at a depth of 150 m below the surface, as illustrated in Figure 4.8. These numerical analyses and simulations provide insights into the stability and behaviour of the crown pillar under various conditions, aiding in the evaluation of potential failure mechanisms.

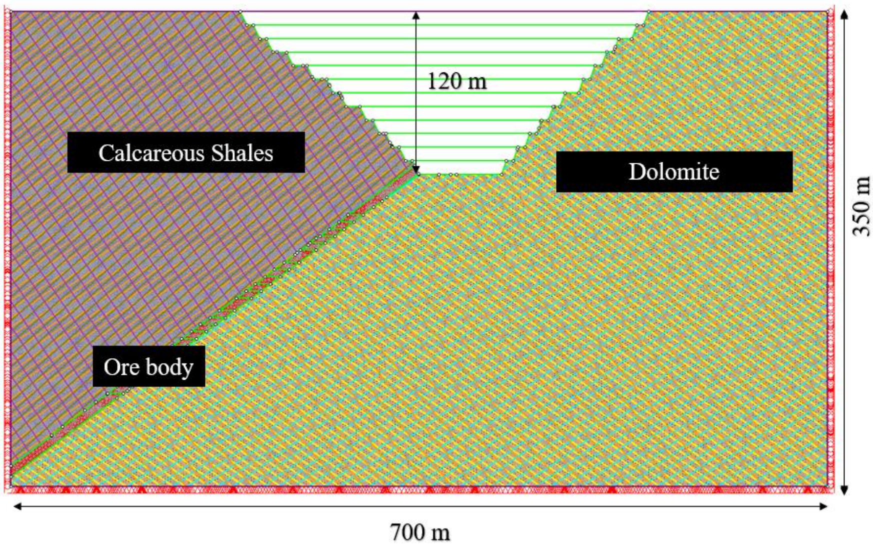

Figure 4. 8 Model consolation with material types

4.7. Horizontal displacement in inclined orebody

Based on the results, this open stope comprises four excavated sections, starting from the top as the first excavation and progressing downward. The stope has a height of 25 m and a width of 10 m, with each excavation utilizing the overhand cut method due to the orebody's excellent GSI of 62.

The analysis of the results reveals a noteworthy observation concerning the hanging wall portion of the structure. Specifically, it exhibits a remarkably high horizontal displacement, reaching up to 200 mm. This substantial displacement can be attributed to the significant impact of joint discontinuity, which is the primary cause of both failures and the resulting large displacements, as shown in Figure 4.9.

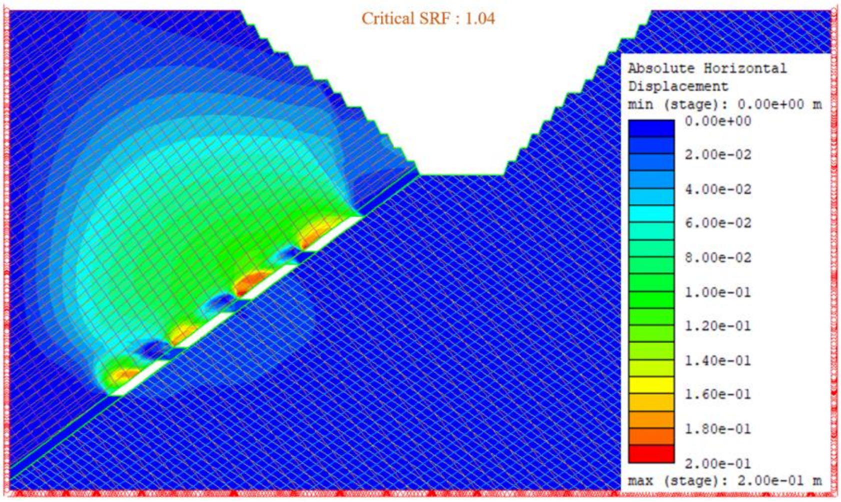

Figure 4. 9 Illustrates the horizontal displacement within all four excavation steps

4.8. The comparison for each excavation open stope in horizontal displacement

Analysing the results reveals distinct trends in the horizontal displacement and safety factors across the different excavation steps. In the first excavation Figure 4.10(a), a notable impact on the hanging wall is evident, with a recorded horizontal displacement of approximately 48.2 mm and a corresponding factor of safety of 1.64. Moving to the second excavation Figure 4.10(b), the displacement increases to 58.2 mm, showing a consistent impact on the hanging wall, while the factor of safety remains relatively stable at 1.37.

The situation changes significantly in the third step of excavation, as depicted in Figure 4.10(c). Here, the horizontal displacement almost doubles, reaching 85.2 mm, accompanied by a reduced factor of safety of approximately 1.17. This suggests a higher risk of instability as the excavation progresses deeper. The fourth and final step of excavation, illustrated in Figure 4.10(d), demonstrates the most substantial horizontal displacement at 200 mm. However, this increase comes at the cost of the lowest factor of safety, which drops to 1.04. It becomes evident that as we delve deeper into the excavation process, the displacement intensifies, primarily due to the removal of the underlying rock, leading to the creation of voids and contributing to the overall instability of the excavation.

These findings underscore the importance of closely monitoring displacement patterns and safety factors as excavation progresses, particularly in deeper stages. Implementing appropriate support measures and engineering controls becomes crucial to mitigate risks associated with increased displacement and maintain the stability of the excavation.

In order to achieve greater stability, the stope height needs to be adjusted. It is not just the stope height that requires alteration; both the stope angle from the hanging wall and the foot side need to be increased to make it more vertical. Currently, the actual angle is 37°, but we can increase both the hanging wall side and foot wall side to approximately 45°. However, this adjustment may cause dilution. The stability, nonetheless, depends on factors such as the GSI, stope size, and the country rock surrounding the open stope.

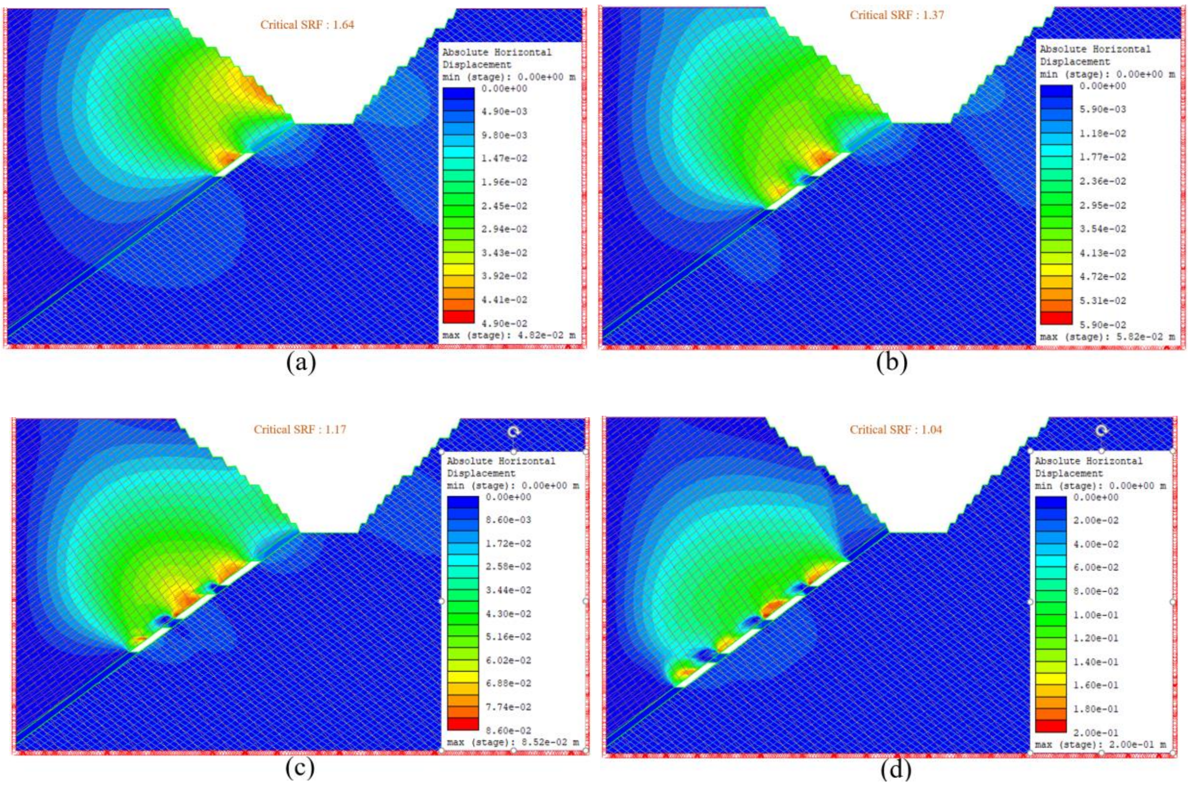

Figure 4. 10 The comparison of horizontal displacement for each excavation step

4.9. The comparison for each excavation open stope in yielded elements

Examining the results of the yielded elements reveals a pattern similar to the horizontal displacement. The failure zones are not as prominent in the first step of excavation, as illustrated in Figure 4.11(a). However, in the second step Figure 4.11(b), the failure zones begin to increase, surpassing those observed in the initial excavation. As we progress to the third excavation Figure 4.11(c), the failure zones become more extensive, affecting a larger area and having a slight impact on the crown pillar. Finally, in Figure 4.11(d), the most significant effects are evident, particularly on the hanging wall and extending to the crown pillar at the surface of the pit. The color scale used in the figures represents the magnitude of failure, with red indicating 100 percent failure and blue indicating no impact.

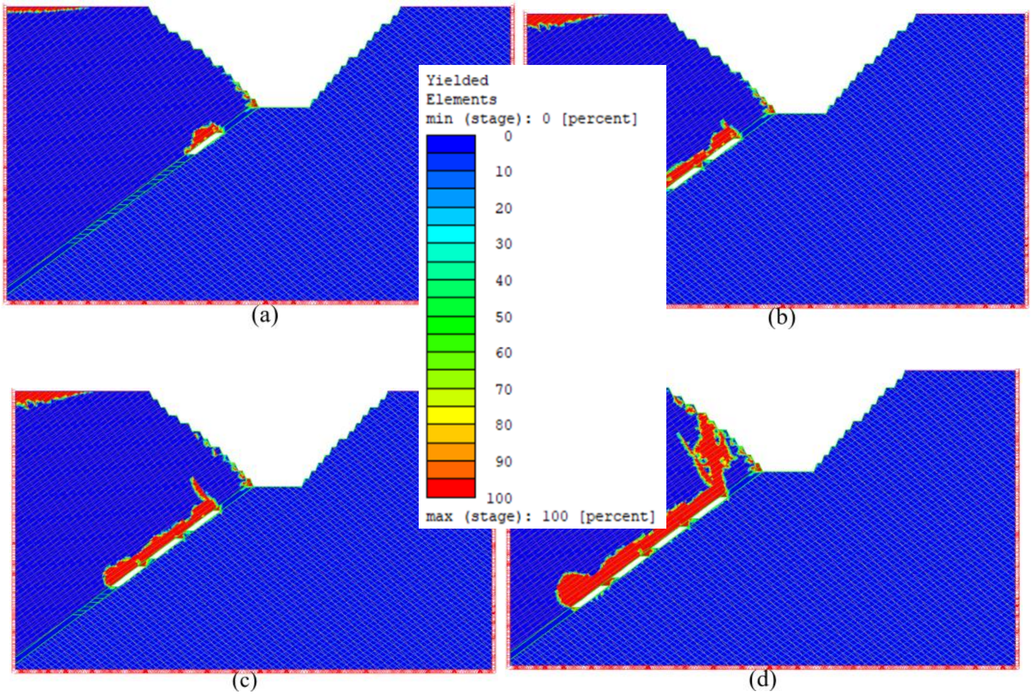

Figure 4. 11 The comparison of yielded elements for each excavation step

4.10. Comparison of horizontal displacement in the hanging wall, footwall, roof and floor

Based on the horizontal displacement observed in both the hanging wall and footwall during the first step, it is evident that the footwall experiences relatively low displacement, measuring below 5 mm. In contrast, the hanging wall exhibits a maximum displacement exceeding 45 mm. This significant displacement in the hanging wall is attributed to its steep inclination, which contributes to the heightened displacement on that side, as shown in Figure 4.12(a). Regarding the roof and floor, the roof demonstrates a displacement of 23 mm, while the floor experiences a much lower displacement, approximately 4 mm. It can be noted that the roof has roughly half the displacement compared to the hanging wall, as illustrated in Figure 4.12(b).

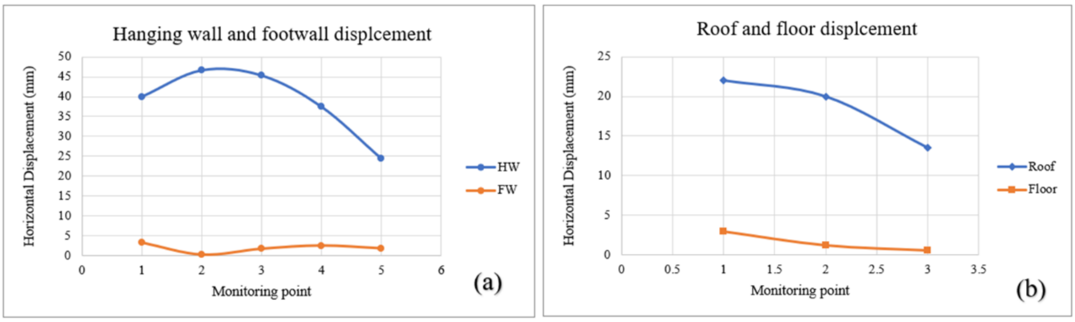

Figure 4. 12 The horizontal displacement in first excavation open stope

Based on the results from this excavation, there is a slight increase in the displacement of both the hanging wall and footwall from the second step approximately 55 mm for the hanging wall and a slight increase to around 8 mm for the footwall, as shown in Figure 4.13(a). Consequently, the displacements in the first and second step excavations do not show significant differences in the results. On the other hand, the roof displacement and floor displacement remain almost the same as in the initial excavation, measuring 24 mm and 4 mm, respectively, as shown in Figure 4.13(b).

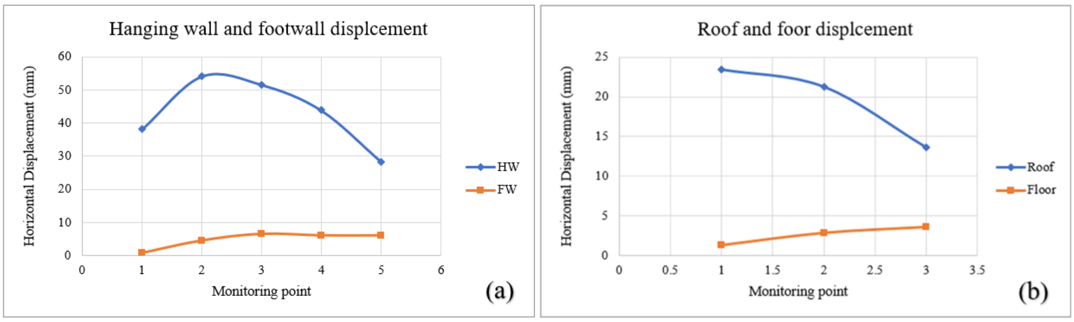

Figure 4. 13 The horizontal displacement in second excavation open stope

The results in this section markedly differ from the first and second excavations. The displacement starts at 60 mm and increases to 180 mm on the hanging wall side, representing a three to fourfold increase compared to the previous sections. In contrast, the footwall only experiences a modest increase to 20 mm, as shown in Figure 4.14(a). This section demonstrates a notable escalation in displacement.

As for the roof, there is also a significant increase, reaching a maximum of 43 mm, while the floor experiences an increase to approximately 15 mm, as illustrated in Figure 4.14(b).

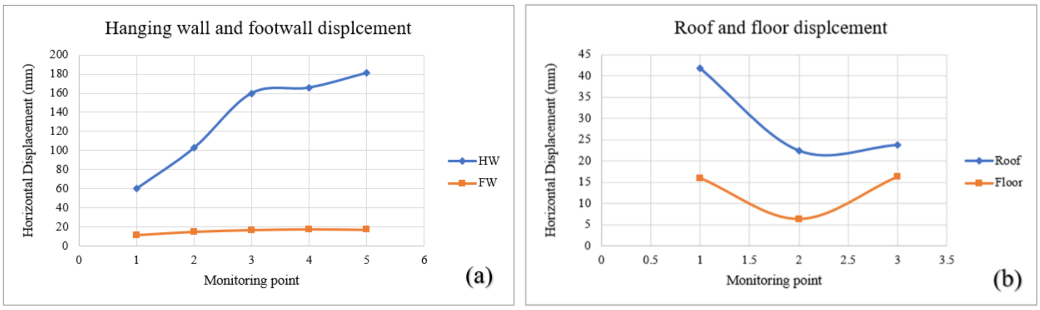

Figure 4. 14 The horizontal displacement in third excavation open stope

The results in this section are nearly identical to the third excavation, as illustrated in Figure 4.15(a). The horizontal displacement increases to about 160 mm for the hanging wall, while the footwall experiences approximately 18 mm of displacement. Similarly, the roof displacement measures around 43 mm, and the floor displacement is approximately 15 mm, as shown in Figure 4.15(b). Therefore, the third and fourth excavations yield almost indistinguishable results. The substantial increase in displacement is attributed to the steeply inclined hanging wall, as well as the presence of bedding and joint sets.

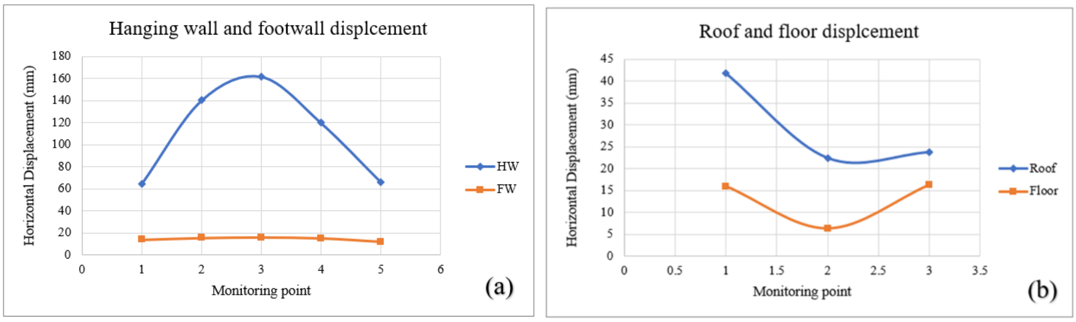

FIGURE 4. 15 THE HORIZONTAL DISPLACEMENTIN FOURTH EXCAVATION OPEN STOPE

In the comparison of the first step excavation between the stope heights of 20 m in Figure 4.16 (a) and 25 m in Figure 4.16 (b), the analysis of the results highlights a significant observation regarding the hanging wall portion of the structure. For a stope height of 20 m, the analysis yielded a Factor of Safety (FOS) of 1.87, accompanied by a horizontal displacement of 44.5 mm. Conversely, the stope height of 25 m resulted in a FOS of 1.04, with a horizontal displacement of 49 mm.

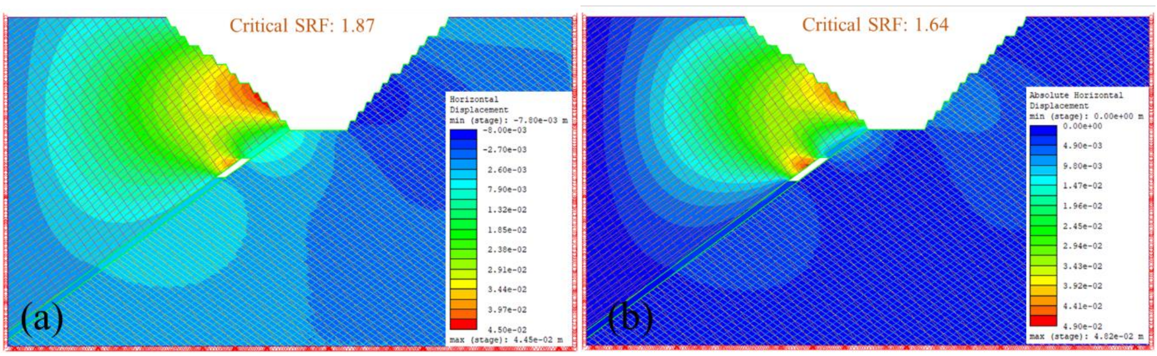

Figure 4. 16 The comparison of different stope heights reveals variations in displacement (1)

In the comparison of the second step excavation in Figure 4.17 (a) at a stope height of 20 m and Figure 4.17 (b) at 25 m, the analysis of the results reveals a significant observation regarding the hanging wall portion of the structure. At a stope height of 20 m (Figure 4.17 (a)), a Factor of Safety (FOS) of 1.55 was obtained with a horizontal displacement of 47.3 mm. In contrast, at a height of 25 m (Figure 4.17 (b)), the FOS was 1.37, accompanied by a horizontal displacement of 56.2 mm.

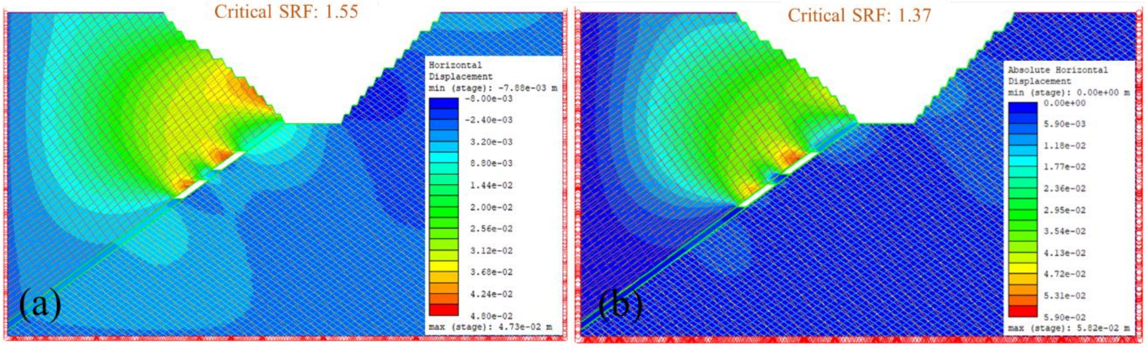

Figure 4. 17 The comparison of different stope heights reveals variations in displacement (2)

In the comparison of the third step excavation in Figure 4.18 (a) at a stope height of 20 m and Figure 4.18 (b) at 25 m, the analysis of the results reveals a significant observation concerning the hanging wall portion of the structure. For a stope height of 20 m, a Factor of Safety (FOS) of 1.37 was obtained with a horizontal displacement of 54.1 mm. In contrast, at a height of 25 m, the FOS was 1.17, accompanied by a horizontal displacement of 85.2 mm.

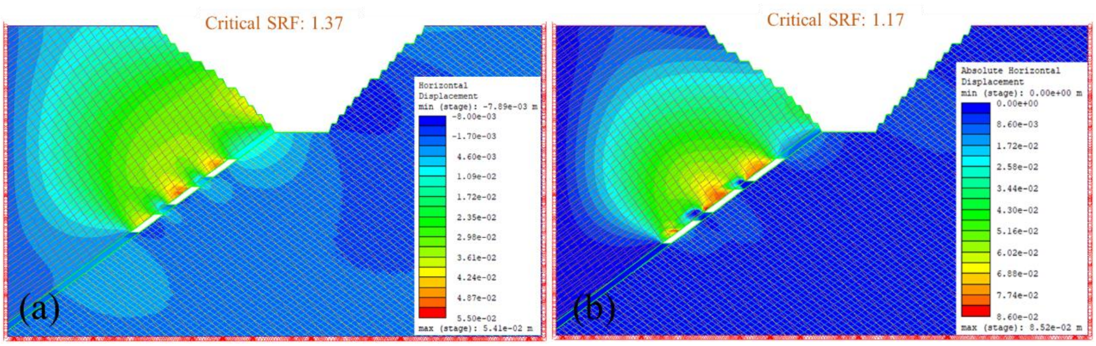

Figure 4. 18 The comparison of different stope heights reveals variations in displacement (3)

However, in the comparison of the fourth step excavation in Figure 4.19 (a) at a stope height of 20 m and Figure 4.19 (b) at 25 m, the analysis of the results reveals a significant observation regarding the hanging wall portion of the structure. For a stope height of 20 m, a Factor of Safety (FOS) of 1.25 was obtained with a horizontal displacement of 60.4 mm. In contrast, at a height of 25 m, the FOS was 1.04, accompanied by a larger horizontal displacement of 200 mm. It's noteworthy that as the depth increases, the Factor of Safety decreases.

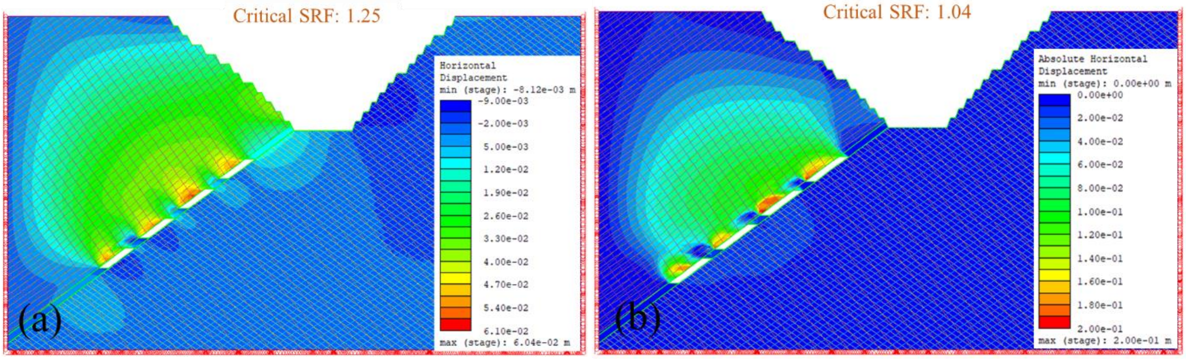

Figure 4. 19 The comparison of different stope heights reveals variations in displacement (4)

4.11. Stability assessment

The relationship between rock mass rating and the stand-up time of an unsupported underground span is depicted in Table 4.1. This table interprets RMR classification ratings concerning stand-up times in the underground mine. To optimize conditions, the underground mine should be oriented so that the dominant joint set strikes perpendicular to the drive direction (Hoek, Brown 1980). This interpretation of RMR classification results relates to stand-up times and rock mass strength parameters. In the Sepon Gold-Copper Mine Deposit, the ore body, footwall, and hanging wall are classified based on laboratory test results and RMR classification, as shown in Table 4.2. Consequently, the open stope requires support with backfill material.

Table 4. 1 Meaning of rock mass classification RMR89 (Hoek, Brown 1980)

Rock mass properties	RMR (rock class)				
	100–81	80–61	60–41	40–21	<20
	I	II	III	IV	V
	Very good rock	Good rock	Fair rock	Poor rock	Very poor rock
Average stand-up time	20 years for 15 m span	1 year for 10 m span	1 week for 5 m span	10 hours for 2.5 m span	30 minutes for 1 m span

Table 4. 2 RMR classification in the mine site

No	Rock type	GSI	RMR89	Depth	RQD
1	Hanging wall	51	66	40	41
2	Footwall	72	83	70.3	60
3	Orebody	62	76	372	90

4.12. Countermeasure for an inclined ore body dip in open stopes by backfilling material

4.12.1. Introduction

The section on "countermeasure for gentle inclined ore body with severe in an open stopes by backfilling material" delves into the strategic approaches adopted to address the stability challenges inherent in an inclined ore body characterized by gentle dip within an open stope. The stability of mining operations is paramount, and in this context, the focus is on employing backfilling material as a proactive and effective countermeasure.

This countermeasure involves the strategic introduction of additional material into the excavated areas, aiming to enhance the structural integrity of the stope and minimize potential risks associated with the unique geological conditions posed by the inclined ore body. The section not only outlines the technical aspects of implementing backfilling but also delves into the underlying rationale driving this approach. By exploring the nuanced intricacies of backfilling in the context of gentle dip in an open stope, the section aims to provide a comprehensive understanding of the countermeasure's feasibility, efficiency, and potential advantages within the mining environment.

4.12.2. Stability assessment of stope with different backfilling materials

Traditionally, backfilling underground has been a common practice in cut and fill mines. Its application in open stope mining serves to mitigate deformation in the surrounding rock mass, creating a stable working platform. Materials commonly used for backfilling include waste rock, tailings, sand, gravel, and various additives. At the Sepon Coper-Gold Mine underground mine, waste rocks from the advancing stope are utilized to provide localized support and a functional working surface. This study involved numerical simulations exploring the effects of mined-out areas with four distinct backfilling materials: waste rock fill, hydraulic fill (a water-solid mixture ranging from 60% to 80% solid content), cemented paste fill (CPF) with a cement-tailing ratio of 1:8, and cemented rock fill (CRF) incorporating 5% cement with waste rock. Detailed properties of these materials are outlined in Table 4.3 (Gonen & Kose, 2011; Naung et al., 2018; Yang et al., 2015). Figure 4.16 displays the resultant failure zones associated with these waste rock backfilling materials.

Table 4. 3 Properties of backfilling materials

Material type	E [MPa]	V	σ [MPa]	φ [deg]	C [MPa]
Hydraulic Fill	181	0.2	0	6.9	0.07
Waste rock Fill	153.1	0.321	0	20.5	0.200

Cemented Paste Fill (CPF)	1130	0.16	1.01	48	1.16
Cemented Rock Fill (CRF)	2850	0.34	0.7	25.4	1.4

4.12.3. The Model simulation with backfilling material

The utilization of backfilling material in the simulation has yielded substantial improvements in the stability of the open stope when compared to its counterpart without backfilling. Notably, the factor of safety has seen a remarkable increase, registering at 3.23. This elevated factor of safety is indicative of a heightened level of stability, providing a robust safeguard against potential instabilities across all four openings, as extensively discussed in the preceding chapter.

Moreover, the impact on total displacement is striking. After incorporating backfilling material, there is an observed reduction of approximately 137 mm in total displacement compared to the earlier scenario of the open stope without backfilling as 200 mm. This reduction in displacement serves as a tangible demonstration of the efficacy of the backfilling approach in not only preventing failures but also in minimizing the overall displacement of the rock mass.

Figure 4.20 below vividly illustrates these findings, portraying a visual representation of the improved stability and reduced displacement achieved through the strategic application of backfilling material. This simulation outcome underscores the importance and effectiveness of employing backfilling as a proactive countermeasure to enhance the safety and stability of mining operations in the context of an inclined ore body with a 37° as gentle dip.

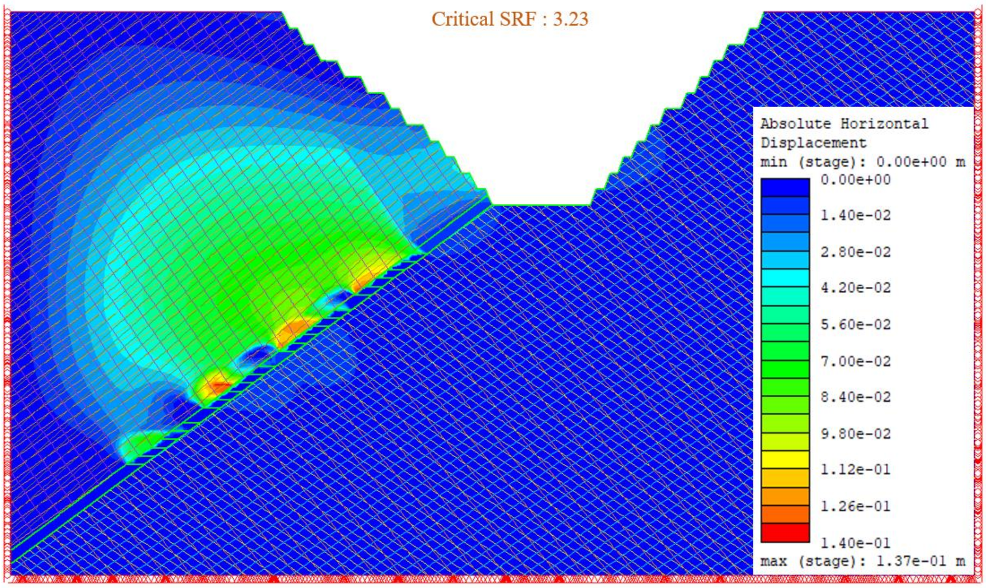

Figure 4. 20 The Model simulation with backfilling material

4.13. Guideline for gentle vein stability

This chapter evaluates stability under conditions of a gently angled ore body while examining the crown and sill pillar stability within the mining area, aiming to establish guidelines for their appropriate thickness. The findings highlight the significant influence of geological factors and ore vein inclination on determining the remaining thickness of the crown pillar. Typically, a steeper dip of the vein heightens the risk to the crown pillar's stability, while weaker geological conditions increase the chance of its collapse. Hence, thoughtful consideration of these factors is essential in designing both the crown and sill pillars.

Based on the study's case, recommendations for crown and sill pillar design are proposed: for hard rock masses, a crown pillar thickness of ≥ 35 m is suggested in an inclined ore vein with a dip of ≥ 35°, ensuring minimal instability risk with proper support systems. Conversely, in weaker rock masses with a gentler dipping vein angle (≤ 35°), a crown pillar thickness of ≥ 40 m is advised to prevent mine collapse. Maintaining the stability of the open stope requires keeping its height within 20 m with a width of 10 m, while the sill pillar should be no less than 10 m to ensure stability.

However, the actual ore body has a very gentle inclination of 37°. To make it more vertical, increasing the angles from the hanging wall and footwall might be necessary, although this could potentially lead to dilution. Moreover, for long-term stability, backfilling the open stope with material, as mentioned in the stand-up time assessment, is crucial.

Additionally, in terms of the limitations inherent in the RS2 simulation, which is confined to a 2D representation and proves to be insufficient, it is strongly recommended to employ RS3. This will enable a comprehensive assessment of the complete reaction of the surrounding rock in the vicinity of the open stope.

4.14. Reference

Bétournay, M. C. (1989). *Surface Crown Pillar Evaluation for Active and Abandoned Metal Mines: Proceedings of the International Conference: Senator Hotel, Timmins, Ontario, Canada, Nov. 15-17, 1989* (Vol. 89, Issue 5). Energy, Mines, and Resources Canada.

Dintwe, T. K. M., Sasaoka, T., Shimada, H., Hamanaka, A., Moses, D. N., Peng, M., Fanfei, M., Liu, S., Ssebadduka, R., & Onyango, J. A. (2022). Numerical simulation of crown pillar behaviour in transition from open pit to underground mining. Geotechnical and Geological Engineering, 1–17.

Gonen, A., & Kose, H. (2011). Stability analysis of open stopes and backfill in longhole stoping method for Asikoy underground copper mine. *Archives of Mining Sciences*, *56*(3), 375–387.

Hoek E., Brown E.T., 1980, *Underground excavations in rock*, Instn. Min. Metall., London. Hoek E., Kaiser P.K., Bawden W.F., 1995, *Support of underground excavations in hard rock,*

Naung, N., Sasaoka, T., Shimada, H., Hamanaka, A., Wahyudi, S., & Pisith, M. (2018). Stability assessment of open stope under overlaying mined-out regions at Modi Taung gold mine, Myanmar. *International Journal of Geosciences*, *9*(9), 547–571.

Tavakoli, M. (1994). Underground metal mine crown pillar stability analysis. *University of Wollongong*. http://ro.uow.edu.au/theses/1280

Trevor, C. (2014). Guidelines for the use of the Scaled Span Method for Surface Crown Pillar Stability Assessment. *Rocscience*. https://www.rocscience.com/help/cpillar/pdf_files/papers/Trevor_Carter_2014.pdf

Yang, Z., Zhai, S., Gao, Q., & Li, M. (2015). Stability analysis of large-scale stope using stage subsequent filling mining method in Sijiaying iron mine. *Journal of Rock Mechanics and Geotechnical Engineering*, *7*(1),

CHAPTER 5
CONCLUSIONS

Laos boasts a rich array of metal and ore deposits including gold, copper, zinc, lead, and nickel. The focus of this research lies in the gold deposit discovered at the Villabuly District Savannakhet Province, known as the Sepon Gold-Copper Mine Deposit. Across Laos, underground mining methods are extensively utilized for various mineral extractions. The choice of mining method typically hinges on ore body characteristics such as thickness, dip, and the competence of the surrounding rock. In instances like Laos, unsupported mining methods are employed to extract mineral deposits characterized as roughly tabular, flat, steeply dipping, and often associated with robust ore and rock. Despite being termed 'unsupported', these methods generally refrain from artificial support systems, although the use of roof bolting and localized support measures is common. In the research area, instability issues arose around the excavated open stope, leading to collapses during shallow depth excavation. These collapses were attributed to the inherent hardness of the underground gold mine in comparison to the host rock, compounded by environmental stress conditions. To mitigate instability, the implementation of underground mining methods like cut and fill comes highly recommended, even though it may result in subsidence. The late introduction of support systems aggravated stope instability within the underground mine. Consequently, this dissertation aims to analyze and propose suitable mine designs and interventions to effectively reduce instability in open stopes, sill pillars, and crown pillars, employing varied vein angles and excavation methods at the Sepon Gold-Copper Mine Deposit. Mine design stands as a critical aspect of mine development. To achieve this objective, the research evaluated site stability under diverse conditions using RS2 software for simulation. Detailed explanations of the results are presented across four chapters:

Chapter 1: This chapter offers an overview of the Sepon Gold-Copper Mine Deposit in Laos, recognized as one of the largest gold-producing regions in Southeast Asia. Laos, rich in mineral resources, encompasses coal and various ore deposits such as copper, gold, zinc, lead, and nickel. The Sepon Gold-Copper Deposit was unearthed at the Vilabuly District, Savannakhet Province, Laos, in 1998. The underground mine employs open stoping and backfill methods, although open stoping predominates in the research area. Additionally, the chapter presents insights into the global gold market's price trends and demand. Furthermore, it outlines the structure and literature review of this dissertation.

Chapter 2: This chapter presents an overview of the research region, situated in the southern central part of Laos. This area is characterized by a complex tectonic structure, exacerbated by fault zones crossing the mine site. Geologically, the host rocks consist of sedimentary formations, including alluvial groups. Notably, the significant granite and associated Sepon Gold-Copper Mine Deposit are situated within the Southeast Asia region. Gold ores are found in formations like jasperoid, decalcified shale, and dolomitized shale. Fieldwork and laboratory tests were conducted to comprehend the mine site conditions and geology. The laboratory tests provided crucial geotechnical properties of the rock mass, including parameters like unconfined compressive strength (UCS), Brazilian tensile strength (BTS), among others. Findings indicate that the hanging wall side of the mine area is weaker than the footwall, while the ore body exhibits stronger properties compared to the hanging wall. This chapter also addresses the problem statement within the research area, which is associated with the challenges posed by the current mining method, particularly in excavating the gentle vein. Furthermore, it outlines the objectives of the study.

Chapter 3: This chapter details the instability conditions observed in the open stoping methods within the underground Gold Copper Mine Deposit at a vein dip of 62°. Various parameters, including stress ratios, geological conditions represented by GSI values, vein inclination angles, stope widths, sill pillar thicknesses, and excavation sequences, were comprehensively evaluated and compared across different open stoping methods. The study, conducted with a GSI value of 35 and 62° inclined veins at the mine site, revealed crucial insights. Weak rock masses with a GSI value of ≤ 35 exhibited susceptibility to instability, necessitating artificial support mechanisms. Analysis of environmental stress conditions highlighted that high vertical stress significantly impacts the stability of excavated stopes at K ≥ 1.5 in underground mines like the Gold-Copper Mine Deposit, while depths of ≥ 130 meters accentuate horizontal stress effects. Moreover, findings regarding vein inclination indicated that inclined veins dipping at ≤ 52° in weak rock mass conditions, such as those found at the Sepon Gold Mine Deposit, pose higher risks of instability or collapse, particularly in the hanging wall section. Regarding sill pillar design, it was noted that underground mines developing larger excavated stopes of ≥ 5 m width should maintain a sill pillar thickness of ≥ 5 m. However, for excavated stopes larger than 10 m, a sill pillar thickness of 10 m suffices. An intriguing discovery was the impact of mining sequencing on underground mine stability, favoring the overhand cut mining sequence approach as the most effective for underground mining.

Chapter 4: This chapter centers on the challenges posed by the 37° gentle vein. The vein's steepness renders it unsuitable for room and pillar mining but quite favorable for open stope excavation. Comparatively, the open stope method proves more suitable in this scenario. Design considerations were based on a stope size of 25 m in height and 10 m in width, with a 10 m sill pillar. Initial excavations showed sustained stability; however, deeper excavations led to increased instability. It was observed that maintaining a stope height of less than 20 m, paired with a 10 m sill pillar, ensures greater stability. Additionally, to ensure long-term stability post-mine closure, the application of backfill material after excavation is recommended. Simulation results demonstrated a substantial improvement in Factor of Safety (FOS) after applying backfill material, with an increase to 3.23, signifying a highly favorable outcome.